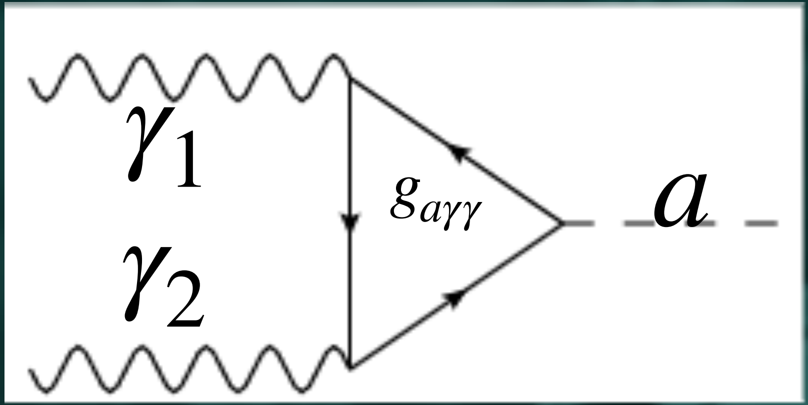

Dark Matter and Quantum Technologies at UWA

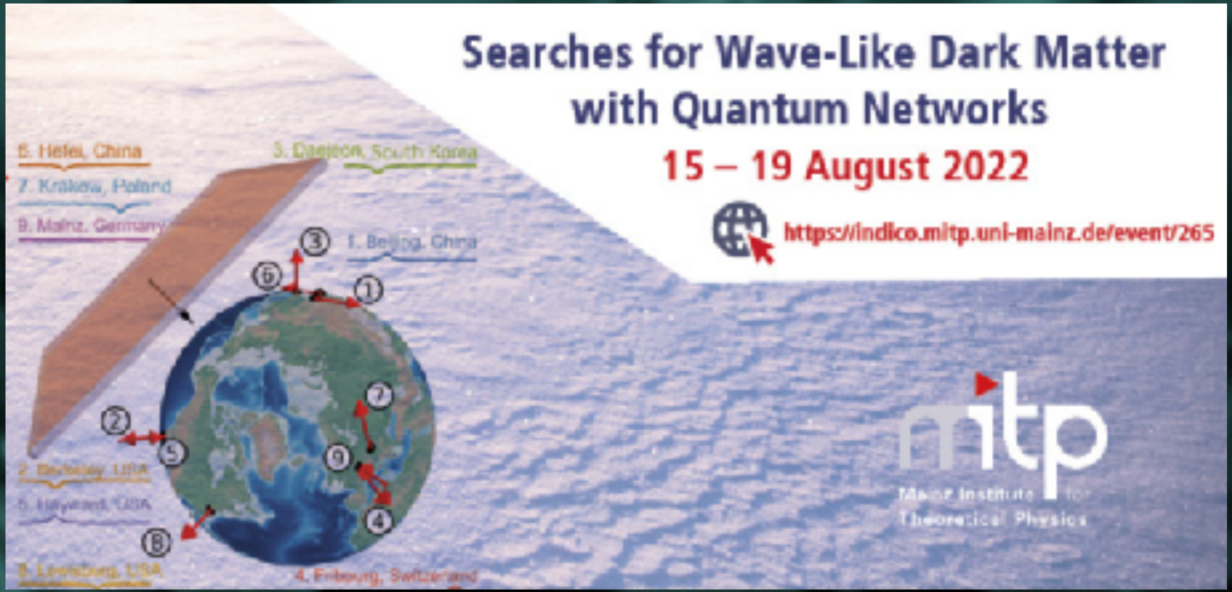

The QDM Lab: https://www.qdmlab.com/

QUANTUM TECHNOLOGIES AND DARK MATTER RESEARCH LAB

EQUS
Australian Research Council Centre of Excellence for Engineered Quantum Systems

THE UNIVERSITY OF WESTERN AUSTRALIA

QDM
Quantum Technologies and Dark Matter Research Lab

ARC CENTRE OF EXCELLENCE FOR DARK MATTER

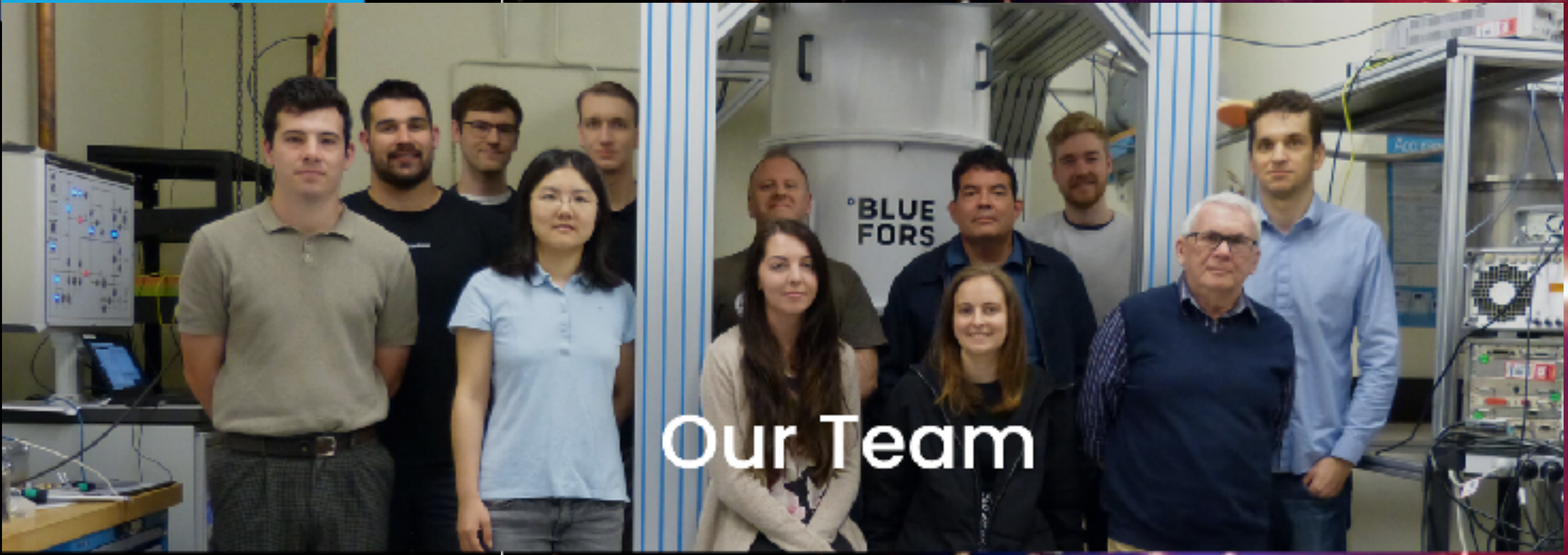

HDR/PHD STUDENTS
Graeme Flower
Catriona Thomson
William Campbell
Aaron Quiskamp
Elrina Hartman

UNDERGRAD STUDENTS
Bryn Roughan (MPE)
Robert Limina (MPE)
Campbell Millar (MPE)
Ishaan Goel (MPE)
Deepali Rajawat (MPE)
Miles Lockwood (Hons)
Aryan Gupta (BPhil)
Michael Hatzon (BPhil)
JoshGreen (BPhil)

ACADEMIC
Michael Tobar
Eugene Ivanov
Maxim Goryachev

POSTDOCS
Ben McAllister
Cindy Zhao
Jeremy Bourhill

TECHNICIAN
Steven Osborne

ADJUNCT
Alexey Veryaskin (Trinity Labs)

https://www.qdmlab.com/

QDM

Quantum Technologies and Dark Matter Research Lab

Home About Virtual Tour Our Team Join QDM News Publications Contact

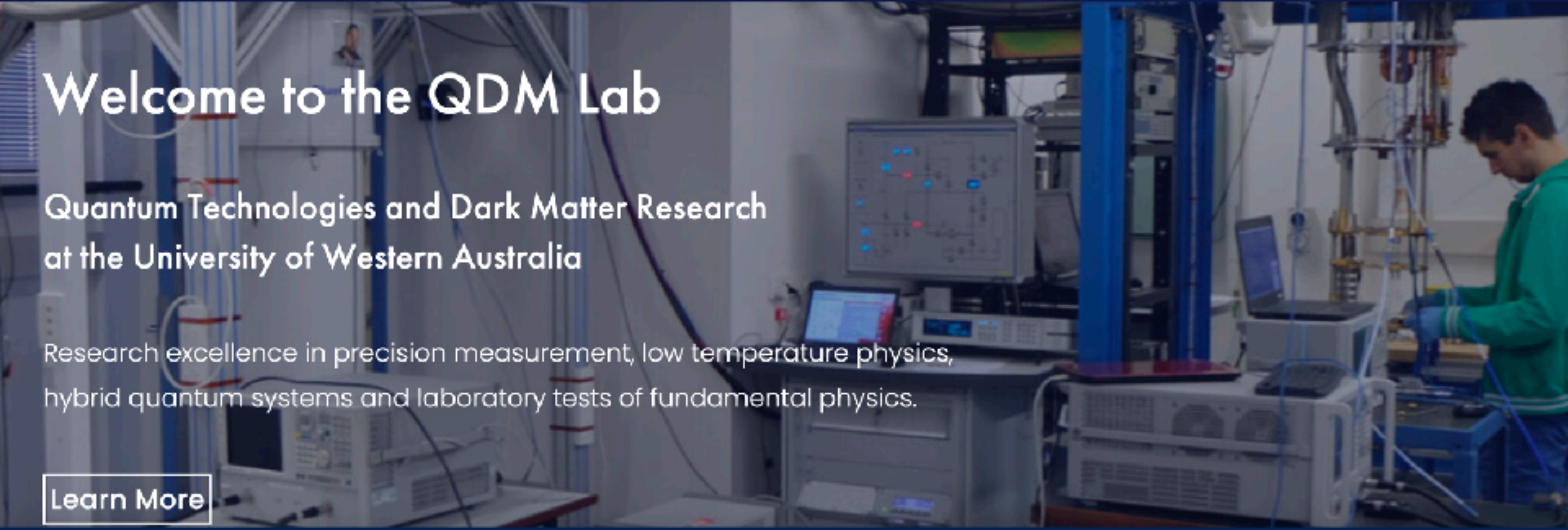

Searching For new Physics

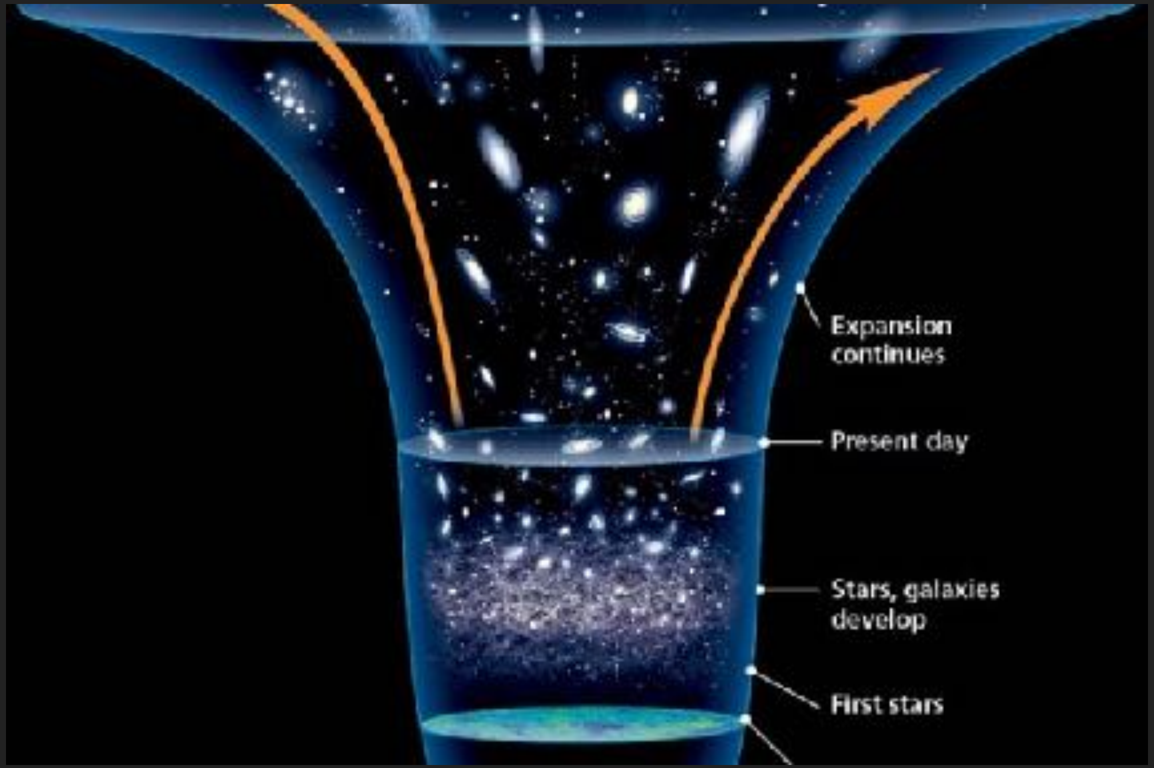

Precision Metrology Technology

PHOTONS

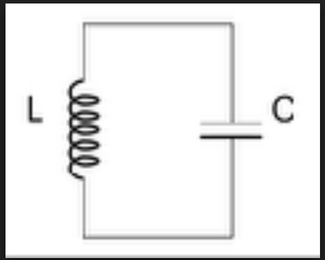

LC-circuits

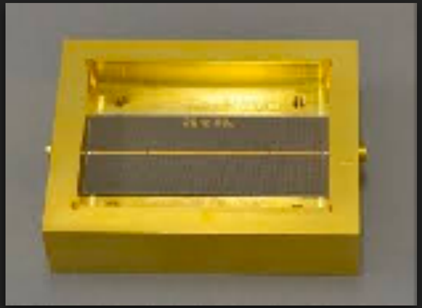

Metallic Cavities

Dielectric Cavities

PHONONS

SAW

BAW

Structures

MAGNONS/SPINS

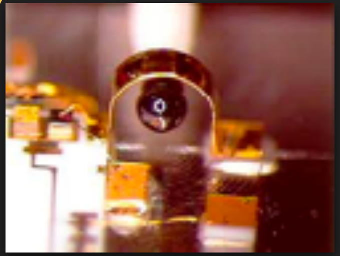

Bulk

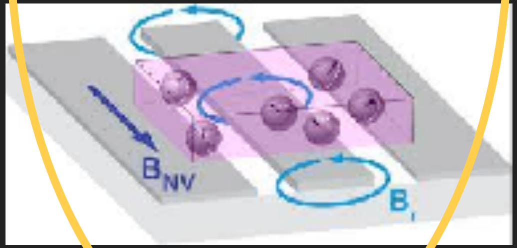

Spin Ensembles

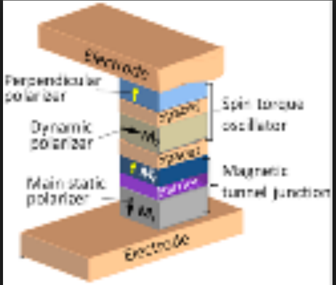

Spin-Torque

ATOMS

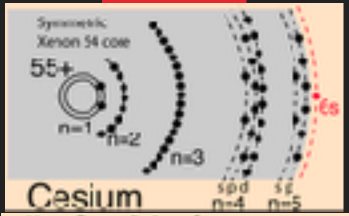

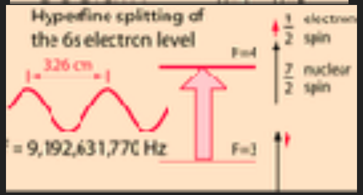

Hyperfine transitions

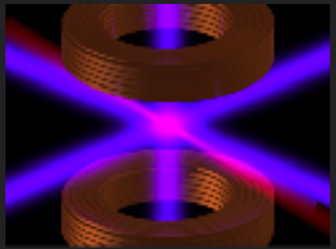

Electron transitions

Nuclear transitions

WIDE RANGE OF PHYICAL PHENOMENA

ARC CENTRE OF EXCELLENCE FOR DARK MATTER

OUTLINE

1) I Can’t talk about everything: Some Overview

2) Phonon Experiments: Do we Always Measure Zero? Interesting Signals in High-Frequency GW detector (Also undertaken LIV Tests and GUP Tests which measured zero)

3) Microwave Photon Experiments: Axion Dark Matter Program at UWA: Focus on Light Axions

Photons (Electromagnetic) vs Phonons (Acoustic)

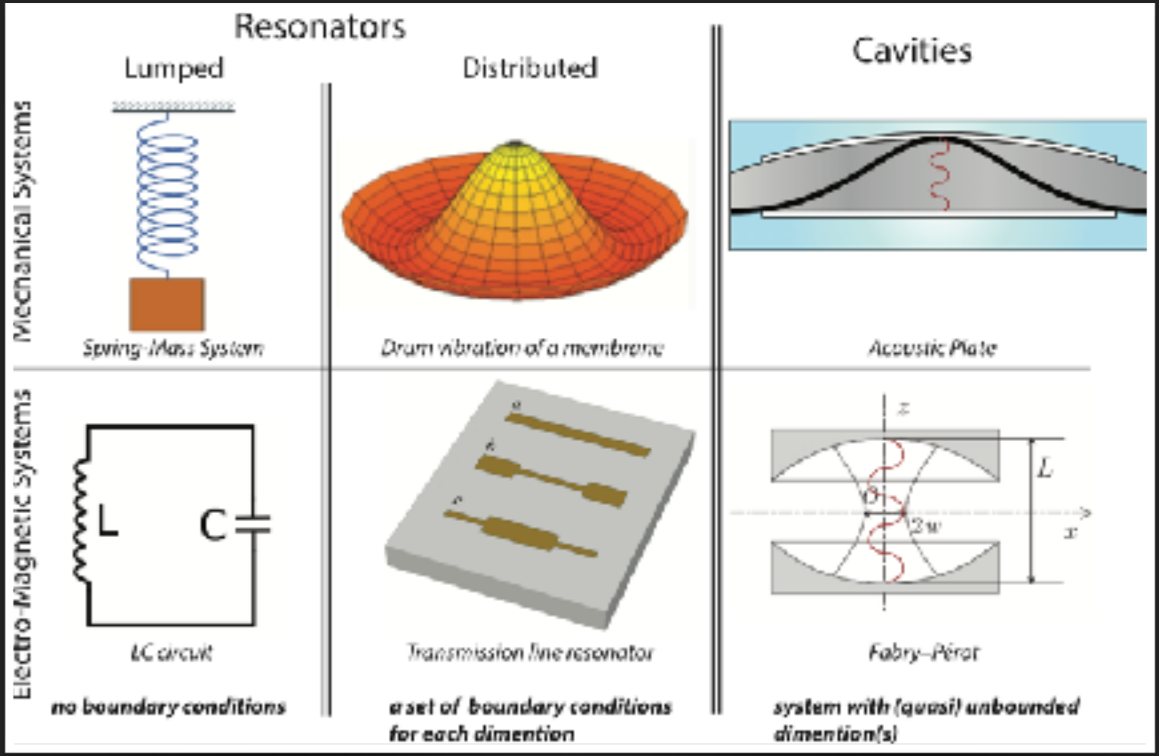

BAW Cavities

APPLIED PHYSICS LETTERS 100, 243504 (2012)

PRL 111, 085502 (2013)

<u>Scientific Reports Vol. 3, 2132 (2013)</u>

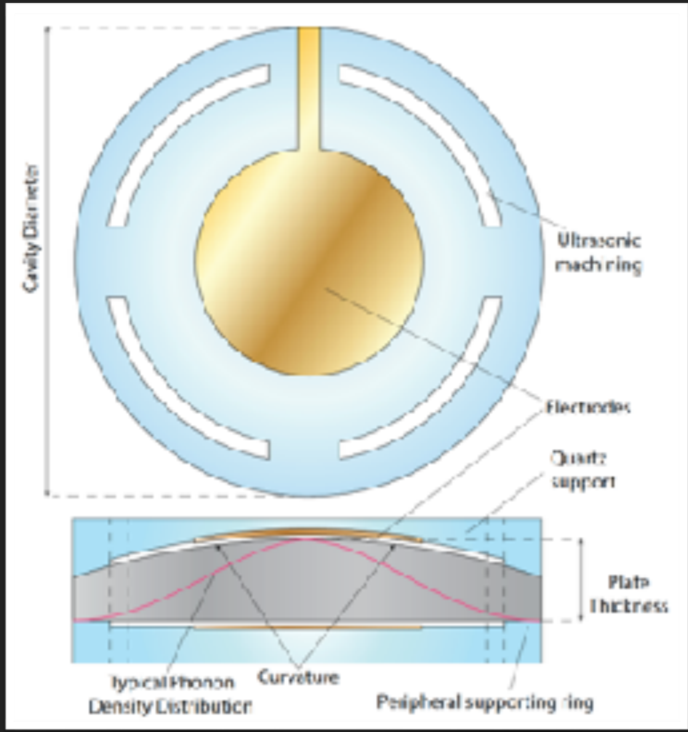

- Frequency range: 1-1000 MHz
- Tree mode family types: 2 transverse and 1 longitudinal
- Piezoelectric Coupling
- Established technology (>70 years for time keeping applications)
- Record high Quality factors ~ 10^{10}

EQUS Australian Research Council Centre of Excellence for Engineered Quantum Systems

ARC CENTRE OF EXCELLENCE FOR DARK MATTER

Lorentz Invariance Tests With BAW Oscillators

Acoustic Tests of Lorentz Symmetry Using Quartz Oscillators

Anthony Lo, Philipp Haslinger, Eli Mizrachi, Loïc Anderegg, Holger Müller, Michael Hohensee, Maxim Goryachev, and Michael E. Tobar

Phys. Rev. X 6, 011018 – Published 24 February 2016

Berkeley
UNIVERSITY OF CALIFORNIA

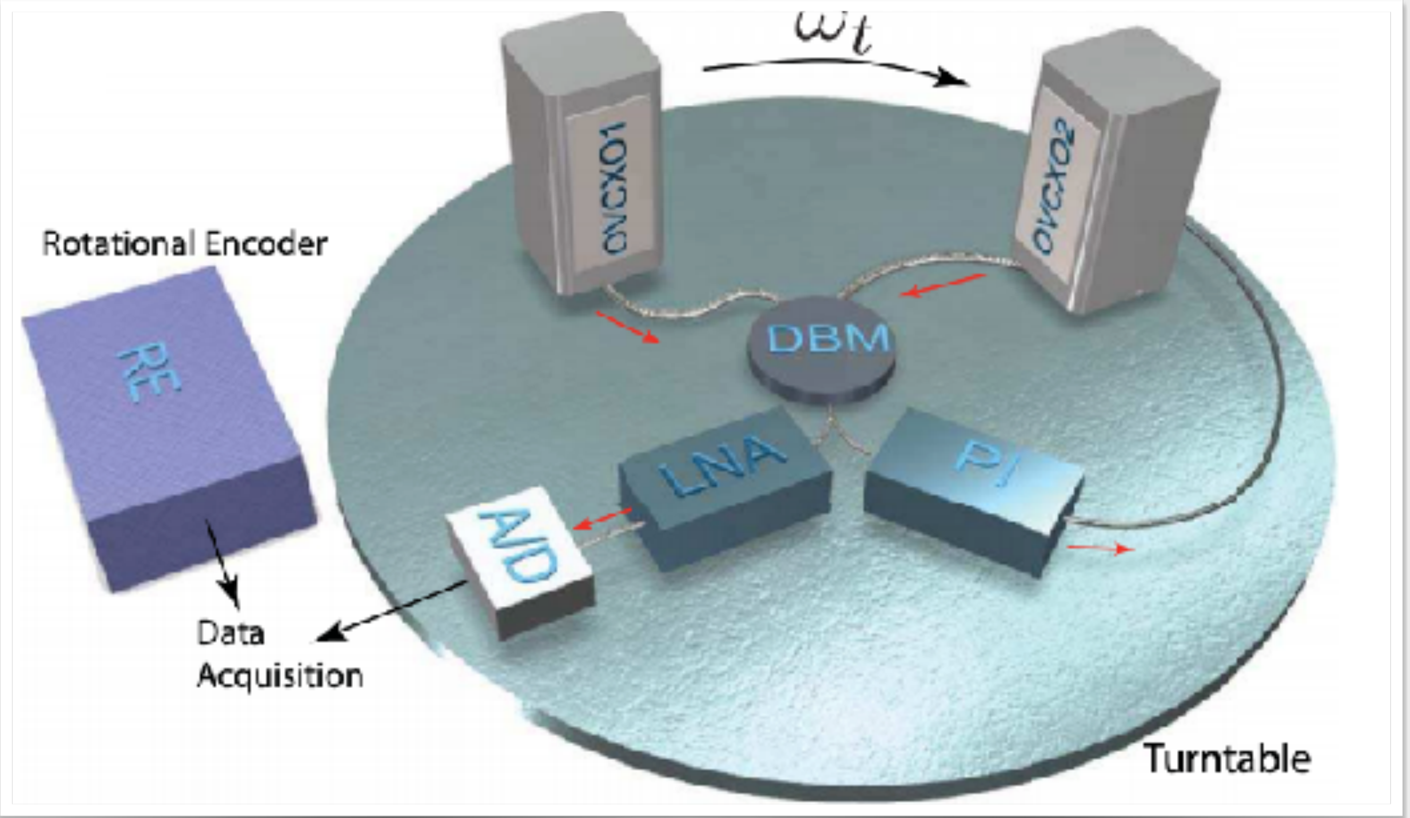

Upper limit on anisotropy of Neutron Mass

EQUS

Quantum Gravity

Testing the generalized uncertainty principle with macroscopic mechanical oscillators and pendulums

P. A. Bushev, J. Bourhill, M. Goryachev, N. Kukharchyk, E. Ivanov, S. Galliou, M. E. Tobar, and S. Danilishin

Phys. Rev. D **100**, 066020 – Published 20 September 2019

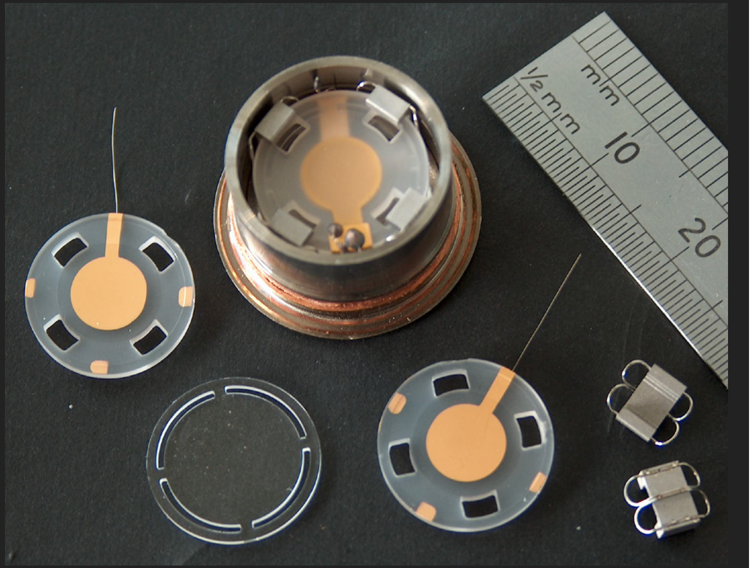

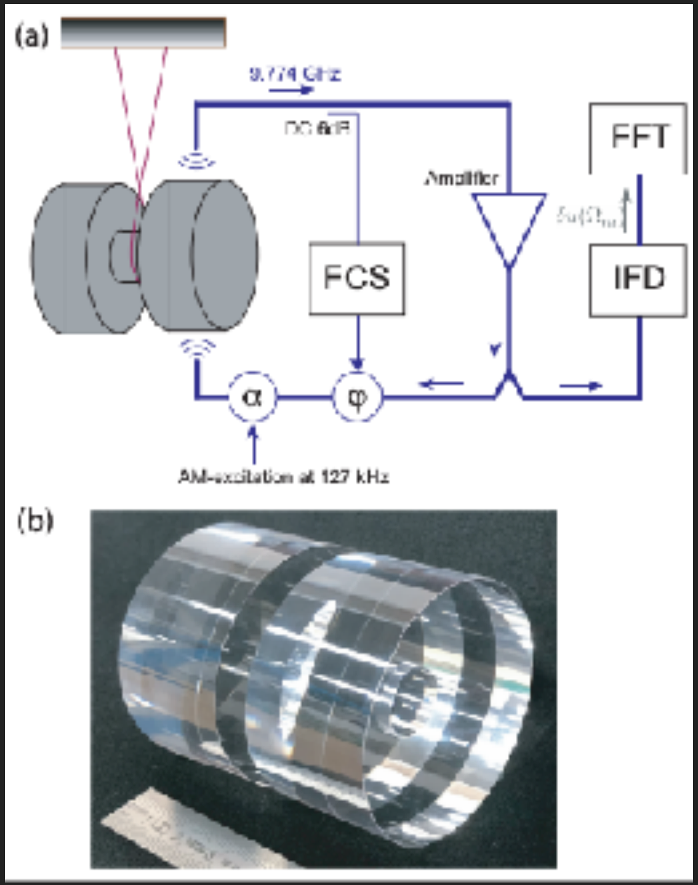

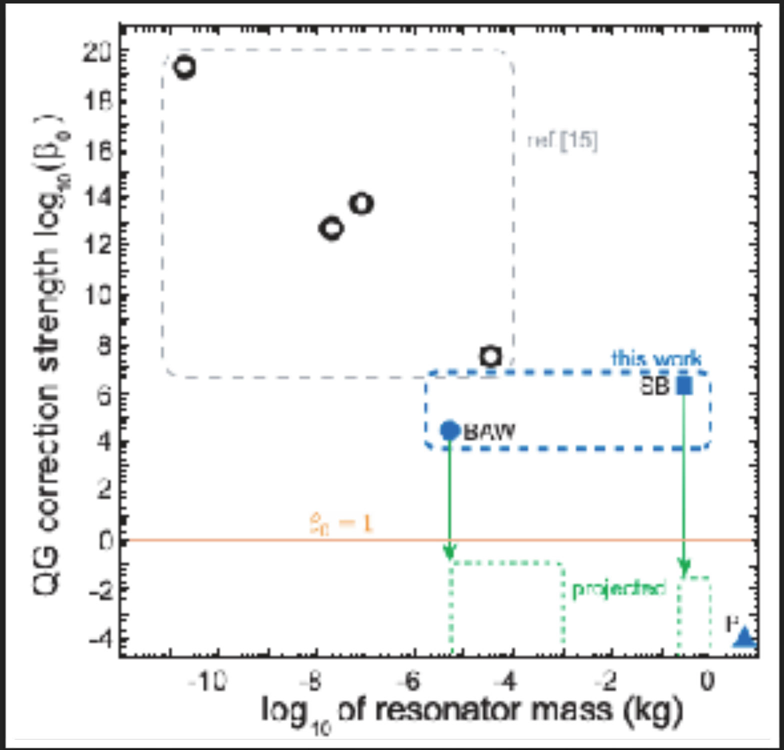

Bulk Acoustic Wave High-Frequency GW Detectors (A Resonant-Mass Detector)

QDM
Quantum Technologies and Dark Matter Research Lab

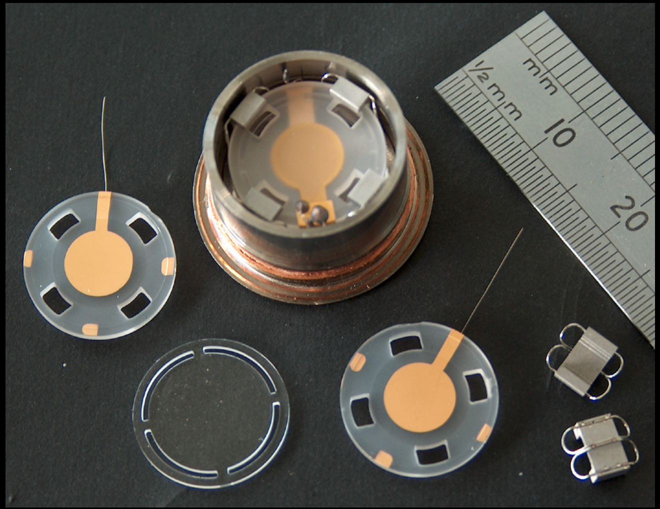

PhD Student

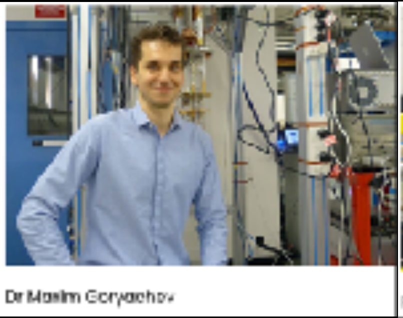

UWA Staff

Ik Siong Heng
Prof. Glasgow

Serge Galliou
Prof. Franche-Comté

Australian Government
Australian Research Council

THE UNIVERSITY OF WESTERN AUSTRALIA

High Frequency Gravitational Waves?

Gravitational wave detection with high frequency phonon trapping acoustic cavities

Maxim Goryachev and Michael E. Tobar

Phys. Rev. D 90, 102005 – Published 24 November 2014

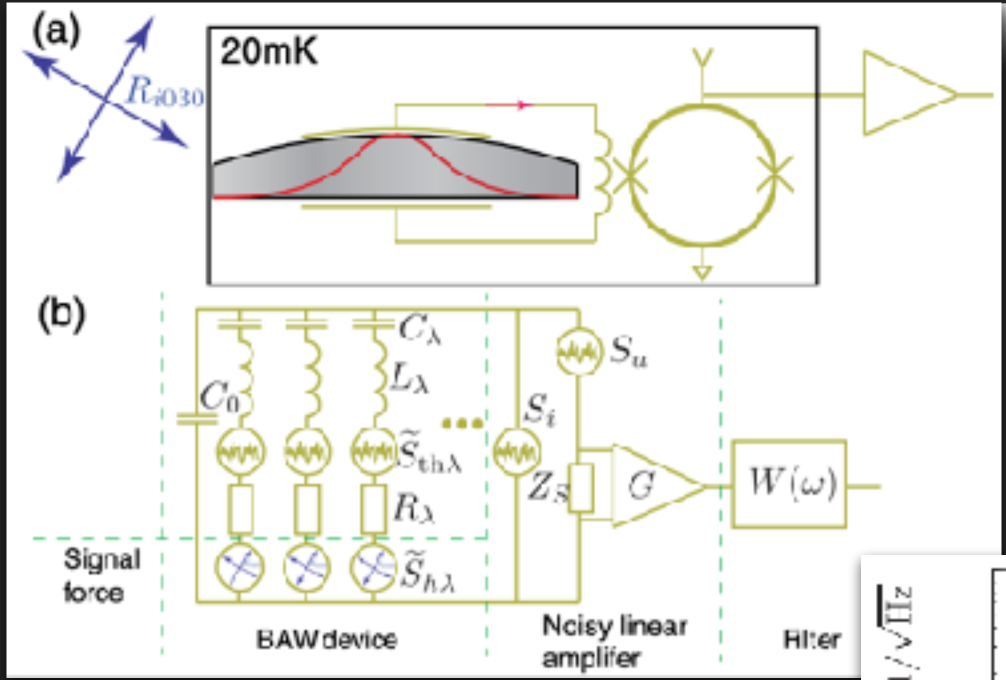

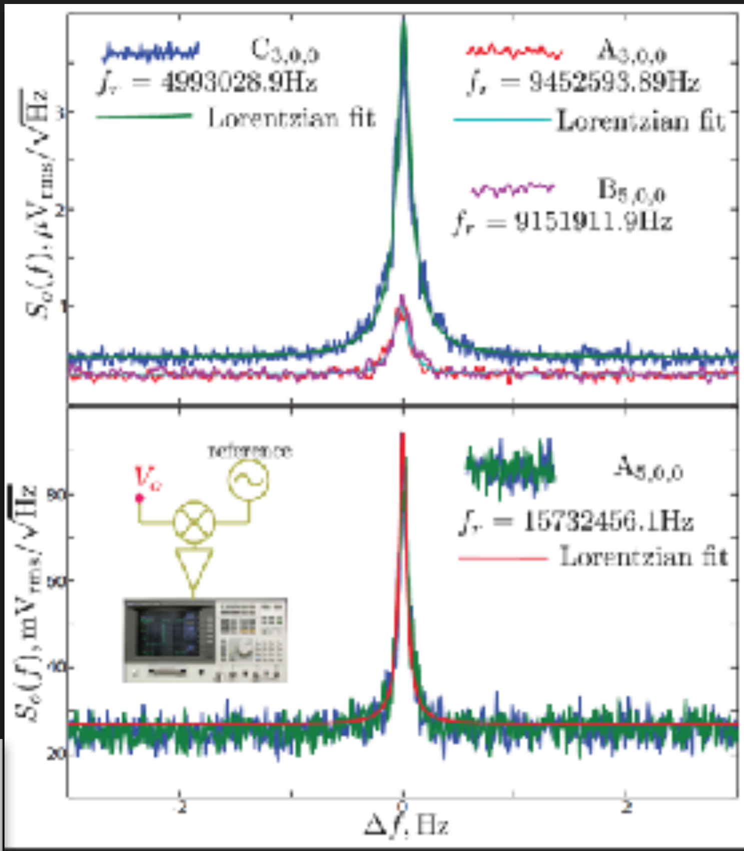

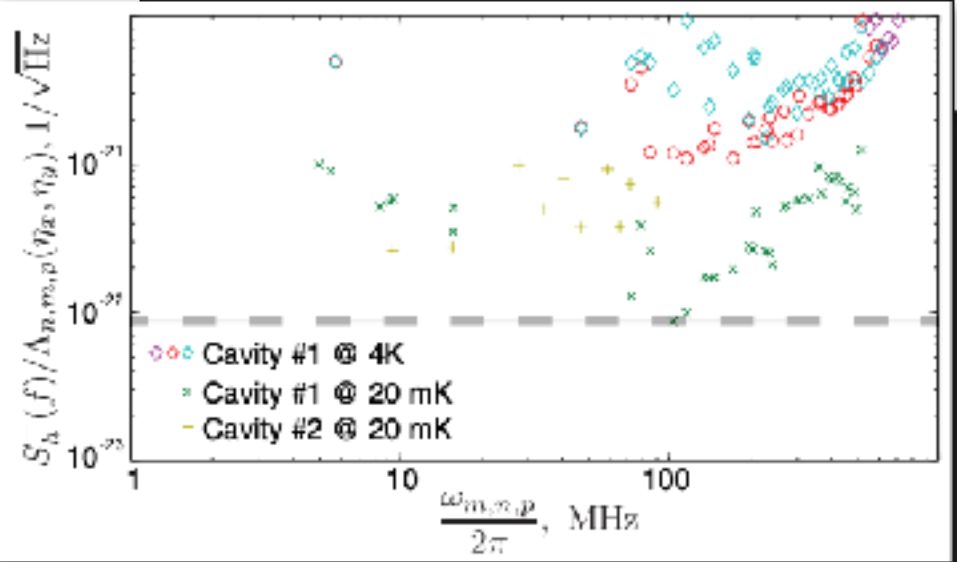

Appl. Phys. Lett. 105, 153505 (2014)

Recent Experiment: First Detection, unlikely! Or not?

PHYSICAL REVIEW LETTERS **127**, 071102 (2021)

Rare Events Detected with a Bulk Acoustic Wave High Frequency Gravitational Wave Antenna

Maxim Goryachev,[1] William M. Campbell,[1] Ik Siong Heng,[2] Serge Galliou,[3] Eugene N. Ivanov,[1] and Michael E. Tobar[1,*]

[1]*ARC Centre of Excellence for Engineered Quantum Systems, ARC Centre of Excellence for Dark Matter Particle Physics, Department of Physics, University of Western Australia, 35 Stirling Highway, Crawley, Western Australia 6009, Australia*

[2]*SUPA, School of Physics and Astronomy, University of Glasgow, Glasgow, Scotland G12 8QQ, United Kingdom*

[3]*Department of Time and Frequency, FEMTO-ST Institute, ENSMM, 26 Chemin de l'Épitaphe, 25000 Besançon, France*

Excluded sources:
LIGO/VIRGO event catalogue, weather perturbations, earthquakes, meteor events / cosmic showers, FRBs

Possible sources:
Internal solid state processes, internal radioactive events, cosmic ray events, HFGW sources, domain walls, WIMPs, dark matter

Recent Experiment

Control and Signal Processing

Cryogenic Part

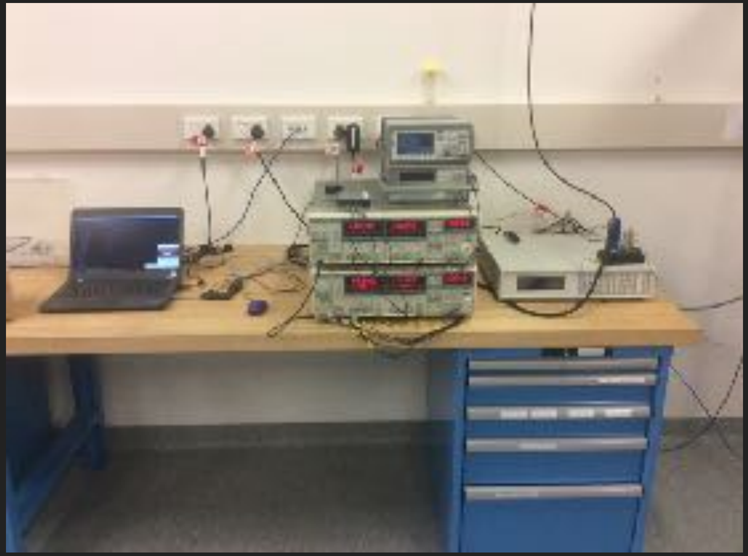

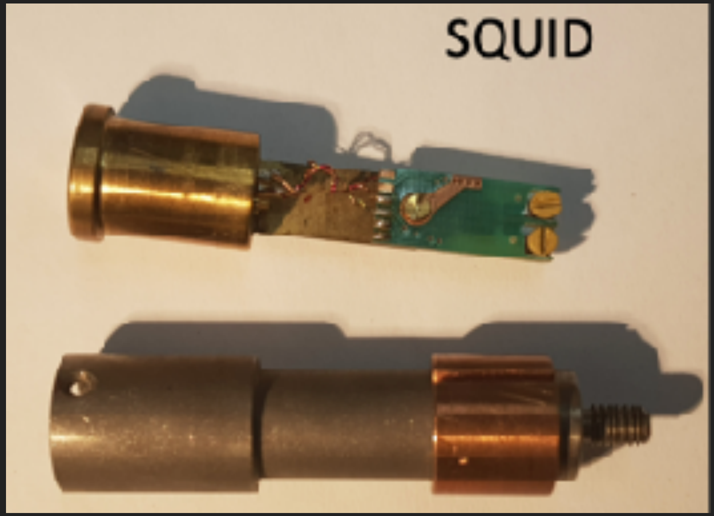

3.4K cryocooler
SQUID electronics

digital downconversion

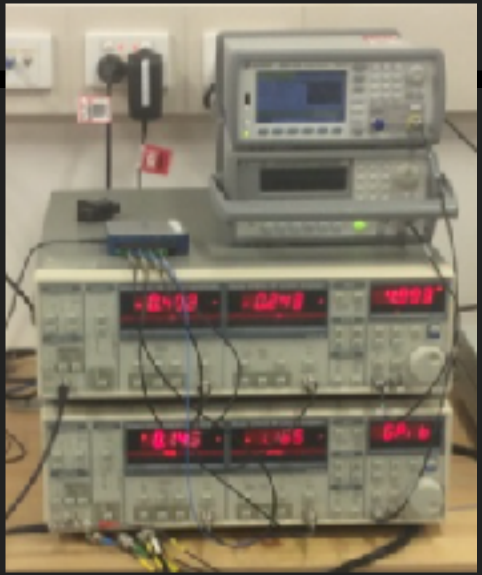

Two standalone lockin amplifiers
Two Signal generators
Locked to an H-maser
Temperature controller
SQUID control
Python data logging

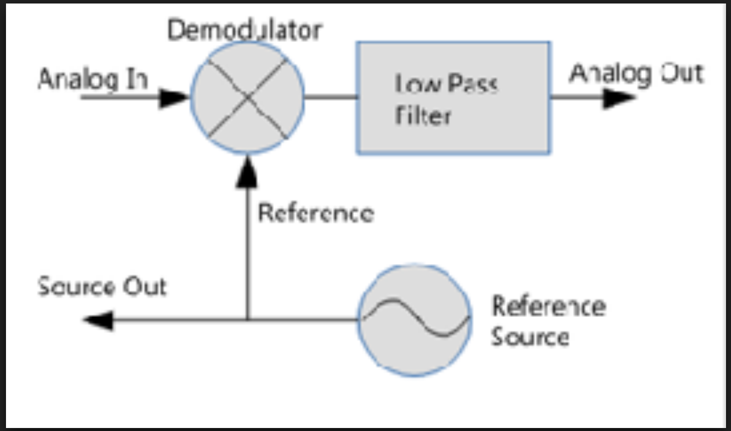

Recent Experiment ?153 days of observation

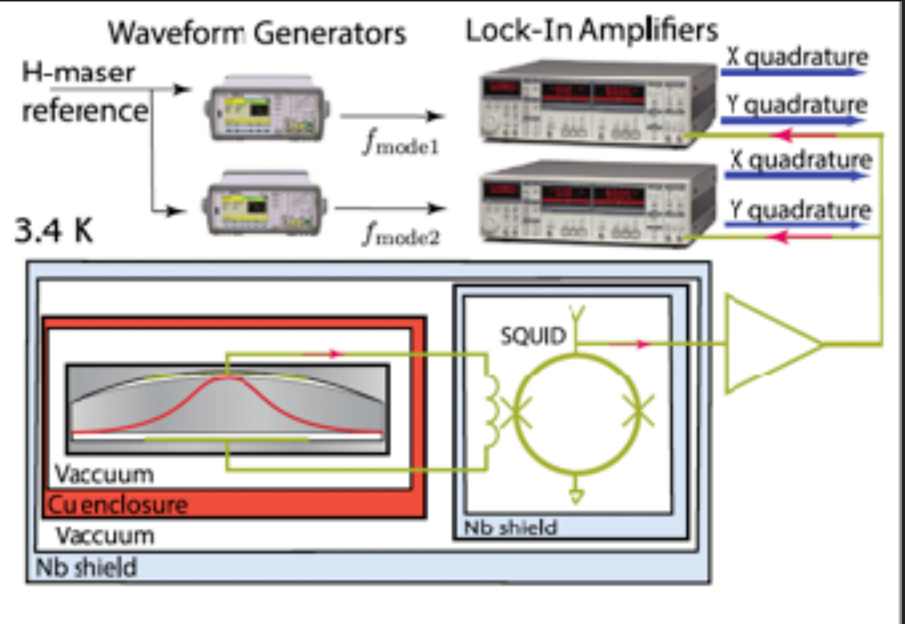

FIG. 1. Experimental setup showing BAW cavity connected to SQUID amplifier and shielding arrangement. Note that 4 and 50 K shields as well as stainless still vacuum chamber not shown.

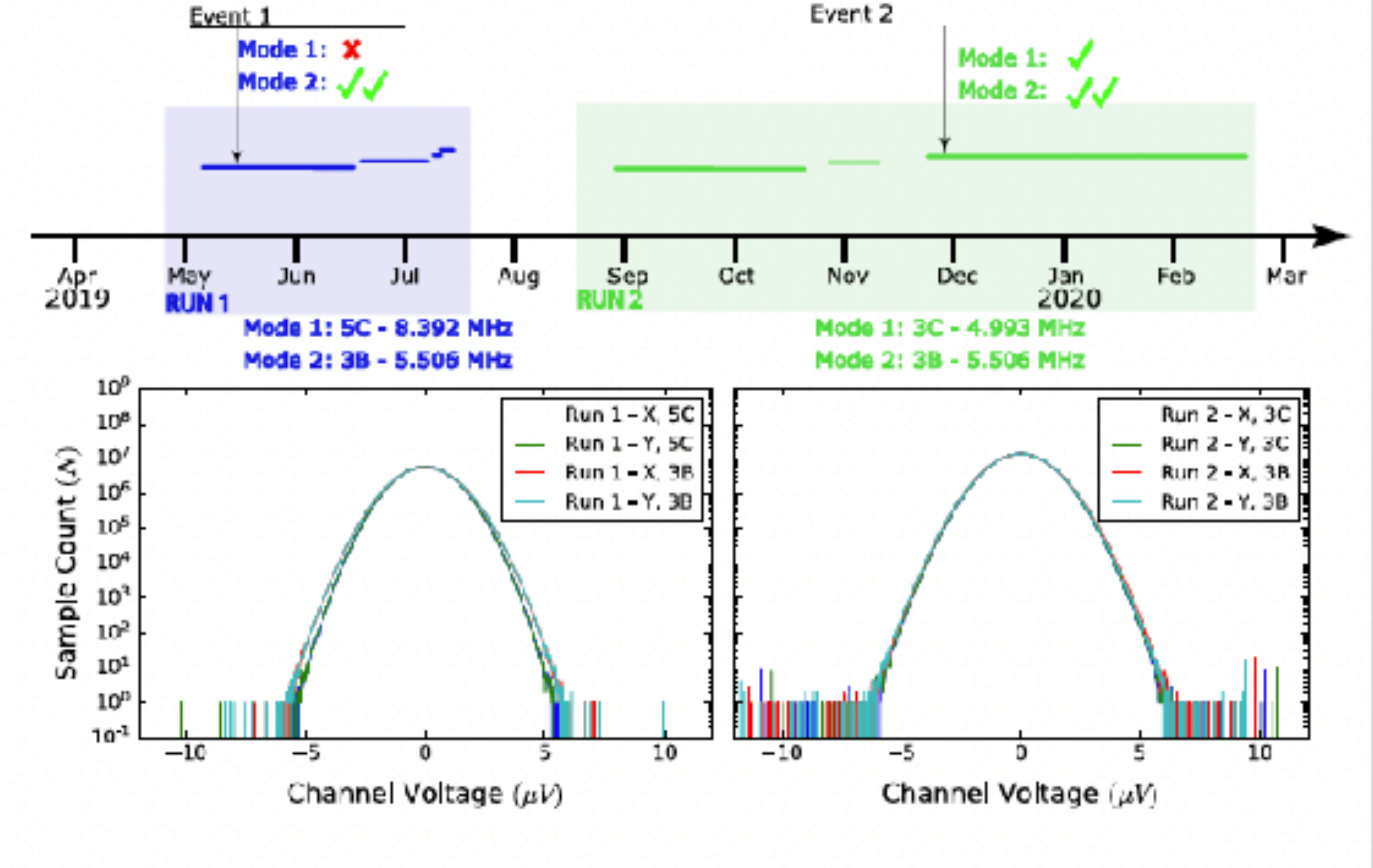

FIG. 2. Timeline of described experiment as well as histogram of total data collection at the detector output. Blue and green lines on timeline show separate data acquisition periods for two runs. Arrows point to the dates of two observed events.

Quantum Technologies and Dark Matter Research Lab

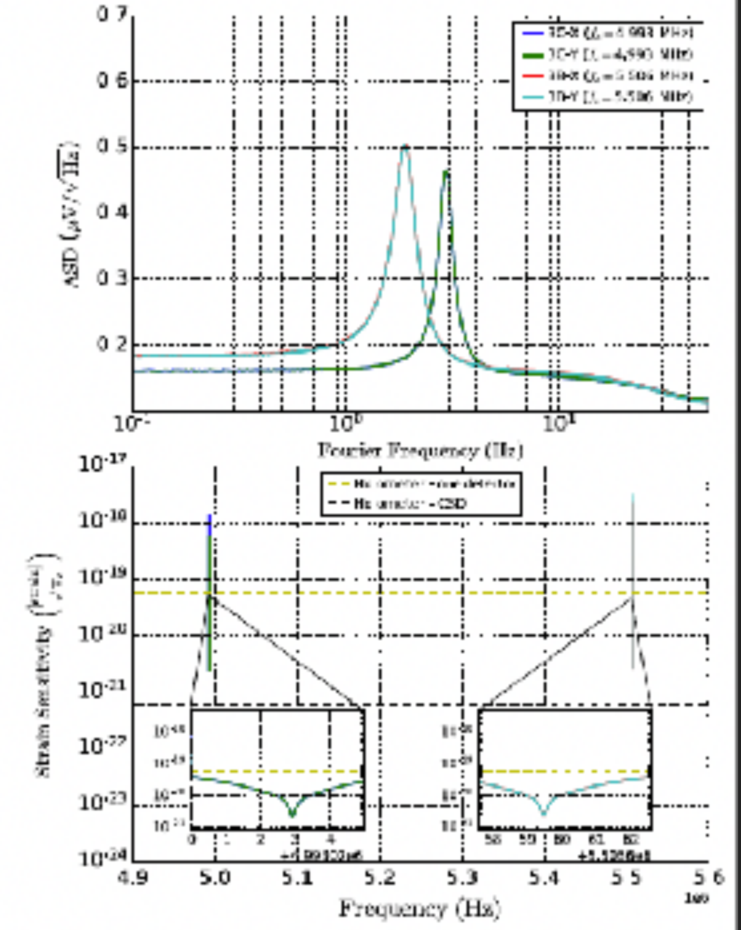

FIG. 3. Top figure displays averaged amplitude spectral density (ASD) of each output channel of lock-ins for longest continuous data taking run; here, each mode has been demodulated from the carrier. Bottom figure shows corresponding spectral strain sensitivity determined for each trace, as well as current best sensitivity in region given by Holometer experiment [6], which uses the cross spectral density (CSD) of two identical interferometers to search for HFGWs.

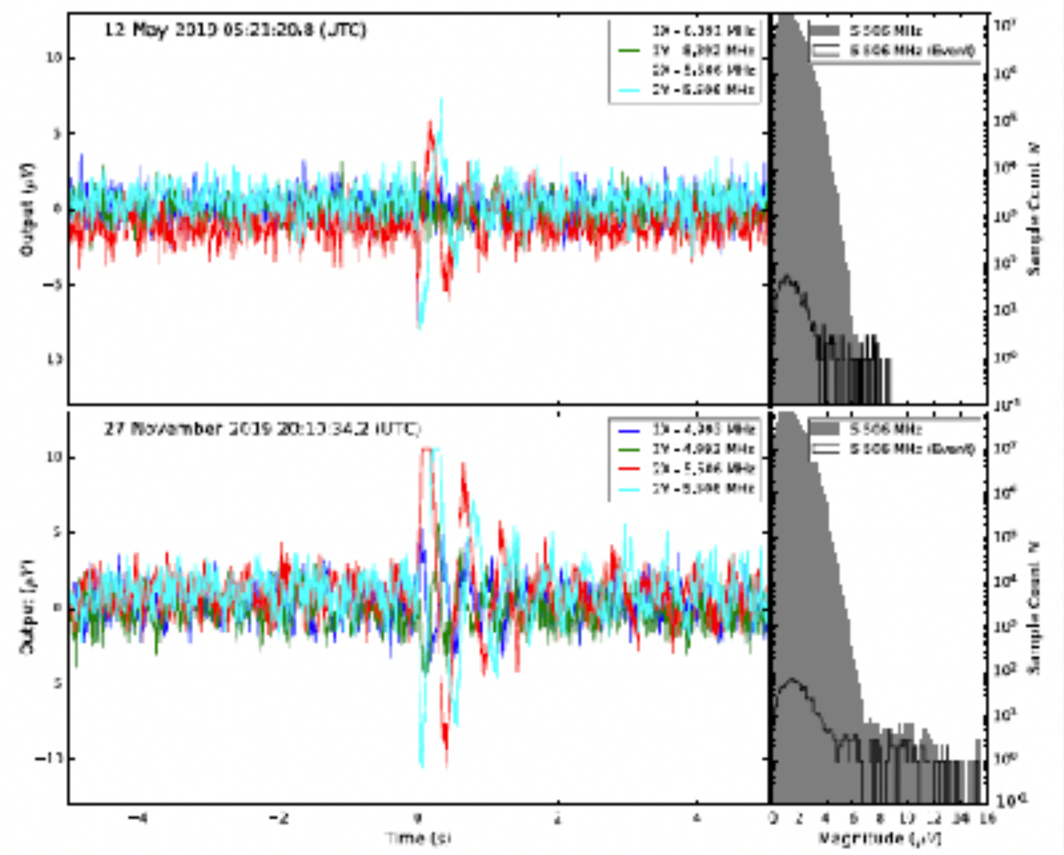

FIG. 4. Time series traces for two event signals detected by system. Each plot shows two quadratures for each mode. Also shown are histograms of output magnitude samples from only the 3B mode from both the entire corresponding run (gray) and just 10 s of data around the event (black). It is clear from this plot that the overwhelming majority of non-Gaussian outliers is due to these signals.

$$H(i\omega) = \frac{\kappa_\lambda^2 \omega_\lambda^2 Z_{\mathrm{SQUID}}^2(-\omega^2/2)h_0\xi}{(i\omega)^2 + \tau_\lambda^{-1} i\omega + \omega_\lambda^2}$$

EQUS
Australian Research Council
Centre of Excellence for
Engineered Quantum Systems

ARC CENTRE OF EXCELLENCE FOR
DARK MATTER

Introducing: the Multimode Acoustic Gravitational wave Experiment (MAGE)

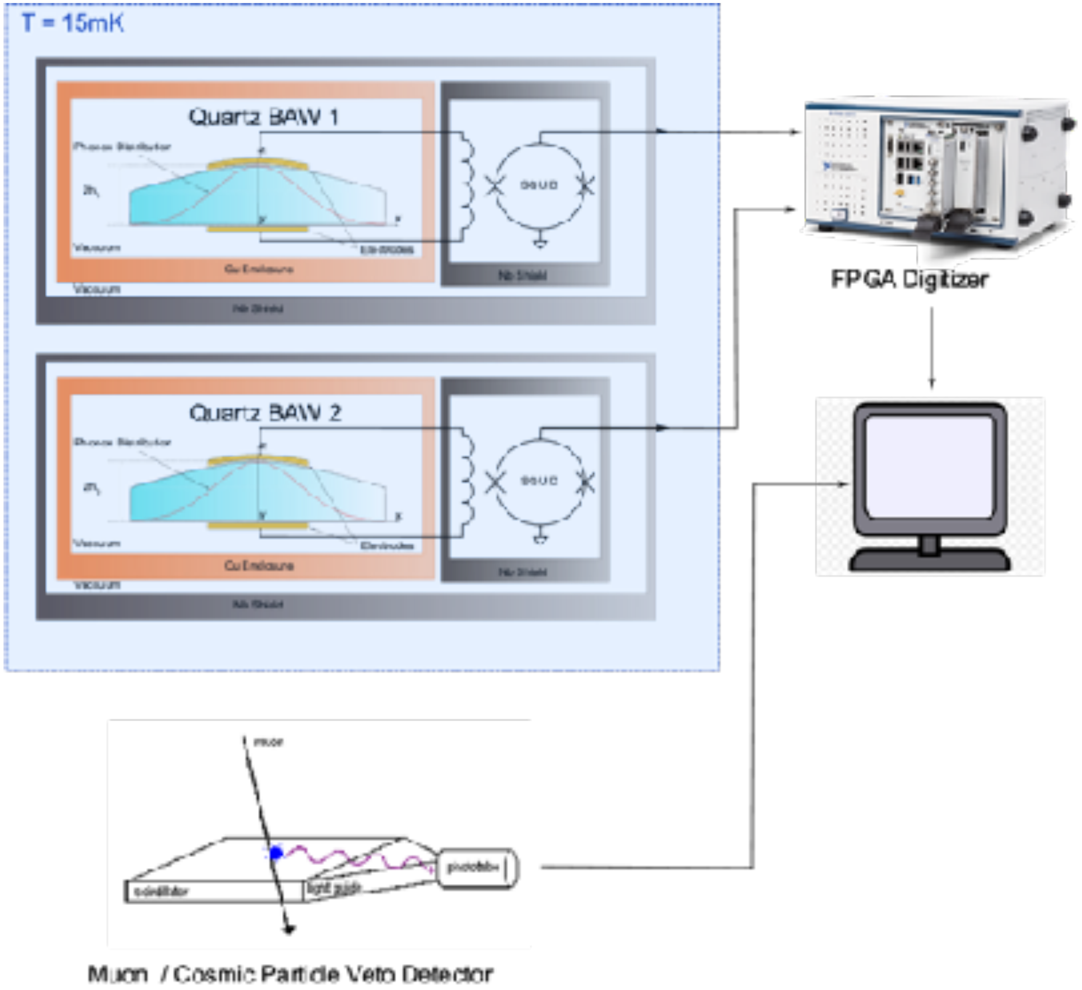

- **MAGE main goals / features:**
- Two identical quartz BAW detectors, maybe more? (funding application)
- Multi-mode Multi-Detector monitoring with FPGA DAQ
- High number of modes 8-10 modes (5-15 MHz range) per crystal
- Wider bandwidth SQUID; 5 – 200 MHz +
- Cosmic particle veto system. Potentially cryogenic ?
- Sub-Kelvin operation -> quantum limited, higher Qs, Quantum Metrology
- Larger mass quartz resonators? Optimize size and mode for sensitivity?

- Current status, waiting for second FPGA DAQ
- Collected one week of data monitoring 8 modes for BAW 1

I have no reason to doubt that Tobar et al can reach their specified experimental precision and accuracy (as mentioned above, they are excellent experimentalists), I have every reason to doubt they will find anything interesting once they reach that sensitivity.

While the investigators have an impressive track record building cavities for precision measurement experiments, two of the three aims (related to high-frequency gravitational waves) are ill-conceived.

The two papers referenced here argue that the entire program of high-frequency gravitational-wave detection does not make sense in light of modern cosmology. Without a compelling answer to this critique, it is difficult to justify supporting experiments to detect megahertz-gigahertz gravitational waves

There are compelling reasons to believe that high-frequency gravitational-wave sources do not exist at the amplitudes probed by the experiments in this Project. Thus, the broader astrophysics community is likely to attribute subsequent detection claims to systematics (issues with the instrument). Even upper limits on high-frequency gravitational waves are likely to be considered uninteresting since we already have much stronger limits from cosmology.

The optomechanical measurement of quantum gravity (Aim 3) is feasible in the sense that the experiment is likely to yield a physically interesting result.

Searching for Axions at UWA

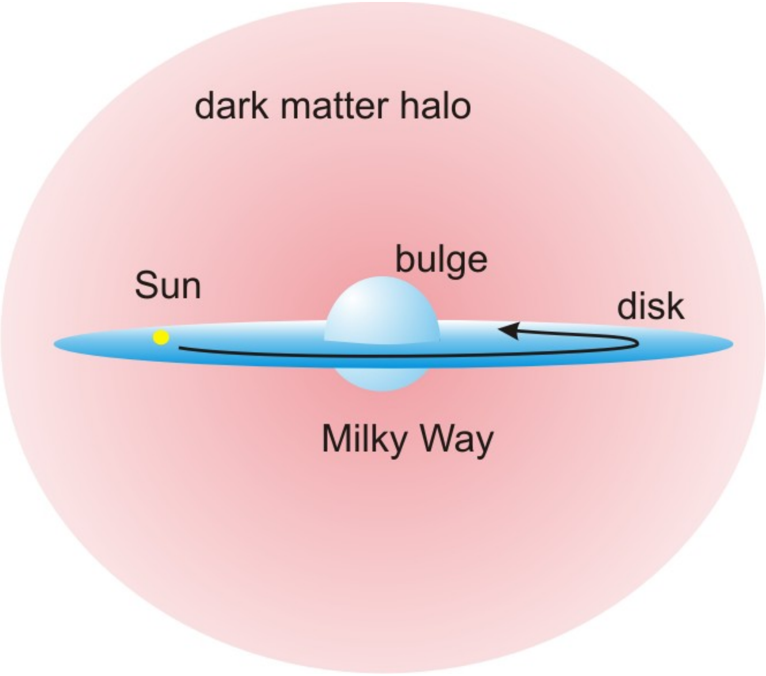

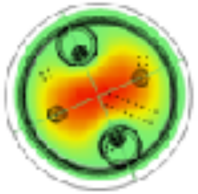

Measure

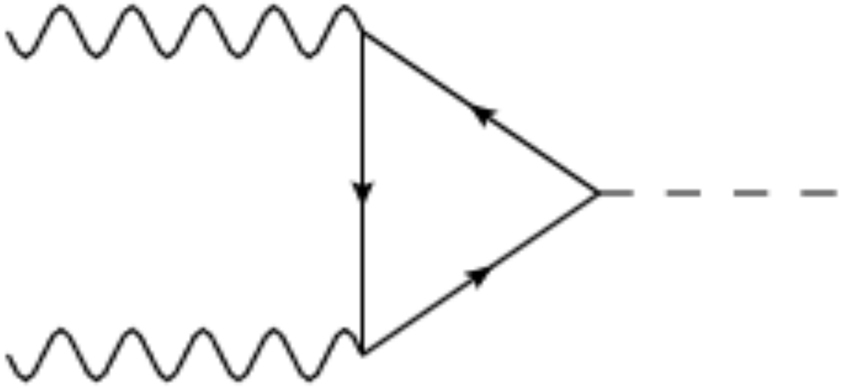

$$c^2 Mass_{axion} = hf_{photon}$$

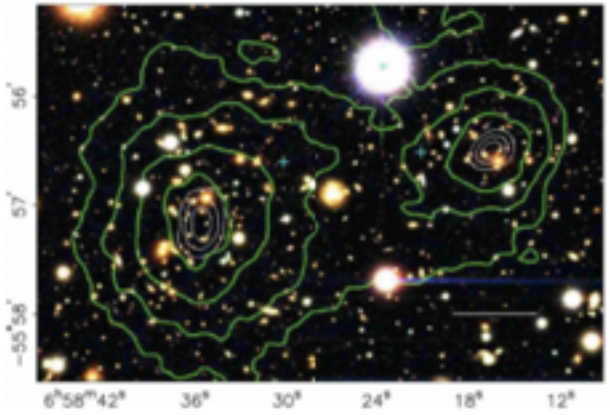

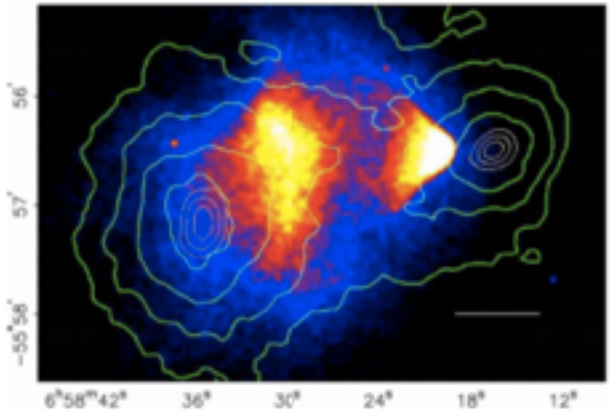

WAVE LIKE DARK MATTER PROGRAM @ UWA

(1) Axion Dark Matter eXperiment (**ADMX**) Project run by Fermilab, run out of Seattle at Washington University. UWA Officially a group member since 2019. PI Gray Rybka

(2) **Oscillating Resonant Group AxioN experiment (ORGAN).** The first Axion experiment at UWA, currently testing Axion Cogenesis.

(3) AC Halloscope with Low Noise Oscillators (UPconversion Low-noise Oscillator Axion Detector (**UPLOAD**) (New Helical Mode Resonator) UWA

(4)Low mass detectors for axions with LCR Circuits, **ADMX-SLIC** (Superconducting Lc-circuit Investigating Cold axions) UF (Sikivie and Tanner) and Broadband Electrical Action Sensing Technique (**BEAST**) UWA

(5)Searches for axions through coupling with electron spins, on hold until axion detected; **Magnon-Cavity** UWA

(6) **Light Scalar Dark Matter** (Dilaton) Clock Comparisons, Acoustic/EM Detectors UWA

Axion Haloscope Dark Matter Experiments at UWA

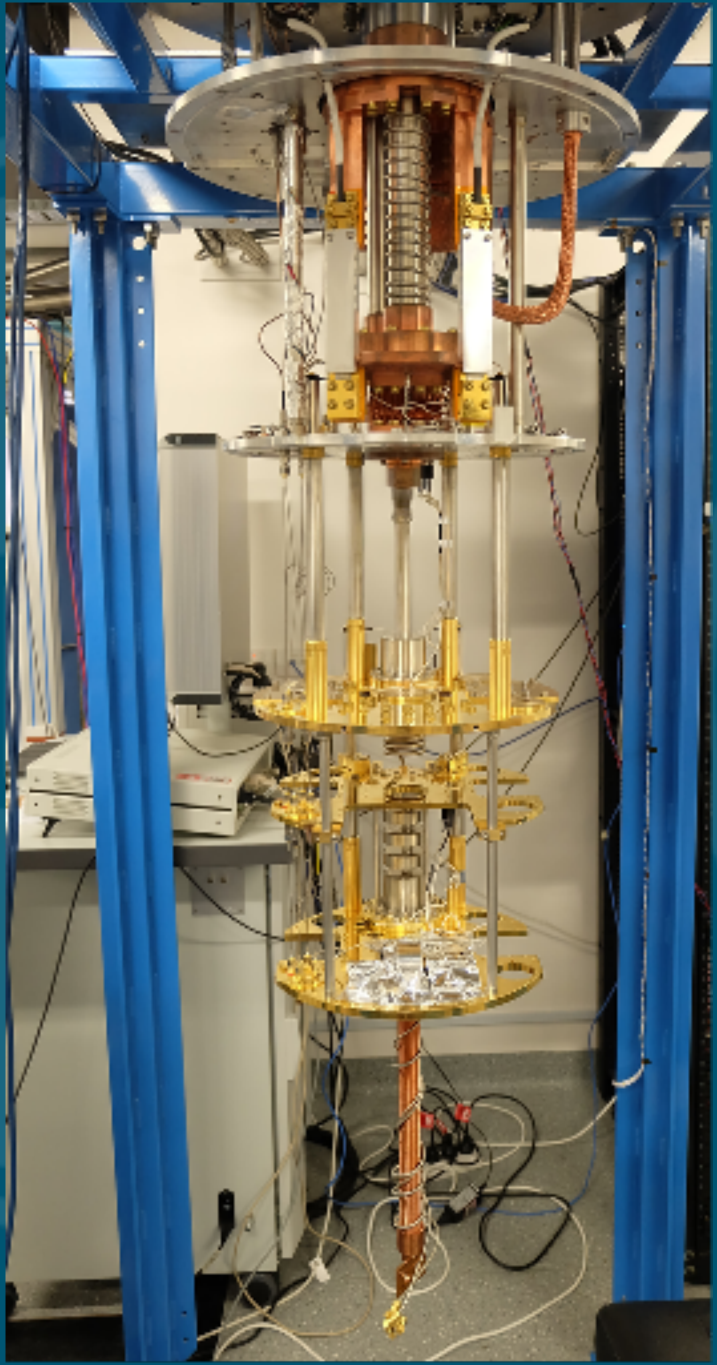

3 Dilution Fridges

14T, 7T and 3T Magnets

Network Analysers and components from rf to 100 GHz

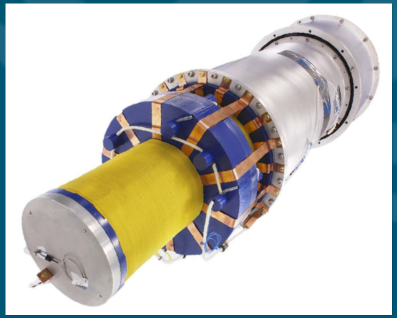

Currently in the Lab: The World’s Lowest Noise Oscillators?

Cryogenic Sapphire Oscillators (CSO) 1989-Now

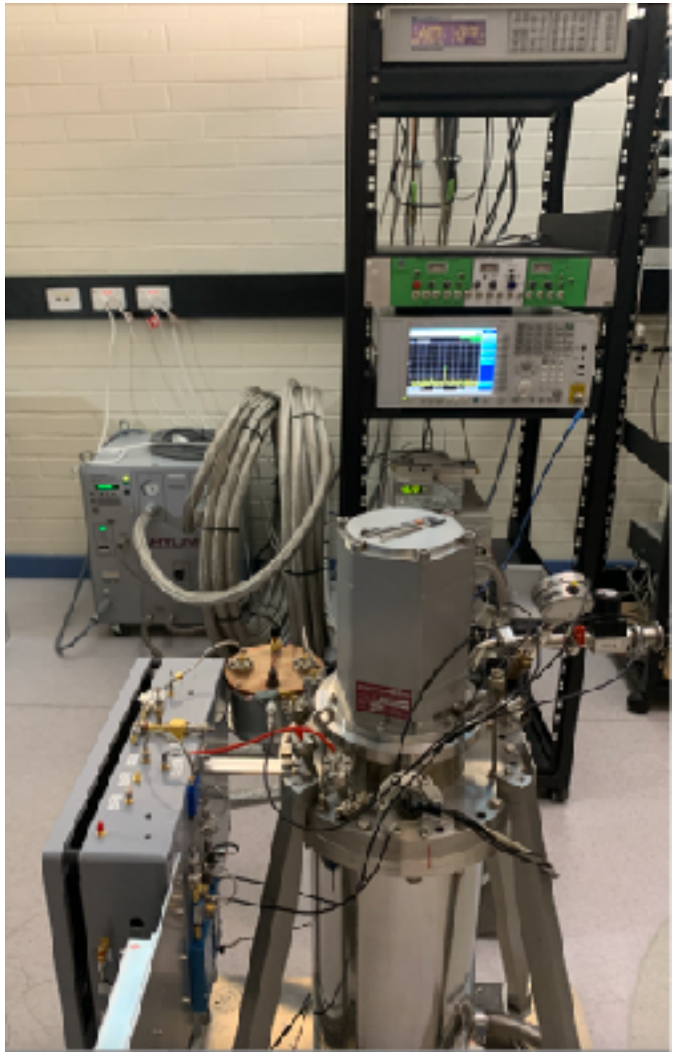

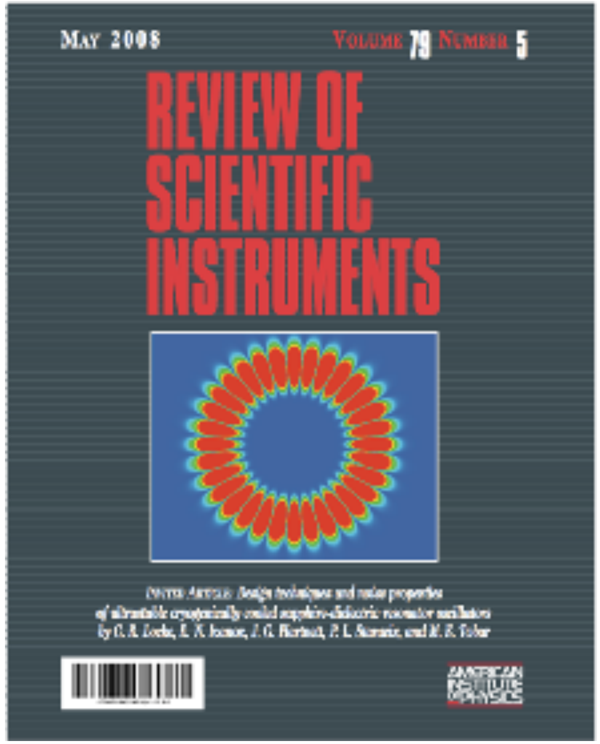

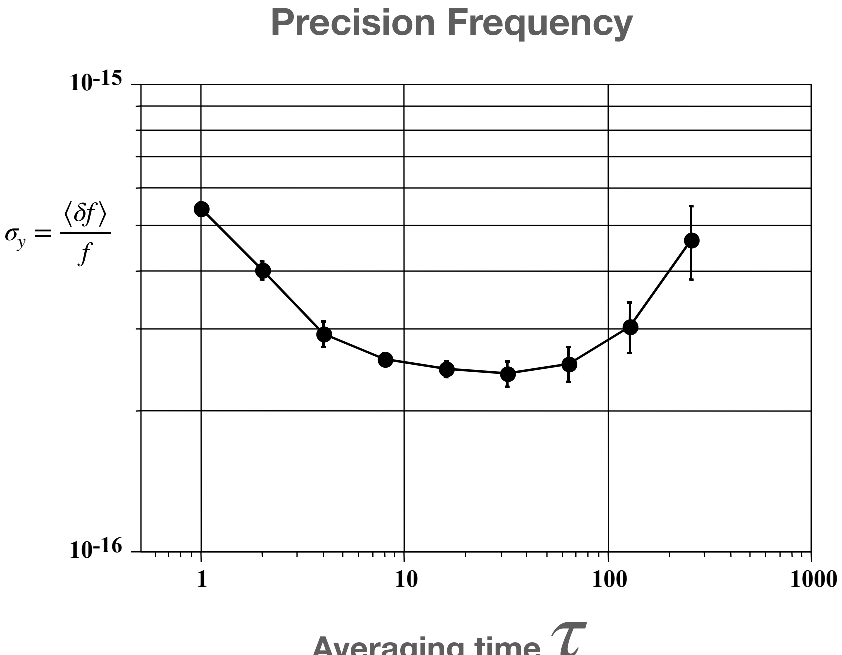

arXiv > hep-ph > arXiv:2208.01640

Search...

Help | Advanced

High Energy Physics – Phenomenology

[Submitted on 1 Aug 2022 (v1), last revised 5 Aug 2022 (this version, v2)]

Twisted Anyon Cavity Resonators with Bulk Modes of Chiral Symmetry and Sensitivity to Ultra-Light Axion Dark Matter

J. F. Bourhill, E. C. I. Paterson, M. Goryachev, M. E. Tobar

In this work, we invent the Anyon Cavity Resonator. The resonator is based on twisted hollow structures, which allow select resonant modes to exhibit non-zero helicity. Depending on the cross-section of the cavity, the modes have more general symmetry than what has been studied before. For example, with no twist, the mode is the form of a boson, while with a 180° twist the symmetry is in the form of a fermion. We show that the generally twisted resonator is in the form of an anyon. The non-zero helicity couples the mode to axions, and we show in the upconversion limit the mode couples to ultra-light axions within the bandwidth of the resonator. The coupling adds amplitude modulated sidebands and allows a simple sensitive way to search for ultra-light axions using only a single mode within the resonator's bandwidth.

Cavity Modes with non-zero Helicity: Couple to Ultra-Light Axions

$$\mathscr{H}_p = \frac{2\,\mathrm{Im}[\int \mathbf{B}_p(\vec{r}) \cdot \mathbf{E}_p^*(\vec{r})\; d\tau]}{\sqrt{\int \mathbf{E}_p(\vec{r}) \cdot \mathbf{E}_p^*(\vec{r})\; d\tau \int \mathbf{B}_p(\vec{r}) \cdot \mathbf{B}_p^*(\vec{r})\; d\tau}},$$

Comparing Instrument Spectral Sensitivity of Dissimilar Electromagnetic Haloscopes to Axion Dark Matter and High Frequency Gravitational Waves

GWs: Spectral Sensitivity

Searching for Low-Mass Axions using Upconversion

Catriona A. Thomson,* Maxim Goryachev, Ben T. McAllister, Eugene N. Ivanov, and Michael E. Tobar†

ARC Centre of Excellence for Engineered Quantum Systems and ARC Centre of Excellence for Dark Matter Particle Physics, Department of Physics, University of Western Australia, 35 Stirling Highway, Crawley, WA 6009, Australia.

(Dated: July 29, 2022)

UPLOAD
New Results: Power and Frequency

SCIENCE ADVANCES | RESEARCH ARTICLE

PHYSICS

Direct search for dark matter axions excluding ALP cogenesis in the 63- to 67-μeV range with the ORGAN experiment

Aaron Quiskamp[1]*, Ben T. McAllister[1,2]*, Paul Altin[3], Eugene N. Ivanov[1], Maxim Goryachev[1], Michael E. Tobar[1]*

ORGAN

PHYSICAL REVIEW D 105, 045009 (2022)

Poynting vector controversy in axion modified electrodynamics

Michael E. Tobar,* Ben T. McAllister, and Maxim Goryachev
ARC Centre of Excellence for Engineered Quantum Systems and ARC Centre of Excellence for Dark Matter Particle Physics, Department of Physics, University of Western Australia, 35 Stirling Highway, Crawley, Western Australia 6009, Australia

(Received 9 September 2021; accepted 28 January 2022; published 15 February 2022)

Resonant Haloscopes: Calculate Systematic way to Calculate Sensitivity
Observable is Power: Real Part of Complex Poynting Theorem: Impedance Match

Reactive Haloscope: Broadband Observable Current/Flux or Voltage: Reactive Part of Poynting Theorem: Impedance Mismatch

Sensitivity of Low-Mass Reactive and Resonant Axion Haloscopes

$$c^2 Mass_{axion} = hf_{photon}$$

Low-Mass: Quasi-Static Regime -> Purely Classical

$$c^2 Mass_{axion} = hf_{photon}??????$$

Physics of the Dark Universe 26 (2019) 100339
Contents lists available at ScienceDirect
Physics of the Dark Universe
journal homepage: www.elsevier.com/locate/dark
ELSEVIER

Modified axion electrodynamics as impressed electromagnetic sources through oscillating background polarization and magnetization

Michael E. Tobar*, Ben T. McAllister, Maxim Goryachev
ARC Centre of Excellence For Engineered Quantum Systems, Department of Physics, School of Physics, Mathematics and Computing, University of Western Australia, 35 Stirling Highway, Crawley WA 6009, Australia

Physics of the Dark Universe 30 (2020) 100624
Contents lists available at ScienceDirect
Physics of the Dark Universe
journal homepage: www.elsevier.com/locate/dark
ELSEVIER

Broadband electrical action sensing techniques with conducting wires for low-mass dark matter axion detection

Michael E. Tobar*, Ben T. McAllister, Maxim Goryachev
ARC Centre of Excellence For Engineered Quantum Systems, Department of Physics, University of Western Australia, 35 Stirling Highway, Crawley WA 6009, Australia

DC Magnetic Haloscopes

Low Mass: Lumped Element Reactive	300 MHz	Middle Mass: Resonant Cavity Reactive and Dissipative	30 GHz	High Mass: Propagating	$\frac{\omega_a}{2\pi}$ Hz
$\lambda_a > d_{exp}$	1.25×10^{-6}	$\lambda_a \sim d_{exp}$	1.25×10^{-4}	$\lambda_a < d_{exp}$	m_a eV

ADMX SLIC
RE-ENTRANT CAVITY
ABRACADABRA
SHAFT
DM RADIO

ADMX
CULTASK
ORGAN
QUAX
RADES

MADMAX
BREAD

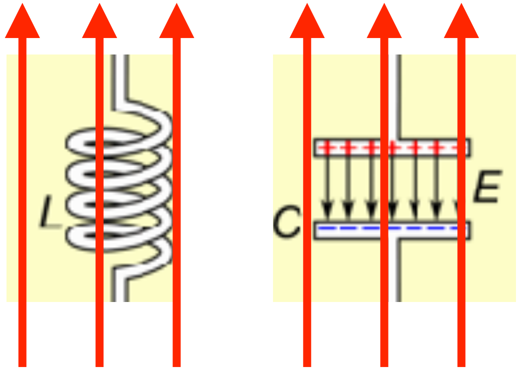

$\overrightarrow{B} = B_{DC}\hat{z}$

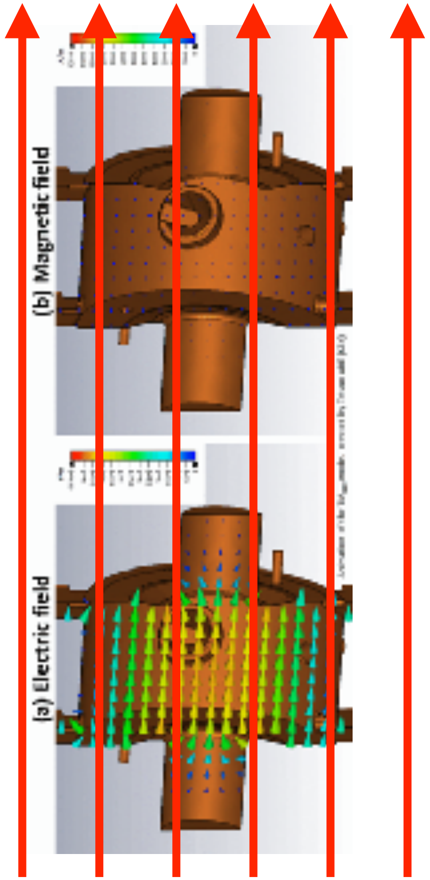

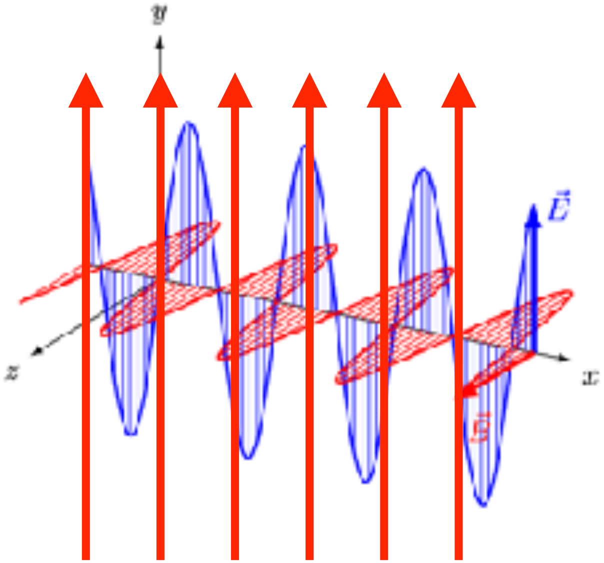

Resonator Measurement: Impedance match; set coupling =1; Take Photons from Source

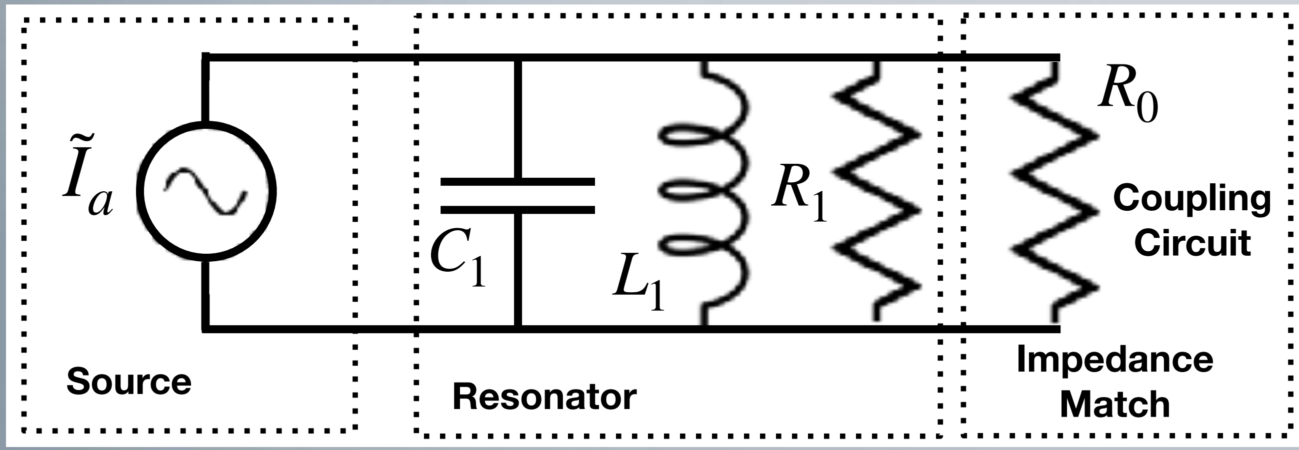

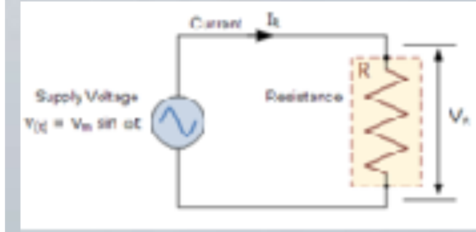

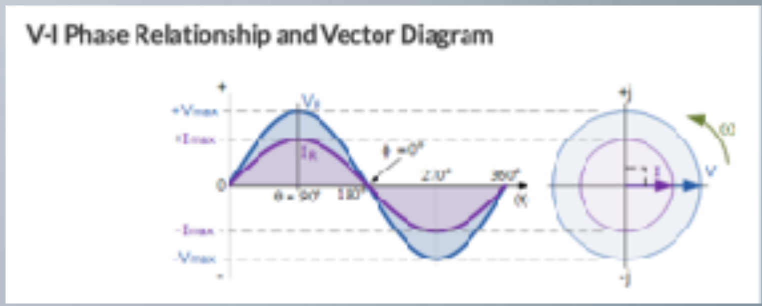

Real Power Measurement, Absorbs Energy: $P_a = I_0^2 R_o = \frac{V_0^2}{R_0}$

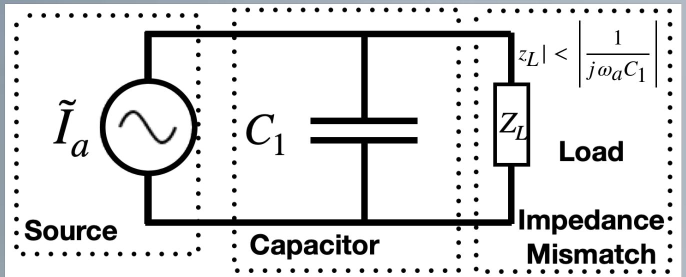

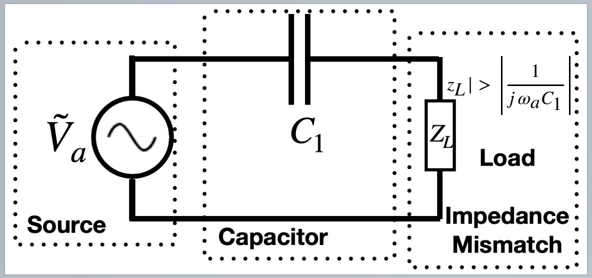

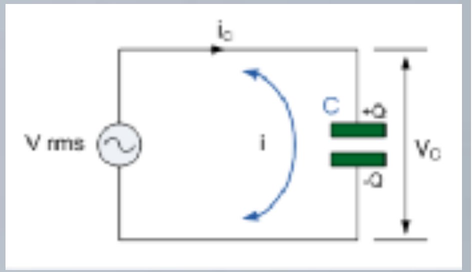

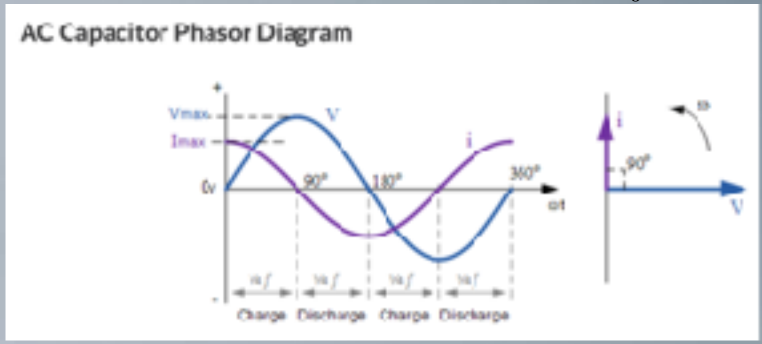

Reactive Power Measurement, Does Not Absorb Energy:

Left eg. Inductive couple SQUID Amplifier (Current of Mag Flux)

Right eg. Capacitive coupled High Impedance Amplifier (Voltage)

Energy oscillates between Source and Capacitor
Do not destroy photons

Reactive power does not propagate or dissipate out of the volume of the detector (ie. no loss): Oscillates in and out of volume

Does not need to be the order of the Compton wavelength in size (sub wavelength phenomena)

Do Not Alter Equations of Motion

REMEMBERING POYNTING THEOREM

- Basic conservation law for electromagnetic energy for AC system
- Describes complex power flow (phasors) in a volume, considering: 1) Sources, 2) Storage, 3) Dissipation, 4) Radiation
- The direction and density of power flow at a point is defined by the instantaneous Poynting vector, $\vec{S}(t)$[W/m²]

Instantaneous Poynting vector in vacuum

$$\vec{S}_1(t) = \frac{1}{\mu_0}\vec{E}_1(t) \times \vec{B}_1(t) = \frac{1}{2}\left(\mathbf{E}_1 e^{-j\omega_1 t} + \mathbf{E}_1^* e^{j\omega_1 t}\right) \times \frac{1}{2\mu_0}\left(\mathbf{B}_1 e^{-j\omega_1 t} + \mathbf{B}_1^* e^{j\omega_1 t}\right)$$

$$= \frac{1}{2\mu_0}\operatorname{Re}\left(\mathbf{E}_1 \times \mathbf{B}_1^*\right) + \frac{1}{2\mu_0}\operatorname{Re}\left(\mathbf{E}_1 \times \mathbf{B}_1 \; e^{-j2\omega_1 t}\right),$$

$$\langle \vec{S}_1 \rangle = \frac{1}{T}\int_0^T \vec{S}_1(t)dt = \frac{1}{T}\int_0^T \left[\frac{1}{2\mu_0}\operatorname{Re}\left(\mathbf{E}_1 \times \mathbf{B}_1^*\right) + \frac{1}{2\mu_0}\operatorname{Re}\left(\mathbf{E}_1 \times \mathbf{B}_1 e^{-2j\omega t}\right)\right] dt = \frac{1}{2\mu_0}\operatorname{Re}\left(\mathbf{E}_1 \times \mathbf{B}_1^*\right)$$

Complex Poynting vector in vacuum

- The corresponding phasor form of the Poynting vector

$$\mathbf{S}_1 = \frac{1}{2\mu_0}\mathbf{E}_1 \times \mathbf{B}_1^* \quad \text{and} \quad \mathbf{S}_1^* = \frac{1}{2\mu_0}\mathbf{E}_1^* \times \mathbf{B}_1,$$

$$\operatorname{Re}\left(\mathbf{S}_1\right) = \frac{1}{2}(\mathbf{S}_1 + \mathbf{S}_1^*) \quad \text{and} \quad j\operatorname{Im}\left(\mathbf{S}_1\right) = \frac{1}{2}(\mathbf{S}_1 - \mathbf{S}_1^*).$$

Time Average Power

Reactive Power

Combing the Poynting vector with Maxwell's Equations -> Leads to Poynting Theorem

1) Instantaneous Poynting Theorem
2) Complex Poynting Theorem

- IN THE TIME DOMAIN THE POYNTING VECTOR, $\vec{S}_1(t)$, REPRESENTS THE INSTANTANEOUS POWER FLOW DUE TO INSTANTANEOUS ELECTRIC AND MAGNETIC FIELDS:

- MORE COMMONLY, PROBLEMS IN ELECTROMAGNETICS ARE SOLVED IN TERMS OF SINUSOIDALLY VARYING FIELDS AT A SPECIFIED FREQUENCY

- IN THE CASE NATURAL TO USE COMPLEX POYNTING THEOREM, $\mathbf{S}_1 = \frac{1}{2\mu_0}\mathbf{E}_1 \times \mathbf{B}_1^*$ and $\mathbf{S}_1^* = \frac{1}{2\mu_0}\mathbf{E}_1^* \times \mathbf{B}_1,$ WHICH ENABLES ONE TO DISTINGUISH BETWEEN REAL POWER FLOW (WATTS) $\mathrm{Re}\left(\mathbf{S}_1\right) = \frac{1}{2}(\mathbf{S}_1 + \mathbf{S}_1^*)$ AND REACTIVE POWER FLOW (VARS)

$$j\,\mathrm{Im}\left(\mathbf{S}_1\right) = \frac{1}{2}(\mathbf{S}_1 - \mathbf{S}_1^*).$$

- STANDARD TECHNIQUE TO ANALYSE ENERGY AND POWER FLOW IN ACTIVE CIRCUITS AND ANTENNA SYSTEMS: APPLY TO AXION ELECTRODYNAMICS

COMPLEX POYNTING THEOREM: CIRCUITS/ANTENNAS

ADVANCED ENGINEERING

ELECTROMAGNETICS

Here Balanis uses $\vec{M}$ as magnetic current

Constantine A. Balanis

Combine complex Poynting vector with complex Maxwell's Equations

Even though magnetic sources do not exist, they can be engineered

Model of Current and Voltage Source

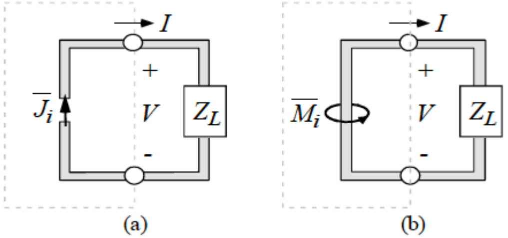

Figure 1.5 Electromagnetic representation of independent circuit sources. (a) Current generator (impressed electric current filament); (b) Voltage generator (impressed magnetic current loop).

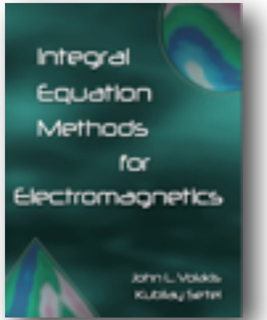

Lectures on
Electromagnetic Field Theory

WENG CHO CHEW

FALL 2020, PURDUE UNIVERSITY

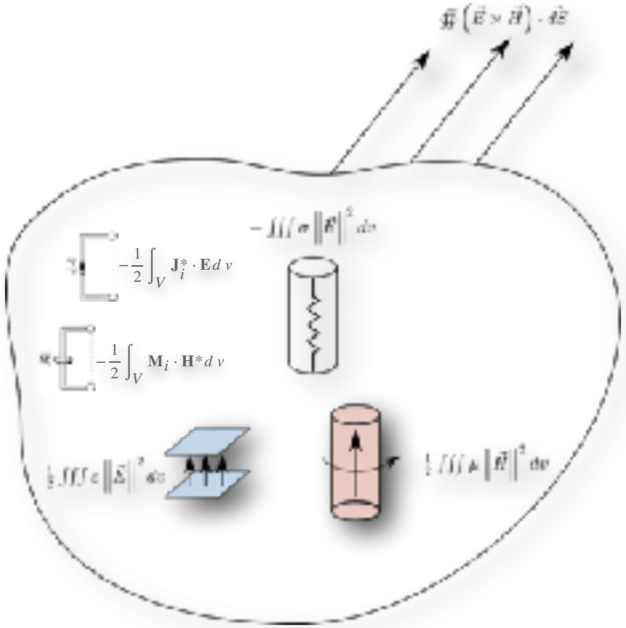

$$-\iiint_V \nabla\cdot(\tfrac{1}{2}\mathbf{E}\times\mathbf{H}^*)\,dv = -\oint_S(\tfrac{1}{2}\mathbf{E}\times\mathbf{H}^*)\cdot d\mathbf{s}$$

$$= \frac{1}{2}\iiint_V(\mathbf{H}^*\cdot\mathbf{M}_i + \mathbf{E}\cdot\mathbf{J}_i^*)\,dv$$

$$+\frac{1}{2}\iiint_V \sigma|\mathbf{E}|^2\,dv + j2\omega\iiint_V(\tfrac{1}{4}\mu|\mathbf{H}|^2 - \tfrac{1}{4}\varepsilon|\mathbf{E}|^2)\,dv$$

or

$$\frac{1}{2}\iiint_V(\mathbf{H}^*\cdot\mathbf{M}_i + \mathbf{E}\cdot\mathbf{J}_i^*)\,dv = \oint_S(\tfrac{1}{2}\mathbf{E}\times\mathbf{H}^*)\cdot d\mathbf{s} + \frac{1}{2}\iiint_V\sigma|\mathbf{E}|^2\,dv$$

$$+j2\omega\iiint_V(\tfrac{1}{4}\mu|\mathbf{H}|^2 - \tfrac{1}{4}\varepsilon|\mathbf{E}|^2)\,dv \qquad (1\text{-}76)$$

which can be written as

$$P_s = P_e + P_d + j2\omega(\overline{W}_m - \overline{W}_e) \qquad (1\text{-}76a)$$

where

$$P_s = -\frac{1}{2}\iiint_V(\mathbf{H}^*\cdot\mathbf{M}_i + \mathbf{E}\cdot\mathbf{J}_i^*)\,dv = \text{supplied complex power (W)} \qquad (1\text{-}76b)$$

$$P_e = \oint_S\left(\frac{1}{2}\mathbf{E}\times\mathbf{H}^*\right)\cdot d\mathbf{s} = \text{exiting complex power (W)} \qquad (1\text{-}76c)$$

$$P_d = \frac{1}{2}\iiint_V\sigma|\mathbf{E}|^2\,dv = \text{dissipated real power (W)} \qquad (1\text{-}76d)$$

$$\overline{W}_m = \iiint_V\tfrac{1}{4}\mu|\mathbf{H}|^2\,dv = \text{time-average magnetic energy (J)} \qquad (1\text{-}76e)$$

$$\overline{W}_e = \iiint_V\tfrac{1}{4}\varepsilon|\mathbf{E}|^2\,dv = \text{time-average electric energy (J)} \qquad (1\text{-}76f)$$

AXION ELECTRODYNAMICS IN HARMONIC PHASOR FORM DC BACKGROUND FIELD

Cavity Electric Field

$$\vec{E}_1(\vec{r},t) = \frac{1}{2}\left(\mathbf{E}_1(\vec{r})e^{-j\omega_1 t} + \mathbf{E}_1^*(\vec{r})e^{j\omega_1 t}\right) = \mathrm{Re}\left[\mathbf{E}_1(\mathbf{r})e^{-j\omega_1 t}\right]$$

Axion Scalar Field

$$a(t) = \frac{1}{2}\left(\tilde{a}e^{-j\omega_a t} + \tilde{a}^* e^{j\omega_a t}\right) = \mathrm{Re}\left(\tilde{a}e^{-j\omega_a t}\right)$$

Axion Phasor

$$\tilde{A} = \tilde{a}e^{-j\omega_a t} \qquad \tilde{A}^* = \tilde{a}^* e^{j\omega_a t}$$

Ampere's law in time dependent form

$$\frac{1}{\mu_0}\nabla \times \vec{B}_1(\vec{r},t)) = \vec{J}_{e_1} + \partial_t\left(\epsilon_0 \vec{E}_1(\vec{r},t) - g_{a\gamma\gamma}a(\vec{r},t)\epsilon_0 c \vec{B}_0(\vec{r},t)\right)$$

Cavity Electric Field Phasor

$$\tilde{\mathbf{E}}_1(\vec{r},t) = \mathbf{E}_1(\vec{r})e^{-j\omega_1 t} \qquad \tilde{\mathbf{E}}_1^*(\vec{r},t) = \mathbf{E}_1^*(\vec{r})e^{j\omega_1 t}$$

Ampere's law in phasor form

$$\frac{1}{\mu_0}\nabla \times \tilde{\mathbf{B}}_1 = \tilde{\mathbf{J}}_{e1} - j\omega_1\epsilon_0\tilde{\mathbf{E}}_1 + j\omega_a g_{a\gamma\gamma}\epsilon_0 c\tilde{A}\vec{B}_0$$

$$\frac{1}{\mu_0}\nabla \times \tilde{\mathbf{B}}_1^* = \tilde{\mathbf{J}}_{e1}^* + j\omega_1\epsilon_0\tilde{\mathbf{E}}_1^* - j\omega_a g_{a\gamma\gamma}\epsilon_0 c\tilde{A}^*\vec{B}_0,$$

Faraday's law in phasor form (Abraham)

$$\nabla \times \tilde{\mathbf{E}}_1 = j\omega_1\tilde{\mathbf{B}}_1$$

$$\nabla \times \tilde{\mathbf{E}}_1^* = -j\omega_1\tilde{\mathbf{B}}_1^*,$$

COMPLEX POYNTING VECTOR FOR A DC AXION HALOSCOPE

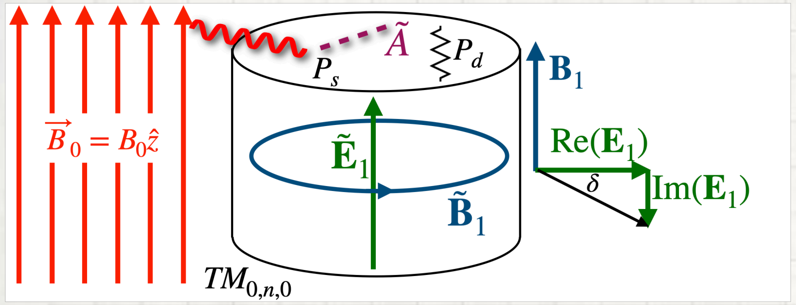

$$\mathrm{Im}(\mathbf{E}_1) = \mathrm{Tan}(\delta)\mathrm{Re}\,(E_1) = \mathrm{Re}\,(E_1)/Q_1$$

$$\mathbf{S}_{EH} = \frac{1}{2\mu_0}\mathbf{E}_1 \times \mathbf{B}_1^* \text{ and } \mathbf{S}_{EH}^* = \frac{1}{2\mu_0}\mathbf{E}_1^* \times \mathbf{B}_1$$

$$\nabla\cdot\mathbf{S} = \frac{1}{2\mu_0}\nabla\cdot(\mathbf{E}_1\times\mathbf{B}_1^*) = \frac{1}{2\mu_0}\mathbf{B}_1^*\cdot(\nabla\times\mathbf{E}_1) - \frac{1}{2\mu_0}\mathbf{E}_1\cdot(\nabla\times\mathbf{B}_1^*)$$

$$\nabla\cdot\mathbf{S}^* = \frac{1}{2\mu_0}\nabla\cdot(\mathbf{E}_1^*\times\mathbf{B}_1) = \frac{1}{2\mu_0}\mathbf{B}_1\cdot(\nabla\times\mathbf{E}_1^*) - \frac{1}{2\mu_0}\mathbf{E}_1^*\cdot(\nabla\times\mathbf{B}_1)$$

Can show

Real part of Poynting Theorem

$$\oint \mathrm{Re}\,(\mathbf{S})\cdot\hat{n}ds = \int\Big(\Big(\frac{j\omega_a}{4}\epsilon_0 g_{a\gamma\gamma}c\vec{B}_0\cdot(\tilde{a}^*\mathbf{E}_1 - \tilde{a}\mathbf{E}_1^*)\Big) - \frac{1}{4}(\mathbf{E}_1\cdot\mathbf{J}_{e1}^* + \mathbf{E}_1^*\cdot\mathbf{J}_{e1})\Big)\,d\tau$$

Can show

Reactive part of Poynting Theorem

$$\oint j\,\mathrm{Im}\,(\mathbf{S})\cdot\hat{n}ds = \int\Big(\Big(\frac{j\omega_1}{2}\Big(\frac{1}{\mu_0}\mathbf{B}_1^*\cdot\mathbf{B}_1 - \epsilon_0\mathbf{E}_1\cdot\mathbf{E}_1^*\Big) + \frac{j\omega_a}{4}\epsilon_0 g_{a\gamma\gamma}c\vec{B}_0\cdot(\tilde{a}^*\mathbf{E}_1 + \tilde{a}\mathbf{E}_1^*) - \frac{1}{4}(\mathbf{E}_1\cdot\mathbf{J}_{e1}^* - \mathbf{E}_1^*\cdot\mathbf{J}_{e1})\Big)\Big)\,d\tau$$

= 0 on resonance

$$\oint\langle\mathbf{S}\rangle\cdot dS = -\frac{1}{4}\int(\mathbf{E}_1\cdot\mathbf{J}_{e1}^* + \mathbf{E}_1^*\cdot\mathbf{J}_{e1})\,d\tau + \frac{j\omega_a\epsilon_0 g_{a\gamma\gamma}}{4}\int c\vec{B}_0\cdot(\tilde{a}^*\mathbf{E}_1 - \tilde{a}\mathbf{E}_1^*)\,d\tau$$

Cavity Power dissipation

Axion power input

= 0 for closed system

$$P_d = \frac{\omega_a\epsilon_0}{2Q}\int\mathbf{E}_1\cdot\mathbf{E}_1^*\,d\tau = \frac{\omega_a U}{Q}$$

$$C_1 = \frac{\left(\int\vec{B}_0\cdot\mathrm{Re}(\mathbf{E}_1)\,dV\right)^2}{B_0^2V_1\int\mathbf{E}_1\cdot\mathbf{E}_1^*\,dV}$$

$$P_1 = \omega_a Q U_1 = g_{a\gamma\gamma}^2\langle a_0\rangle^2\omega_a Q_1\epsilon_0 c^2 B_0^2 V_1 C_1$$
$$= g_{a\gamma\gamma}^2\rho_a Q_1\epsilon_0 c^5 B_0^2 V_1 C_1\frac{1}{\omega_a},$$

known power output for a Sikivie Haloscope

CONSIDERATION OF POYNTING VECTOR IN AXION ELECTRODYNAMICS: THE ABRAHAM-MINKOWSKI CONTROVERSY

* Poynting vector in Electrodynamics -> Over a century of Controversy, chose $\mathbf{S}_{\mathrm{M}} = \frac{1}{\epsilon_0 \mu_0}(\mathbf{D} \times \mathbf{B})$ or $\mathbf{S}_{\mathrm{A}} = (\mathbf{E} \times \mathbf{H})$ in matter ?

* Pfeifer et. al., Momentum of an electromagnetic wave in dielectric media, Reviews of Modern Physics 79(4), 1197-1216 (2007). -> Addresses the Abraham-Minkowski controversy, conclude: both valid depends on system.

* Kinsler et al., Four Poynting theorems, Eur. J. Phys. 30 (2009) 983–993. Enables interpretation of four Poynting vectors and interaction with the medium -> choosing the best Poynting vector depend on the medium and experimental set up.

* DJ Griffiths, Resource Letter EM-1: Electromagnetic Momentum, Am. J. Phys. 80, 7 (2012) -> Abraham–Minkowski controversy regarding the field momentum in polarizable and magnetizable media: Correct one depends on the detailed nature of the material.

VII. MOMENTUM OF PHOTONS

$$\begin{cases} p_{\mathrm{A}} = \dfrac{1}{n}\left(\dfrac{h\nu}{c}\right) & \text{(Abraham)} \\ p_{\mathrm{M}} = n\left(\dfrac{h\nu}{c}\right) & \text{(Minkowski)} \end{cases}$$

$$\mathbf{P}_{\mathrm{total}} = \mathbf{P}_{\mathrm{kinetic}} + \int \mathbf{g}_A \, d^3\mathbf{r} = \mathbf{P}_{\mathrm{canonical}} + \int \mathbf{g}_M \, d^3\mathbf{r}.$$

$$\Delta\theta' = \begin{cases} n\,\Delta\theta & \text{(Abraham)} \\ \dfrac{1}{n}\,\Delta\theta & \text{(Minkowski)} \end{cases}$$

Size of the central maximum in single-slit diffraction

Measured by Jones et al, when media does not move

Low-Mass Axions -> Macroscopic Description similar to a Macroscopic Description of an Electricity Generator

GENERATING ELECTRICITY FROM DARK MATTER

[2] arXiv:2109.04056 [pdf, other]

Abraham and Minkowski Poynting vector controversy in axion modified electrodynamics

Michael E Tobar, Ben T McAllister, Maxim Goryachev

Comments: Typos fixed, more references added

Subjects: High Energy Physics - Phenomenology (hep-ph); Instrumentation and Methods for Astrophysics (astro-ph.IM); General Relativity and Quantum Cosmology

Microscopic Quantum Phenomena

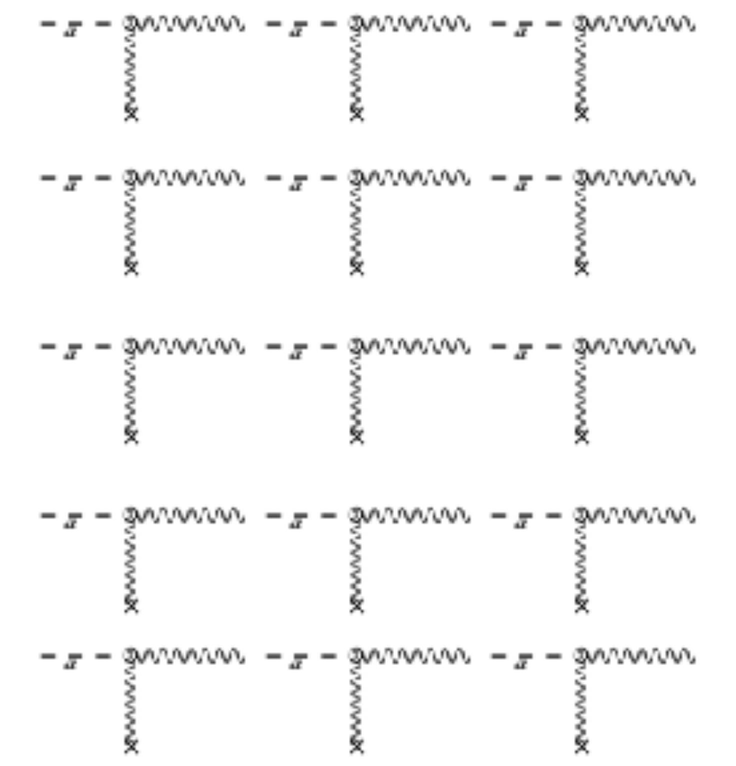

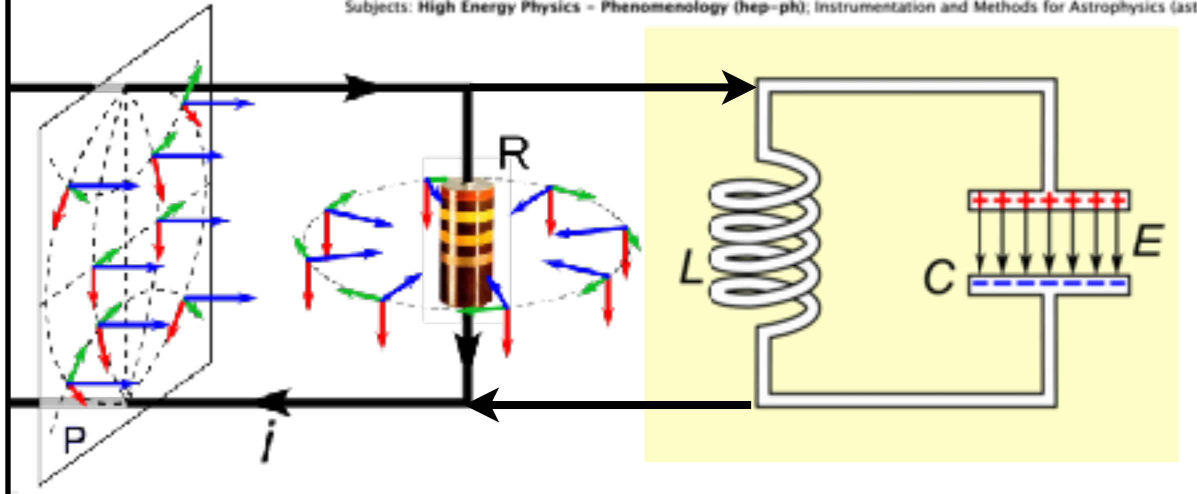

Physics of the Dark Universe

Broadband electrical action sensing techniques with conducting wires for low-mass dark matter axion detection

Michael E Tobar, Ben T McAllister, Maxim Goryachev

PHYSICAL REVIEW APPLIED 15, 014007 (2021)

Electrodynamics of Free- and Bound-Charge Electricity Generators Using Impressed Sources

Michael E. Tobar, Ben T. McAllister, and Maxim Goryachev

ARC Centre of Excellence for Engineered Quantum Systems and ARC Centre of Excellence for Dark Matter Particle Physics, Department of Physics, University of Western Australia, 35 Stirling Highway, Crawley, Western Australia 6009, Australia

Understanding Electricity Generation

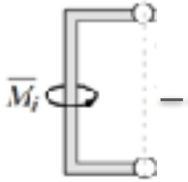

$$-\frac{1}{2}\int_V \mathbf{M}_i \cdot \mathbf{H}^* dv$$

Ensemble of Microscopic Quantum Phenomena -> Classical Macroscopic Description

Well known Classical Equations of Motion

Raymond Y. Chiao

Raymond Chiao outside his UC Merced Lab

arXiv > physics

Physics > Classical Physics

Active Electric Dipole Energy Sources: Transduction via Electric Scalar and Vector Potentials

Michael E. Tobar, Raymond Y. Chiao, Maxim Goryachev

$$-\frac{1}{2}\int_V \mathbf{J}_i^* \cdot \mathbf{E} dv$$

GENERAL FORM OF MAXWELL'S EQUATIONS IN MATTER

Bound Electric and/or Magnetic Current Models?

1) Modified Ampere's Law (mmf generator)

$$\nabla \times B = \mu_0(\vec{J}_f + \vec{J}_b)\ ;\quad \vec{J}_b = \vec{J}_P + \vec{J}_M = \partial_t \overrightarrow{P} + \nabla \times \overrightarrow{M}$$

$$\varrho_P = -\nabla \cdot \overrightarrow{P} \quad \leftrightarrow \quad \nabla \cdot \vec{J}_P = -\partial_t \rho_b$$

Dielectric term

Polarization Current

Permanent Magnet term

2) Modified Faraday's Law (emf generator)

$$\nabla \times \overrightarrow{D} = -\epsilon_0\mu_0\partial_t(\overrightarrow{H} + \overrightarrow{M}) + \nabla \times \overrightarrow{P} = -\epsilon_0\mu_0\partial_t\overrightarrow{H} - \epsilon_0\vec{J}_{mb}$$

$$\vec{J}_{mb} = \vec{J}_{mM} + \vec{J}_{mP} = \mu_0\partial_t\overrightarrow{M} - \frac{1}{\epsilon_0}\nabla \times \overrightarrow{P}$$

$$\varrho_M = -\mu_0\nabla \cdot \overrightarrow{M}$$

$$\nabla \cdot \vec{J}_{mM} = -\partial_t\varrho_M$$

Magnetisation Magnetic Current

Permanent Electret term
(Non-conservative,
Metastable)

Permanent Magnet

$$\rightarrow \nabla \times \overrightarrow{M} \neq 0$$

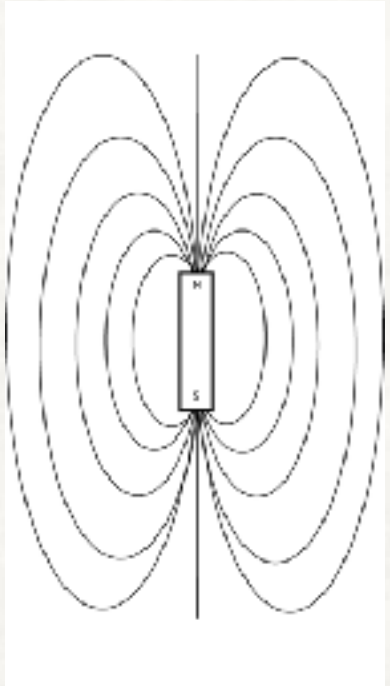

Model as fictitious bound
monopole currents
or fictitious bound
"Ampèrian" currents

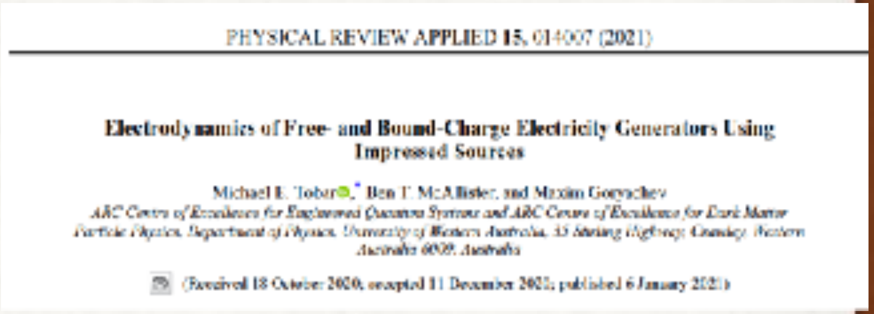

PHYSICAL REVIEW APPLIED 15, 014007 (2021)

Electrodynamics of Free- and Bound-Charge Electricity Generators Using Impressed Sources

Michael E. Tobar,* Ben T. McAllister, and Maxim Goryachev

ARC Centre of Excellence for Engineered Quantum Systems and ARC Centre of Excellence for Dark Matter Particle Physics, Department of Physics, University of Western Australia, 35 Stirling Highway, Crawley, Western Australia 6009, Australia

(Received 18 October 2020; accepted 11 December 2020; published 6 January 2021)

Bound Charge Voltage Source
Electret

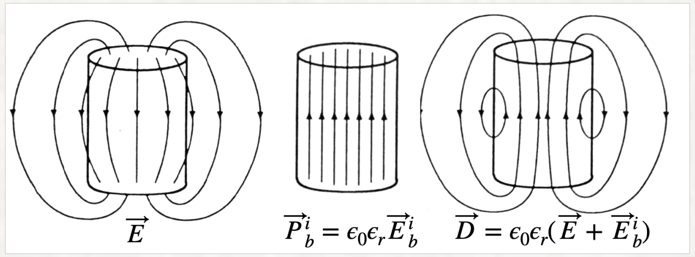

Polarization can also be defined
in free charge voltage source

$$\nabla \times \overrightarrow{P} \neq 0$$

$$\epsilon_0\nabla \times \overrightarrow{E}_i$$

Engineers call impressed field
Could label as Fictitious or Pseudo Electric field

Four Poynting theorems

Paul Kinsler,* Alberto Favaro, and Martin W. McCall
Blackett Laboratory, Imperial College, Prince Consort Road, London SW7 2AZ, United Kingdom.
(Dated: November 9, 2016)

The Poynting vector is an invaluable tool for analysing electromagnetic problems. However, even a rigorous stress-energy tensor approach can still leave us with the question: is it best defined as $\vec{E} \times \vec{H}$ or as $\vec{D} \times \vec{B}$? Typical electromagnetic treatments provide yet another perspective: they regard $\vec{E} \times \vec{B}$ as the appropriate definition, because $\vec{E}$ and $\vec{B}$ are taken to be the fundamental electromagnetic fields. The astute reader will even notice the fourth possible combination of fields: i.e. $\vec{D} \times \vec{H}$. Faced with this diverse selection, we have decided to treat each possible flux vector on its merits, deriving its associated energy continuity equation but applying minimal restrictions to the allowed host media. We then discuss each form, and how it represents the response of the medium. Finally, we derive a propagation equation for each flux vector using a directional fields approach; a useful result which enables further interpretation of each flux and its interaction with the medium.

Published in Eur. J. Phys. **30**, *983 (2009).*[1]
This arXiv version has updates not present in the published version.

arXiv:0908.1721v4

II. MAXWELL'S EQUATIONS

Maxwell's equations for the electric field $\vec{E}$ and magnetic field $\vec{B}$ in a medium are

$$\nabla \cdot \vec{E} = \frac{1}{\epsilon_0}\rho_b + \frac{1}{\epsilon_0}\rho_f = \frac{1}{\epsilon_0}\rho \tag{1}$$

$$\nabla \cdot \vec{B} = 0 \tag{2}$$

$$\nabla \times \vec{E} = -\partial_t \vec{B} \tag{3}$$

$$\nabla \times \vec{B} = \mu_0 \vec{J}_b + \mu_0 \vec{J}_f + \mu_0 \epsilon_0 \partial_t \vec{E}, \tag{4}$$

where $(\rho_b, \vec{J}_b)$ and $(\rho_f, \vec{J}_f)$ are respectively the bound and free (charge, current) densities. As an alternative, we can define an electric polarization P and magnetization M, and

$$\vec{J}_b = \vec{J}_P + \vec{J}_M = \partial_t \vec{P} + \nabla \times \vec{M} \tag{5}$$

$$\rho_b = -\nabla \cdot \vec{P} \tag{6}$$

$$\vec{D} = \epsilon_0 \vec{E} + \vec{P} \tag{7}$$

$$\vec{H} = \frac{1}{\mu_0}\vec{B} - \vec{M}. \tag{8}$$

These allow us to rewrite Maxwell's equations as

$$\nabla \cdot \vec{D} = \rho_f \tag{9}$$

$$\nabla \cdot \vec{B} = 0 \tag{10}$$

$$\nabla \times \vec{E} = -\mu_0 \partial_t \left(\vec{H} + \vec{M}\right) \tag{11}$$

$$\nabla \times \vec{H} = \vec{J}_f + \partial_t \vec{D} = \vec{J}_f + \partial_t \left(\epsilon_0 \vec{E} + \vec{P}\right). \tag{12}$$

We can even rewrite eqn. (11) in the unconventional form

$$\nabla \times \vec{D} = -\epsilon_0 \mu_0 \partial_t \left(\vec{H} + \vec{M}\right) + \nabla \times \vec{P} \tag{13}$$

$$= -\epsilon_0 \mu_0 \partial_t \vec{H} - \epsilon_0 \mu_0 \vec{K}_b, \tag{14}$$

where we have defined

$$\vec{K}_b = \vec{K}_P + \vec{K}_M = -\frac{1}{\epsilon_0 \mu_0} \nabla \times \vec{P} + \partial_t \vec{M}, \tag{15}$$

$$\sigma_b = -\nabla \cdot \vec{M}. \tag{16}$$

This $\vec{K}_b$ appears in the same place as a monopole current would if such were allowed; σ_b is the *bound* magnetic pole density. Note that $\vec{K}_b$ and σ_b are merely a way of representing the (local) material response; we are not claiming that some process actually generates true magnetic monopoles inside the material [14][2]. Strictly speaking, this is also true of the bound electric charge and its currents – they are a mechanism used solely to represent the behaviour of the medium.

Further, and just as for the ficticious bound electric charge density, the ficticious bound monopole density necessarily integrates to zero over all space. Thus the material response could, in principle, be re-represented as magnetic dipoles instead of monopoles.

Electromotive force

From Wikipedia, the free encyclopedia

Not to be confused with Electromagnetic field.

In electromagnetism and electronics, **electromotive force (emf,** denoted $\mathcal{E}$ and measured in volts)[1] is the electrical action produced by a non-electrical source.[2] Devices (known as *transducers*) provide an emf[3] by converting other forms of energy into electrical energy,[3] such as batteries (which convert chemical energy) or generators (which convert mechanical energy).[2] Sometimes an analogy to water pressure is used to describe electromotive force.[4] (The word "force" in this case is not used to mean forces of interaction between bodies).

Fictitious Force

- EMF per unit length [V/m], is like a Fictitious Electric field
- Does not conform to Maxwell's equations
- Outside Maxwell's equations
- Engineers call it an Impressed Electric Field

VOLTAGE SOURCE

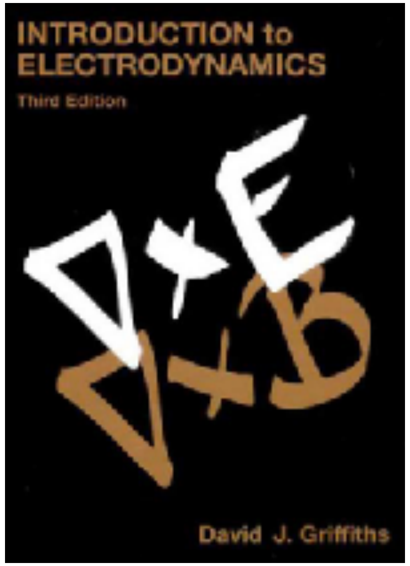

Chapter 7 **7.1.2 Electromotive Force**

The upshot of all this is that there are really *two* forces involved in driving current around a circuit: the *source*, $\mathbf{f}_s$, which is ordinarily confined to one portion of the loop (a battery, say), and the *electrostatic* force, which serves to smooth out the flow and communicate the influence of the source to distant parts of the circuit:

$$\mathbf{f} = \mathbf{f}_s + \mathbf{E}. \tag{7.8}$$

The physical agency responsible for $\mathbf{f}_s$ can be any one of many different things: in a battery it's a chemical force; in a piezoelectric crystal mechanical pressure is converted into an

$$\boxed{\mathcal{E} = \oint \mathbf{f} \cdot d\mathbf{l} = \oint \mathbf{f}_s \cdot d\mathbf{l}.}$$

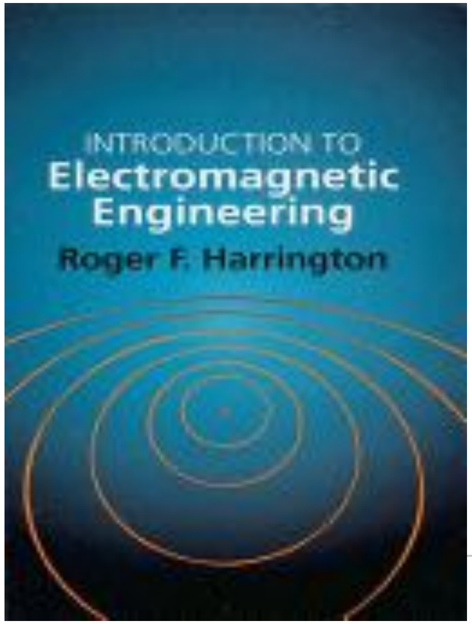

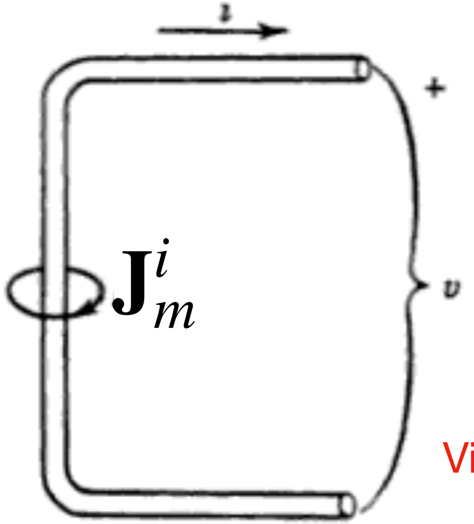

$$\mathbf{J}_m^i$$

$$\oint \mathbf{f}_s \cdot d\mathbf{l} \neq 0$$

$$\mathbf{J}_m^i = -\nabla \times \mathbf{f}_S$$

Via Faraday's Law

$$\mathcal{E} = \oint_C [\boldsymbol{E} + \boldsymbol{v} \times \boldsymbol{B}] \cdot d\boldsymbol{\ell}$$
$$+ \frac{1}{q} \oint_C \text{Effective chemical forces} \cdot d\boldsymbol{\ell}$$
$$+ \frac{1}{q} \oint_C \text{Effective thermal forces} \cdot d\boldsymbol{\ell}\,,$$
$$+ \ldots\ldots\ldots\ldots$$

Surface equivalence principle

How to include external forces to Maxwell's equations?

ELECTRET VOLTAGE SOURCE

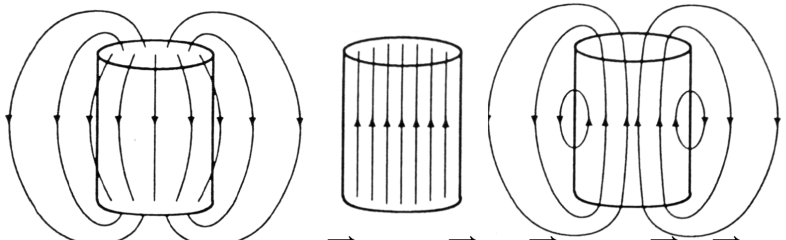

Bulk polarization modifies the boundary Luttinger theorem

PHYSICAL REVIEW RESEARCH 3, 023011 (2021)

Electric polarization as a nonquantized topological response and boundary Luttinger theorem

Xue-Yang Song,[1,2] Yin-Chen He,[2] Ashvin Vishwanath,[1] and Chong Wang[2]
[1]Department of Physics, Harvard University, Cambridge, Massachusetts 02138, USA
[2]Perimeter Institute for Theoretical Physics, Waterloo, Ontario N2L 2Y5, Canada

(Received 22 February 2021; accepted 5 March 2021; published 2 April 2021)

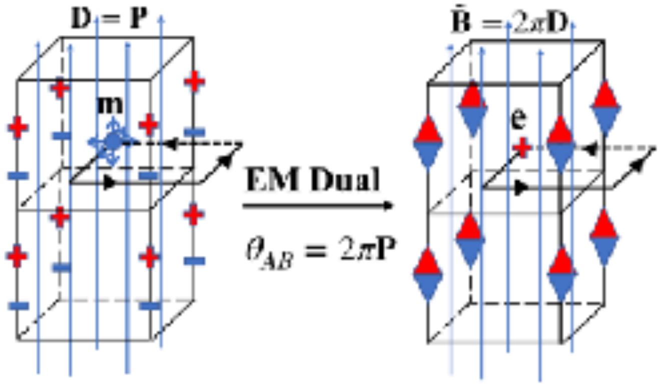

FIG. 2. The semiclassical picture relates projective representation of monopoles to polarization by electromagnetic duality that exchanges magnetic monopole and electric charge. The electric displacement field (left) $\mathbf{D} = \mathbf{P}$ is mapped to magnetic field (right) $\tilde{\mathbf{B}} = 2\pi\mathbf{D}$ and the monopole to an electric charge. The Aharonov-Bohm (AB) phase θ_{AB} seen by the electric charge is proportional to magnetic field (right), hence the monopole Berry phase proportional to displacement field (left).

PHYSICAL REVIEW RESEARCH 3, 023011 (2021)

TABLE I. Polarization density $\mathbf{P}$ is related to the properties of the monopoles in dimensions $d = 1, 2, 3$.

	Monopole property	Polarization
1D	Berry phase	$\Phi = 2\pi P$
2D	Momentum	$\mathbf{k}_{\mathcal{M}} = 2\pi\hat{z} \times \mathbf{P}$
3D	Projective momentum	$T_j^{-1}T_i^{-1}T_jT_i = \exp(i2\pi\epsilon^{ijk}P_k)$

We summarize the connection between bulk polarization and monopole (instanton) properties in $d = 1, 2, 3$ in Table I.

APPENDIX C: POLARIZATION AND OTHER TOPOLOGICAL QUANTITIES

$$\frac{\Theta}{4\pi^2}\mathbf{E}\cdot\mathbf{B}, \tag{C1}$$

$$\Delta\mathbf{P} = \frac{\Theta}{4\pi^2}\mathbf{B}. \tag{C2}$$

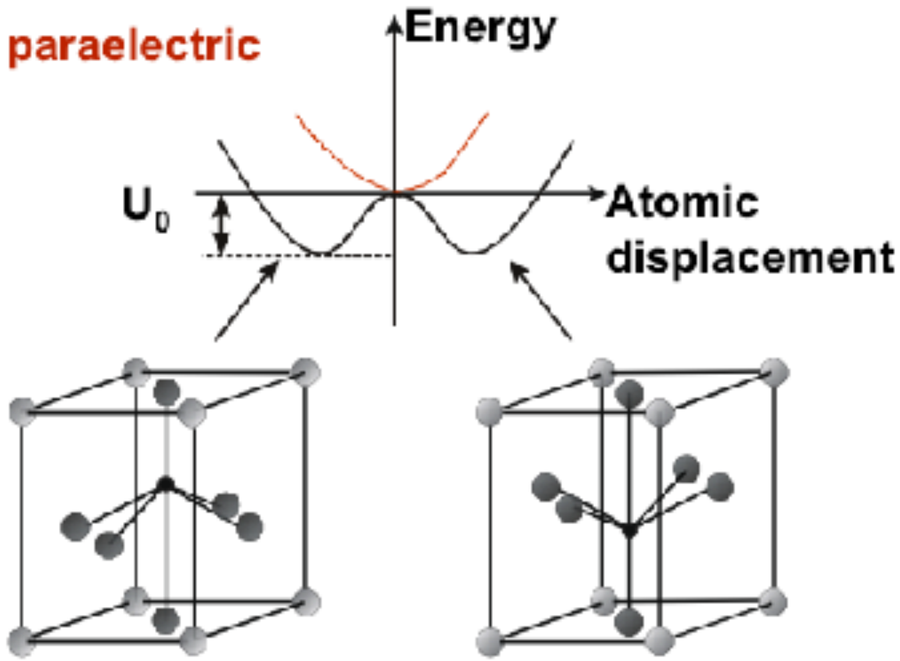

Perovskite Oxide Ferroelectrics

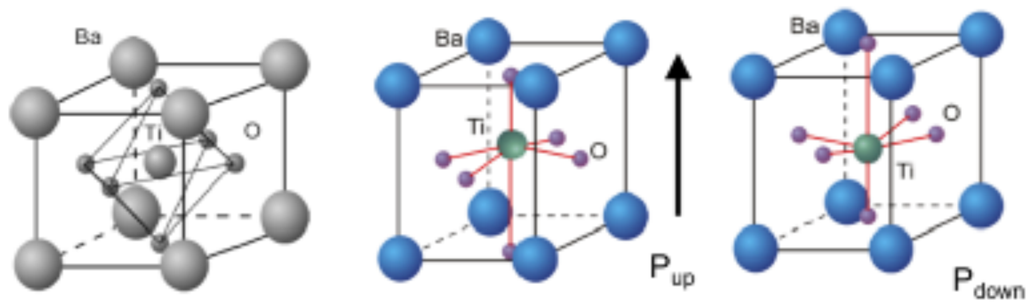

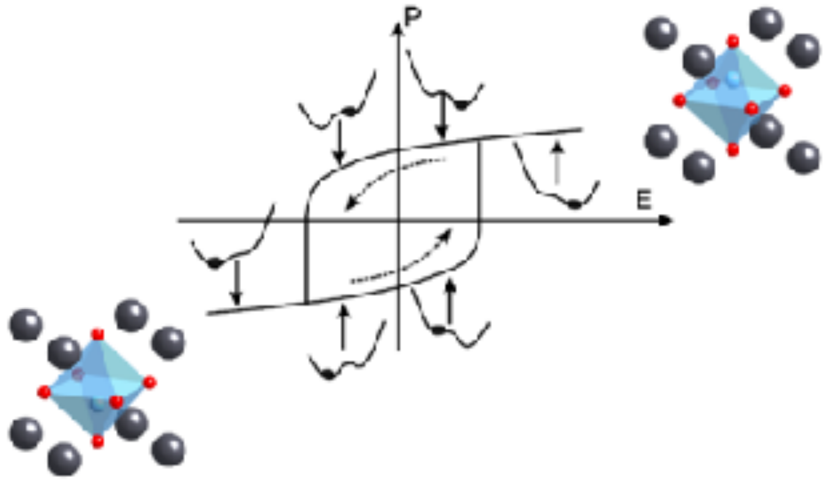

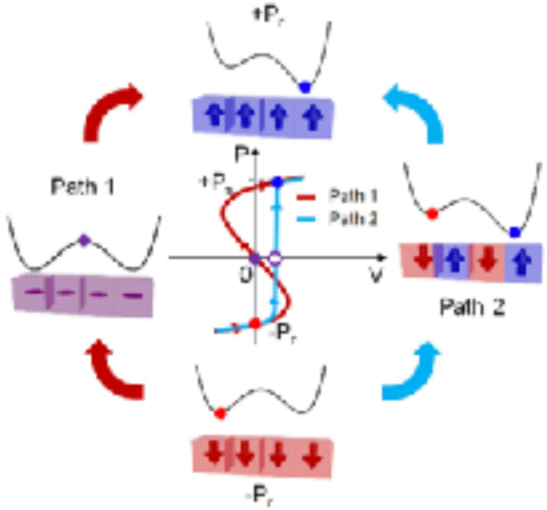

WIKIPEDIA

Article Talk

Electret microphone

An **electret microphone** is a type of electrostatic capacitor-based microphone, which eliminates the need for a polarizing power supply by using a permanently charged material.

Energy harvester

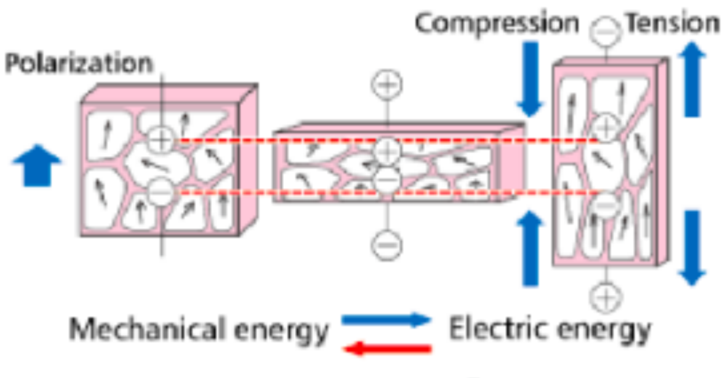

Berry Phase

arXiv > physics > arXiv:2101.00945

Physics > Classical Physics

Active Electric Dipole Energy Sources: Transduction via Electric Scalar and Vector Potentials

Michael E. Tobar, Raymond Y. Chiao, Maxim Goryachev

Modern polarisation theory is based on heuristic replacement of the position vector, by the $\vec{k}$-derivative operator: $\vec{r} \rightarrow i\,\nabla_{\vec{k}}$

Thus, Berry phase is considered in momentum space rather that position space

Potentials

$$\vec{E} = -\vec{\nabla} V - \frac{\partial \vec{A}}{\partial t}$$

$$\frac{1}{\epsilon_0}\vec{P} = -\frac{1}{\epsilon_0}\vec{\nabla} \times \vec{C} + \vec{\nabla} V$$

$$\frac{1}{\epsilon_0}\vec{D} = -\frac{1}{\epsilon_0}\vec{\nabla} \times \vec{C} - \frac{\partial \vec{A}}{\partial t}$$

$$\vec{B} = \vec{\nabla} \times \vec{A} - \mu_0 \frac{\partial \vec{C}}{\partial t}$$

ELECTRIC POLARIZATION AS A NONQUANTIZED ...

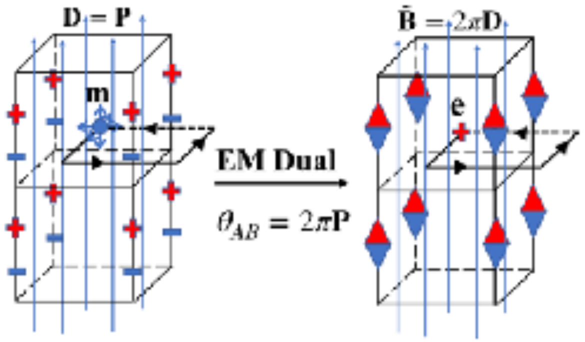

FIG. 2. The semiclassical picture relates projective representation of monopoles to polarization by electromagnetic duality that exchanges magnetic monopole and electric charge. The electric displacement field (left) $\mathbf{D} = \mathbf{P}$ is mapped to magnetic field (right) $\tilde{\mathbf{B}} = 2\pi\mathbf{D}$ and the monopole to an electric charge. The Aharonov-Bohm (AB) phase θ_{AB} seen by the electric charge is proportional to magnetic field (right), hence the monopole Berry phase proportional to displacement field (left).

Berry phase review

Why do we write the phase in this form?
Does it depend on the choice of reference wavefunctions?

$$\phi = \oint \mathcal{A}\cdot d\mathbf{k}, \quad \mathcal{A} = \langle \psi_k | -i\nabla_k | \psi_k \rangle$$

If the ground state is non-degenerate, then the only freedom in the choice of reference functions is a local phase:

$$\psi_k \rightarrow e^{i\chi(k)}\psi_k$$

Under this change, the "Berry connection" $\mathcal{A}$ changes by a gradient

$$\mathcal{A} \rightarrow \mathcal{A} + \nabla_k \chi$$

just like the vector potential in electrodynamics.

So loop integrals of $\mathcal{A}$ will be gauge-invariant, as will the curl of $\mathcal{A}$, which we call the "Berry curvature". $\mathcal{F} = \nabla \times \mathcal{A}$

$\vec{C}$ Electric Vector Potential

- Macroscopic description of an underlying higher dimensional emergent system.
- Electric Berry Phase in Position Space
- Occurs due to External Impressed Force per unit charge

This model allows the definition of Berry Phase in position space

Axion-Photon Coupling

- Axion is predicted to couple to photons, coupling parameter, $g_{a\gamma\gamma}$
- Two-photon transition, interaction Hamiltonian density $\mathscr{H} = \mathscr{H}_{\mathrm{EM}} + \mathscr{H}_a + \mathscr{H}_{int}$: $\mathscr{H}_{int} = \varepsilon_0 c g_{a\gamma\gamma} a \mathbf{E} \cdot \mathbf{B}$

Equation of Motion: Maxwell's Equations

$$\nabla \times \vec{B}_1 = \mu_0 \epsilon_0 \partial_t \vec{E}_1 + \mu_0 \vec{J}_{e1}$$
$$\nabla \times \vec{E}_1 = -\partial_t \vec{B}_1$$
$$\nabla \cdot \vec{B}_1 = 0$$
$$\nabla \cdot \vec{E}_1 = \epsilon_0^{-1} \rho_{e_1}$$

Axion Equation of Motion: Klein-Gordon equation for massive spin 0 particle

$$\left(\Box + \frac{m_a^2 c^2}{\hbar^2} \right) a = - g_{a\gamma\gamma} \varepsilon_0 c \mathbf{E} \cdot \mathbf{B}$$
$$\Box = c^{-2} \partial_t \partial_t - \nabla^2$$

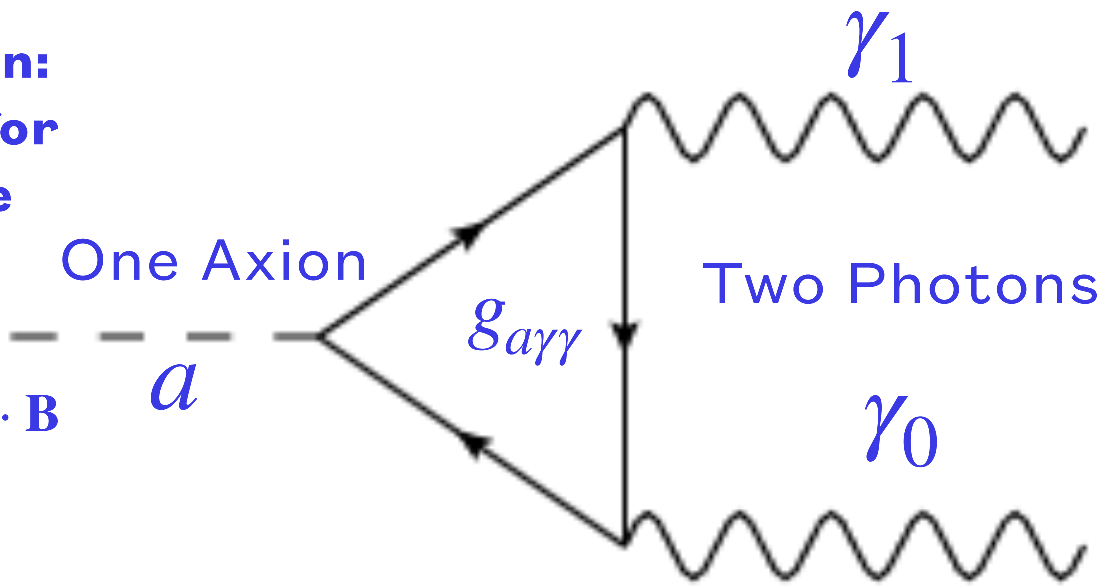

$$\nabla \times \vec{B}_0 = \mu_0 \epsilon_0 \partial_t \vec{E}_0 + \mu_0 \vec{J}_{e0}$$
$$\nabla \times \vec{E}_0 = -\partial_t \vec{B}_0$$
$$\nabla \cdot \vec{B}_0 = 0$$
$$\nabla \cdot \vec{E}_0 = \epsilon_0^{-1} \rho_{e_0}$$

Axion Coupling to two Photonic Degree of Freedoms Modifies Electrodynamics

Haloscopes

- Axions convert into photons in presence of strong background electromagnetic field

1) Background field (subscript zero)

2) Created Photon Field (subscript 1)

Axion Equation of Motion:

Klein-Gordon equation for massive spin 0 particle

$$a(t) = \frac{1}{2}\left(\tilde{a}e^{-j\omega_a t} + \tilde{a}^* e^{j\omega_a t}\right)$$
$$= \mathrm{Re}\left(\tilde{a}e^{-j\omega_a t}\right)$$

Modified Axion Electrodynamics

(Represents two photons)

$$\nabla \cdot \vec{E} = \frac{\rho_e}{\varepsilon_0} + c g_{a\gamma\gamma} \vec{B} \,.\, \nabla a$$
$$\nabla \times \vec{B} - \frac{1}{c^2}\partial_t \vec{E} =$$
$$\mu_0 \vec{J}_e - g_{a\gamma\gamma}\epsilon_0 c\left(\vec{B}\,\partial_t a + \nabla a \times \vec{E}\right)$$
$$\nabla \cdot \vec{B} = 0$$
$$\nabla \times \vec{E} + \partial_t \vec{B} = 0$$

$$\epsilon_0 \nabla \cdot \vec{E}_1 = \rho_{e1} + \rho_{ab}$$
$$\frac{1}{\mu_0}\nabla \times \vec{B}_1 - \epsilon_0 \partial_t \vec{E}_1 = \vec{J}_{e1} + \vec{J}_{ab} + \vec{J}_{ae}$$

$$\rho_{ab} = g_{a\gamma\gamma}\epsilon_0 c \nabla \cdot \left(a(t)\vec{B}_0(\vec{r},t)\right)$$
$$\vec{J}_{ab} = -\, g_{a\gamma\gamma}\epsilon_0 c \partial_t \left(a(t)\vec{B}_0(\vec{r},t)\right)$$
$$\vec{J}_{ae} = -\, g_{a\gamma\gamma}\epsilon_0 c \nabla \times \left(a(t)\vec{E}_0(\vec{r},t)\right)$$
$$\nabla \cdot \vec{J}_{ab} = -\,\partial_t \rho_{ab}$$

Source Terms generate Photons->
From background fields mixing with axion

Photonic Haloscope Equations in terms of Auxiliary Fields

Modified Axion Electrodynamics

(Represents two photons)

$$\nabla \cdot \vec{E} = \frac{\rho_e}{\varepsilon_0} + c g_{a\gamma\gamma} \vec{B} \,.\, \nabla a$$

$$\nabla \times \vec{B} - \frac{1}{c^2} \partial_t \vec{E} =$$

$$\mu_0 \vec{J}_e - g_{a\gamma\gamma} \epsilon_0 c \left(\vec{B} \partial_t a + \nabla a \times \vec{E} \right)$$

$$\nabla \cdot \vec{B} = 0$$

$$\nabla \times \vec{E} + \partial_t \vec{B} = 0$$

Applied Background Field

$$\nabla \times \vec{B}_0 = \mu_0 \epsilon_0 \partial_t \vec{E}_0 + \mu_0 \vec{J}_{e_0}$$

$$\nabla \times \vec{E}_0 = - \partial_t \vec{B}_0$$

$$\nabla \cdot \vec{B}_0 = 0$$

$$\nabla \cdot \vec{E}_0 = \epsilon_0^{-1} \rho_{e_0}$$

$$\vec{\nabla} \cdot \vec{D}_1 = \rho_{e1}$$

$$\vec{\nabla} \times \vec{E}_1 = - \partial_t \vec{B}_1$$

$$\vec{\nabla} \cdot \vec{B}_1 = 0$$

$$\frac{1}{\mu_0} \vec{\nabla} \times \vec{B}_1 = \vec{J}_{e1} + \epsilon_0 \partial_t \vec{E}_1 - g_{a\gamma\gamma} \epsilon_0 c \vec{B}_0 \partial_t a$$

$$\frac{1}{\epsilon_0} \nabla \times \vec{D}_1 = - \partial_t \vec{B}_1 - g_{a\gamma\gamma} c \nabla \times (a \vec{B}_0)$$

$\nabla a = 0$

$$\frac{1}{\epsilon_0} \nabla \times \vec{D}_1 = - \partial_t \vec{B}_1 - \frac{g_{a\gamma\gamma} a}{c} \partial_t \vec{E}_0 - g_{a\gamma\gamma} a c \mu_0 \vec{J}_{e0}$$

Constitutive Relations(in vacuum)

$$\frac{1}{\epsilon_0} \vec{D}_1 = \vec{E}_1 - g_{a\gamma\gamma} c a \vec{B}_0$$

Measure Created Photon

$$\nabla \cdot \left(\vec{E}_1(\vec{r}, t) - g_{a\gamma\gamma} a(t) c \vec{B}_0(\vec{r}, t) \right) = \frac{\rho_{e_1}}{\epsilon_0}$$

$$\nabla \times \left(\vec{B}_1(\vec{r}, t) + \frac{g_{a\gamma\gamma} a(t)}{c} \vec{E}_0(\vec{r}, t) \right)$$

$$- \frac{1}{c^2} \partial_t \left(\vec{E}_1(\vec{r}, t) - g_{a\gamma\gamma} a(\vec{r}, t) c \vec{B}_0(\vec{r}, t) \right) = \mu_0 \vec{J}_{e_1}$$

$$\nabla \cdot \vec{B}_1(\vec{r}, t) = 0$$

$$\nabla \times \vec{E}_1(\vec{r}, t) + \partial_t \vec{B}_1(\vec{r}, t) = 0.$$

Eg. Solenoidal DC Magnetic field: Defined by a surface when λ_a > Experiment

$$\vec{B}_{DC}(\vec{r}) = \frac{\mu_0}{4\pi}\int_{\Omega}\frac{\vec{\nabla}\times\vec{J}^{i}_{DC}(\vec{r}')}{|\vec{r}-\vec{r}'|}\mathrm{d}^3\vec{r}',$$

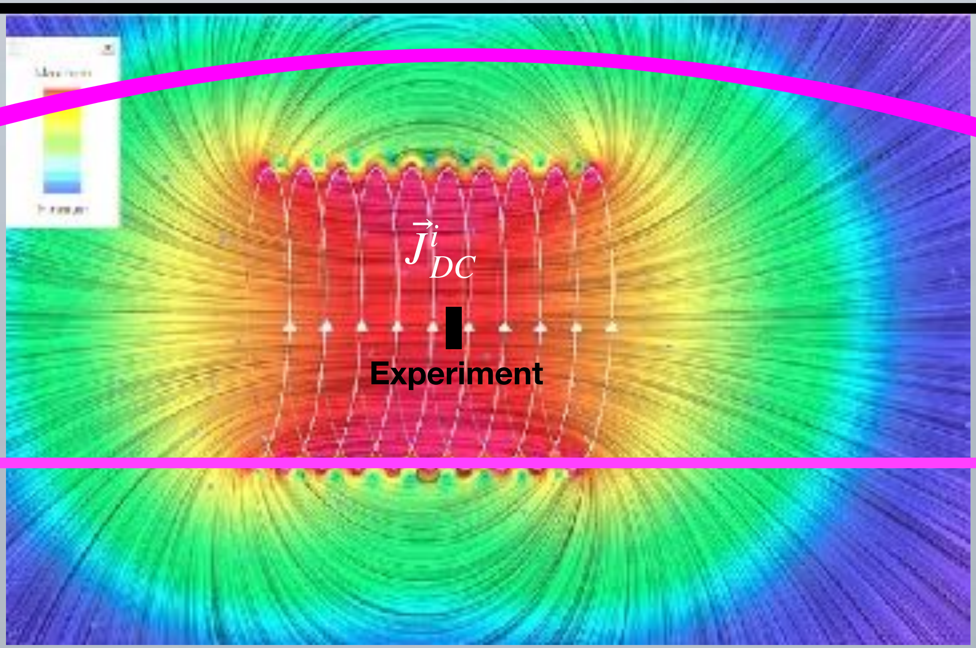

$\frac{\lambda_a}{2}$

$$\frac{1}{\epsilon_0}\vec{D}_1 = \vec{E}_1 - g_{a\gamma\gamma}ca\vec{B}_{DC}$$

$$\frac{1}{\epsilon_0}\vec{P}_{1a} = -g_{a\gamma\gamma}a(t)c\vec{B}_{DC}(\vec{r},t) = -\frac{1}{4\pi}\int_{\Omega}\frac{\vec{\nabla}\times\vec{J}^{i}_{ma}(\vec{r}',t)}{|\vec{r}-\vec{r}'|}\mathrm{d}^3\vec{r}'$$

$$\frac{1}{\epsilon_0}\nabla\times\vec{P}_{a1} = -g_{a\gamma\gamma}a(t)c\mu_0\vec{J}_{DC}$$

$$\vec{J}^{i}_{ma}(\vec{r},t) = g_{a\gamma\gamma}a(t)c\mu_0\vec{J}^{i}_{DC}(\vec{r})$$

Like an Electric Polarization with non-zero Curl:
Extra surface term in the solution to the equation of motion
This surface cannot go to infinity due to the solenoidal nature of a DC magnetic field
Assuming the total derivative is zero also assumes all surfaces go to infinity
Polarization generated by axion induced fictitious magnetic current boundary -> similar to an electret or voltage source : Has an Electric Vector Potential!

Capacitor under DC Magnetic Field: Quasi-static limit

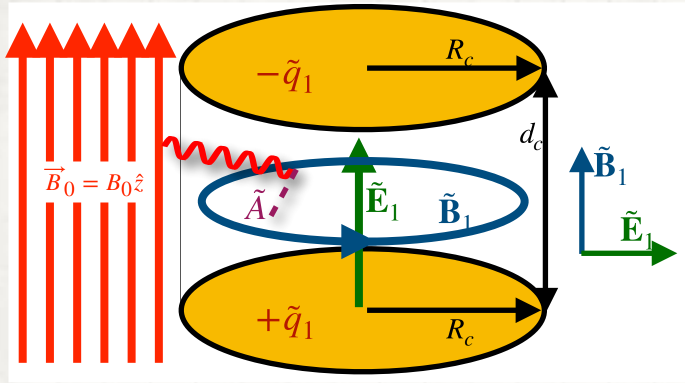

To First order: Real part of Poynting Theorem $= 0$: Reactive part of Poynting Theorem $\neq 0$

$$\oint j\,\mathrm{Im}\left(\mathbf{S}_{EH}\right)\cdot\hat{n}ds = j\omega_a\int\left(\frac{1}{2\mu_0}\mathbf{B}_1^*\cdot\mathbf{B}_1 - \frac{\epsilon_0}{2}\mathbf{E}_1^*\cdot\mathbf{E}_1 + \frac{\epsilon_0}{2}g_{a\gamma\gamma}a_0c\vec{B}_0\cdot Re(\mathbf{E}_1)\right)dV$$

$$\oint j\,\mathrm{Im}\left(\mathbf{S}_{DB}\right)\cdot\hat{n}ds = j\omega_a\int\left(\frac{1}{2\mu_0}\mathbf{B}_1^*\cdot\mathbf{B}_1 - \frac{\epsilon_0}{2}\mathbf{E}_1^*\cdot\mathbf{E}_1 + \epsilon_0 g_{a\gamma\gamma}a_0c\vec{B}_0\cdot Re(\mathbf{E}_1) - \frac{\epsilon_0 g_{a\gamma\gamma}^2a_0^2c^2}{2}\vec{B}_0\cdot\vec{B}_0\right)dV$$

$$\oint j\,\mathrm{Im}\left(\mathbf{S}_{DB}\right)\cdot\hat{n}ds \approx -j\omega_a\int\left(\frac{\epsilon_0 g_{a\gamma\gamma}^2a_0^2c^2}{2}\vec{B}_0\cdot\vec{B}_0\right)dV$$

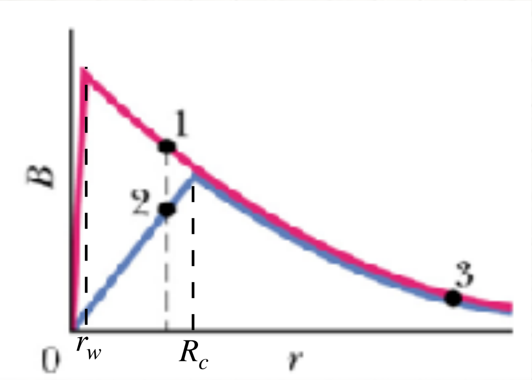

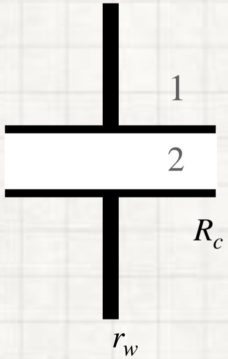

3

First order: Ignore fringing

$$\mathbf{E}_1 = \frac{\tilde{q}_1}{\pi R_c^2\epsilon_0}\hat{z} \qquad \mathbf{B}_1 = -j\omega_a\mu_0\tilde{q}_1\frac{r}{\pi R_c^2}\hat{\theta} \qquad \frac{U_m}{U_e} = \frac{\int_{V_c}\mathbf{B}_1\cdot\mathbf{B}_1^*dV}{\epsilon_0\mu_0\int_{V_c}\mathbf{E}_1\cdot\mathbf{E}_1^*dV} = \frac{R_c^2\omega_a^2}{8c^2} = \frac{\pi^2R_c^2}{2\lambda_a^2}$$

Sensitivity assuming the Modified Minkowski Poynting Vector

$$\nabla\times\vec{D}_1 = \epsilon_0\nabla\times\vec{E}_1 - g_{a\gamma\gamma}\epsilon_0c\nabla\times(a\vec{B}_0) = -\epsilon_0(\partial_t\vec{B}_1 + g_{a\gamma\gamma}a(t)\mu_0c\vec{J}_{e0})$$

$$jP_a = \oint j\,\mathrm{Im}\left(\mathbf{S}_{DB}\right)\cdot\hat{n}ds \approx -j\omega_a\int\left(\frac{\epsilon_0 g_{a\gamma\gamma}^2a_0^2c^2}{2}\vec{B}_0\cdot\vec{B}_0\right)dV$$

$$U_c = g_{a\gamma\gamma}^2\langle a_0\rangle^2\epsilon_0c^2B_0^2V_1$$

$$\mathscr{V}_{rms} = g_{a\gamma\gamma}\langle a_0\rangle cB_0d_c = g_{a\gamma\gamma}d_c\frac{c}{\omega_a}B_0\sqrt{\rho_ac^3}$$

Sensitivity assuming the Modified Abraham Poynting Vector

$$\nabla\times\vec{E}_1 = -\partial_t\vec{B}_1$$

$$jP_a = \oint j\,\mathrm{Im}\left(\mathbf{S}_{EH}\right)\cdot\hat{n}ds = \frac{j\omega_a g_{a\gamma\gamma}a_0\epsilon_0c}{2}\int\left(\vec{B}_0\cdot\mathrm{Re}(\mathbf{E}_1)\right)\frac{\pi^2r^2}{\lambda_a^2}\,dV$$

$P_a = \omega_aU_c$, where $U_c = g_{a\gamma\gamma}^2\langle a_0\rangle^2\epsilon_0c^2B_0^2V_1\left(\frac{\pi^2Rc^2}{2\lambda_a^2}\right)^2$ $\qquad U_c = \frac{1}{2}\tilde{\mathscr{V}}\tilde{\mathscr{V}}^*C_a \qquad \left(C_a = \frac{\pi R_c^2\epsilon_0}{d_c}\right)$

$$\mathscr{V}_{rms} = g_{a\gamma\gamma}\langle a_0\rangle cB_0d_c\left(\frac{\pi R_c}{\sqrt{2}\lambda_a}\right)^2 = g_{a\gamma\gamma}d_c\frac{c}{\omega_a}B_0\sqrt{\rho_ac^3}\left(\frac{\pi R_c}{\sqrt{2}\lambda_a}\right)^2$$

Electric Action of the Axion, $a(t)$, mixing with $\vec{B}_0$
-> Creates Electromagnetic Energy at ω_a

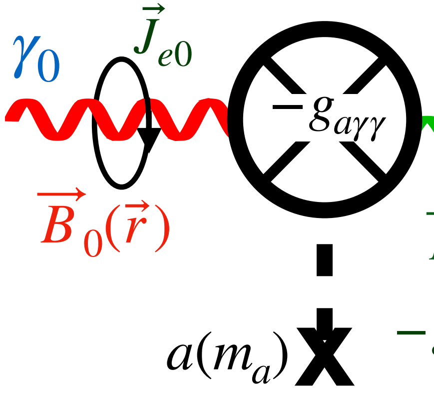

$\vec{E}_{1a}(\vec{r},t) = -g_{a\gamma\gamma}\left(a(t)c\vec{B}_0(\vec{r})\right)$

$a(t) = a_0 \sin(\omega_a t)$

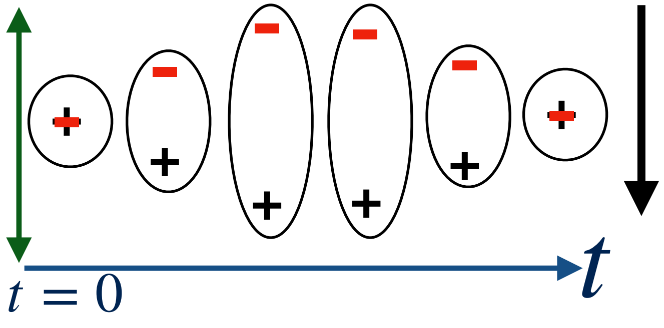

$\vec{J}_{ab}(\vec{r},t) = \epsilon_0 \dfrac{\partial \vec{E}_{1a}(\vec{r},t)}{\partial t}$

$\vec{E}_{1a}$

A fictitious Electric Field


Physics of the Dark Universe 30 (2020) 100624

Contents lists available at ScienceDirect

Physics of the Dark Universe

journal homepage: www.elsevier.com/locate/dark

ELSEVIER

Broadband electrical action sensing techniques with conducting wires for low-mass dark matter axion detection

Michael E. Tobar *, Ben T. McAllister, Maxim Goryachev

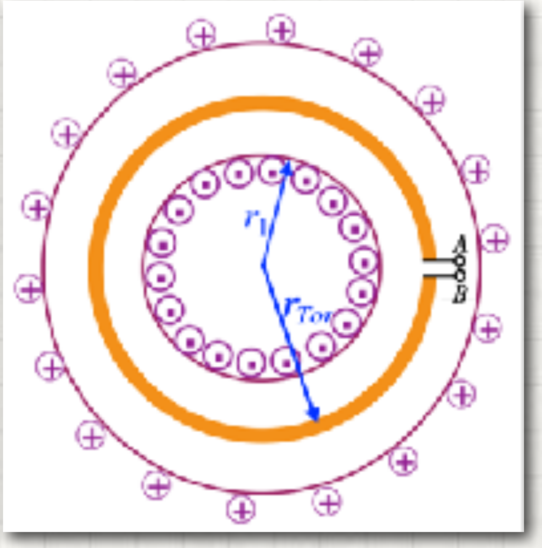

$$\oint \langle \vec{S} \rangle \cdot dS = -\frac{1}{4}\int (\mathbf{E}_1 \cdot \mathbf{J}_{e1}^* + \mathbf{E}_1^* \cdot \mathbf{J}_{e1})\, d\tau + \frac{1}{4}\int c\vec{B}_0 \cdot (g_{a\gamma\gamma}\tilde{a}\mathbf{J}_{e1}^* + g_{a\gamma\gamma}\tilde{a}^*\mathbf{J}_{e1})\, d\tau - \int \frac{1}{4} g_{a\gamma\gamma}\vec{J}_{e0} \cdot (\tilde{a}c\mathbf{B}_1^* + \tilde{a}^* c\mathbf{B}_1)\, d\tau$$

Increase Sensitivty by Increasing Topology: Toroidal Magnet

Toroidal Magnet

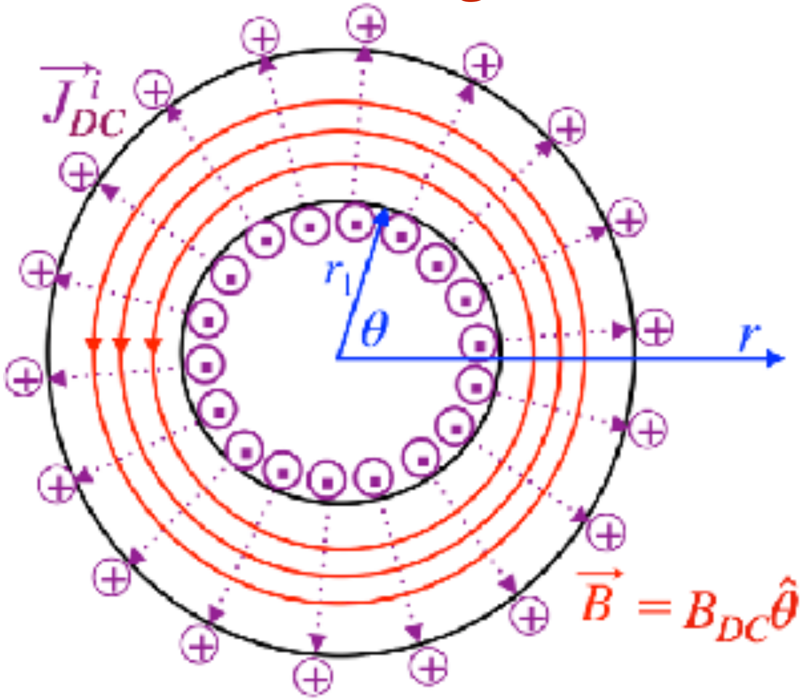

Static External Fields

$$\vec{\nabla}\cdot\vec{B}_{DC}(\vec{r}) = 0 \quad \vec{\nabla}\times\vec{B}_{DC}(\vec{r}) = \mu_0\vec{J}^i_{DC}$$

$$B_{DC} = \mu_0 N_l I^i_{DC\ Tor}$$

$$I^i_{fDC\ enc} = N I^i_{DC\ Tor} = 2\pi r\frac{B_{DC}}{\mu_0}$$

$$N = 2\pi r N_l$$

Axion Induced Fields

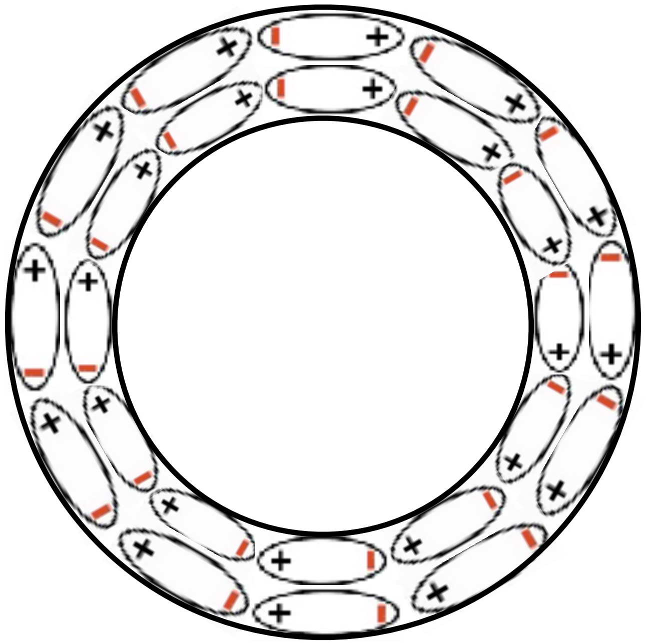

$$\vec{E}^i_{aB} = -g_{a\gamma\gamma}a_0 c B_{DC}\sin(\omega_a t)\hat{\theta}$$

$$\mathscr{E} = \oint_P \vec{E}^i_{aB}\cdot d\vec{l}$$

$$\mathscr{E} = -I^i_{ma\ enc} = -g_{a\gamma\gamma}a_0 c B_{DC} 2\pi r\sin(\omega_a t)$$

Topological Readout

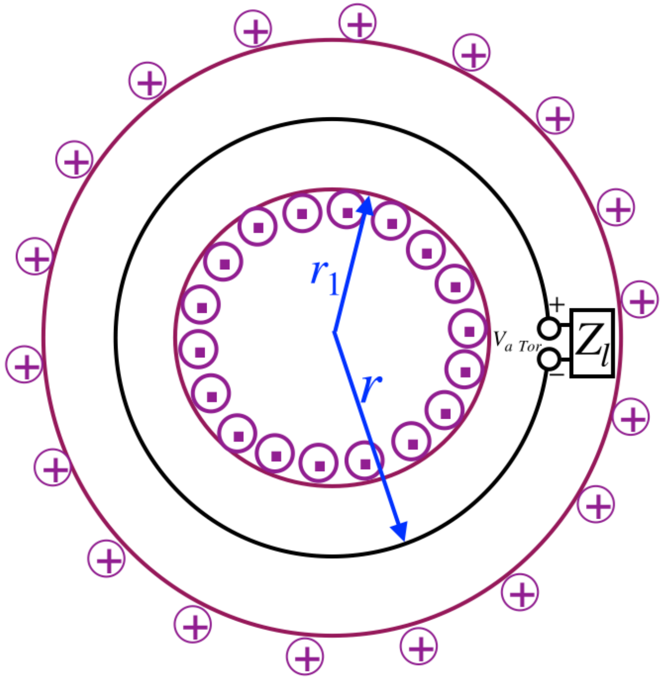

$$V_{a\ Tor} = g_{a\gamma\gamma}a_0 c B_{DC} 2\pi r N_c\sin(\omega_a t)$$

N_c No. of turns of pickup coil

$$V^{RMS}_{a\ Tor} = g_{a\gamma\gamma}2\pi r N_c\left(\frac{c}{\omega_a}\right)B_{DC}\sqrt{\rho_D M c^3}$$

- Axion Modified Abraham Poynting theorem is consistent with the total derivative being zero: Ignores $-g_{a\gamma\gamma}c\nabla\times(a\overrightarrow{B}_0)\neq 0$
- To be true it is well known that all surface terms $\rightarrow 0$ as $\lambda_a \rightarrow \infty$
- Minkowski Poynting theorem identifies surface terms $\neq 0$ as $\lambda_a \rightarrow \infty$
- Fictitious Magnetic Current Boundary Term: Similar to an Electret or Voltage Source
- Macroscopic emergent description of the QCD axion-photon anomaly (which microscopically is a quantum effect)
- Abraham or Minkowski? Should be determined experimentally -> Analogies with ED suggest Minkowski is Correct

Curl Force

PRL 103, 108101 (2009) PHYSICAL REVIEW LETTERS week ending 4 SEPTEMBER 2009

Direct Measurement of the Nonconservative Force Field Generated by Optical Tweezers

Pinyu Wu,[1] Rongxin Huang,[1] Christian Tischer,[2] Alexandr Jonas,[3] and Ernst-Ludwig Florin[1,*]
[1]Center for Nonlinear Dynamics and Department of Physics, University of Texas at Austin, Austin, Texas 78712, USA
[2]European Molecular Biology Laboratory, 69117 Heidelberg, Germany
[3]Institute of Scientific Instruments, Academy of Sciences of the Czech Republic, 61264 Brno, Czech Republic
(Received 15 March 2009; published 1 September 2009)

$$\mathbf{F} = -\underbrace{\nabla V}_{\text{conservative}} + \underbrace{\nabla\times\mathbf{A}}_{\text{non-conservative}} \equiv \underbrace{\mathbf{F}_{\text{grad}}}_{\text{conservative}} + \underbrace{\mathbf{F}_{\text{curl}}}_{\text{non-conservative}}. \quad (1)$$

where the nonconservative force $\mathbf{F}_{\text{curl}}$ satisfies

$$\nabla\times\mathbf{F} = \nabla\times\mathbf{F}_{\text{curl}} = \nabla(\nabla\cdot\mathbf{A}) - \nabla^2\mathbf{A} \neq 0.$$

Classical and quantum complex Hamiltonian curl forces

M V Berry
H H Wills Physics Laboratory, Tyndall Avenue, Bristol BS8 1TL, United Kingdom
Received 23 June 2020, revised 20 July 2020
Accepted for publication 7 August 2020
Published 10 September 2020

Abstract

Quantized Hamiltonian Curl Forces and Squeezed Light

P. Strange

(Dated: July 3, 2018)

In this paper we discuss quantum curl forces. We present both the classical and quantum theory of linear curl forces. The quantum theory is shown to reproduce the classical theory precisely if appropriate combinations of eigenfunctions are chosen. A series of examples are used to illustrate the theory and to demonstrate its limitations. Furthermore we are able to point out an analogy between the quantum theory of curl forces and some of the squeezed light states of quantum optics.

IOP PUBLISHING JOURNAL OF PHYSICS A: MATHEMATICAL AND THEORETICAL
J. Phys. A: Math. Theor. 46 (2013) 422001

FAST TRACK COMMUNICATION

Physical curl forces: dipole dynamics near optical vortices

KEY ISSUES REVIEW

Non-conservative optical forces

Journal of Physics A: Mathematical and Theoretical

FAST TRACK COMMUNICATION

Physical curl forces: dipole dynamics near optical vortices

To cite this article: M V Berry and Pragya Shukla 2013 J. Phys. A: Math. Theor. 46 422001

THE EUROPEAN PHYSICAL JOURNAL D

Curl forces and their role in optics and ion trapping

Electret-> Curl Force
Electric Vector Potential

$$\nabla\times\vec{D} = -\epsilon_0\mu_0\partial_t(\vec{B}) + \nabla\times\vec{P}$$

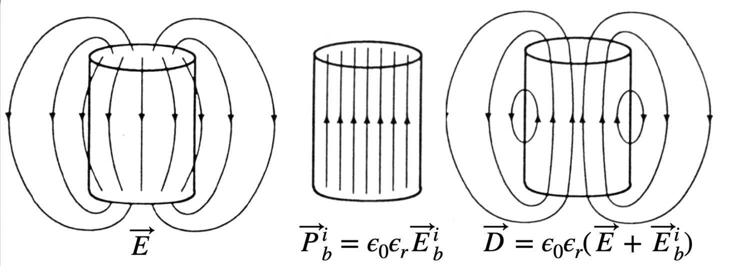

Curl Force in Axions Electrodynamics

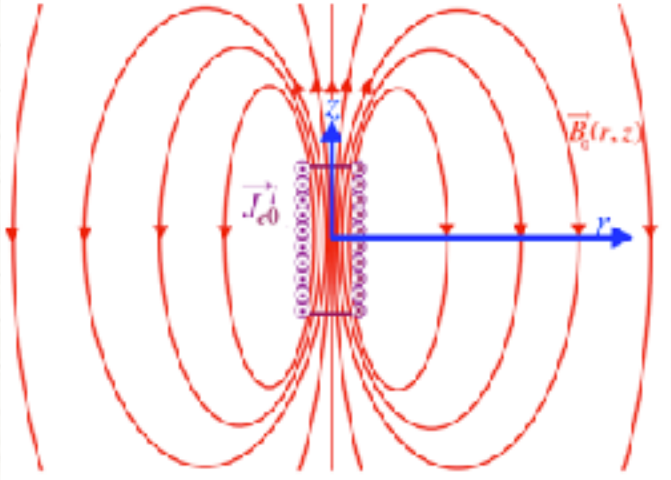

$$\vec{B}_0(\vec{r}) = \frac{\mu_0}{4\pi}\int_\Omega \frac{\nabla\times\vec{J}^i_{DC}(\vec{r}')}{|\vec{r}-\vec{r}'|}d^3\vec{r}'$$

$$\vec{E}_{a1}(\vec{r},t) = -g_{a\gamma\gamma}a(t)c\vec{B}_0(\vec{r})$$

$$= -\frac{1}{4\pi}\int_\Omega \frac{\nabla\times\vec{J}^i_{ma}(\vec{r}',t)}{|\vec{r}-\vec{r}'|}d^3\vec{r}'$$

Fictitious Electric field

$$\vec{J}_{m1a} = g_{a\gamma\gamma}a(t)\mu_0 c\vec{J}_{e0}$$

Axion Modified Faraday's Law

$$\frac{1}{\epsilon_0}\nabla\times\vec{D}_1 = \nabla\times\vec{E}_1 - g_{a\gamma\gamma}c\nabla\times(a\vec{B}_0) = -(\partial_t\vec{B}_1 + g_{a\gamma\gamma}a(t)c\mu_0\vec{J}_{e0})$$

Physics of the Dark Universe

Broadband electrical action sensing techniques with conducting wires for low-mass dark matter axion detection
Michael E. Tobar, Ben T. McAllister, Maxim Goryachev

Physics of the Dark Universe

Modified axion electrodynamics as impressed electromagnetic sources through oscillating background polarization and magnetization
Michael E. Tobar, Ben T. McAllister, Maxim Goryachev

Magnetic Vector Potential generates a Conservative Force -> Not a non-conservative Curl force arXiv:2208.01640 [pdf, other]

Twisted Anyon Cavity Resonators with Bulk Modes of Chiral Symmetry and Sensitivity to Ultra-Light Axion Dark Matter

J. F. Bourhill, E. C. I. Paterson, M. Goryachev, M. E. Tobar

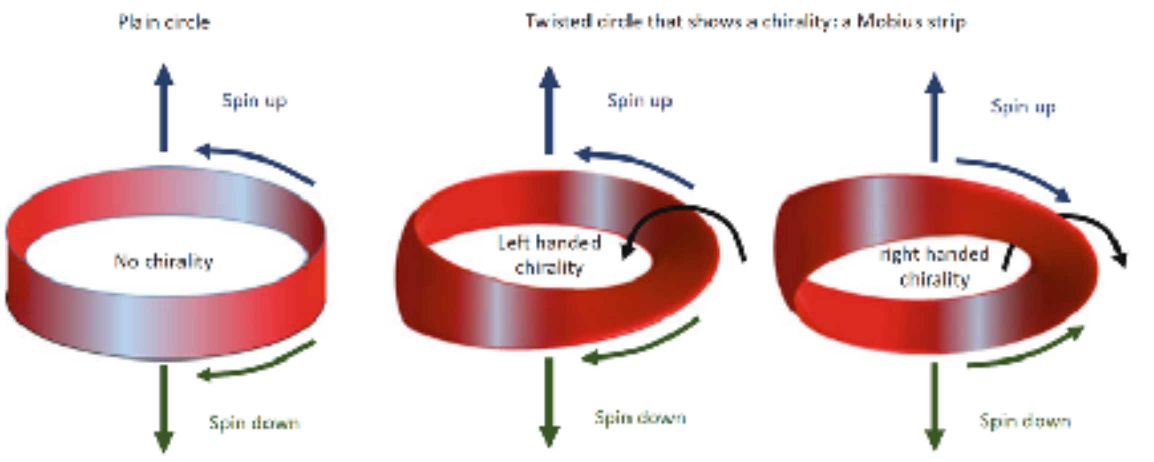

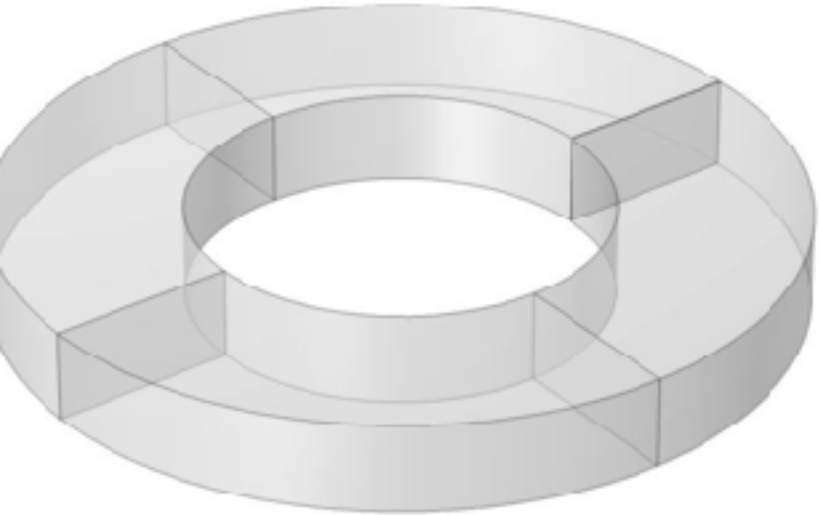

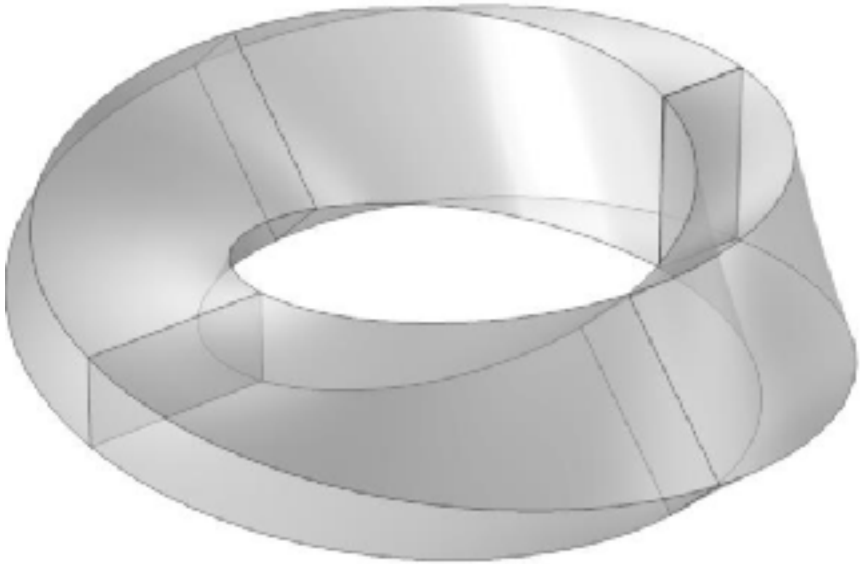

Fermions Come in Two Chiralities, Called Left and Right. Bosons Do Not

Torus

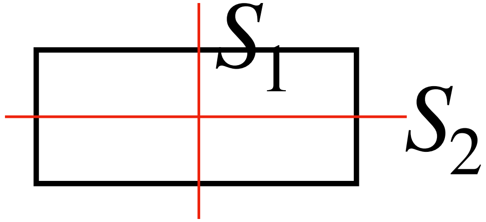

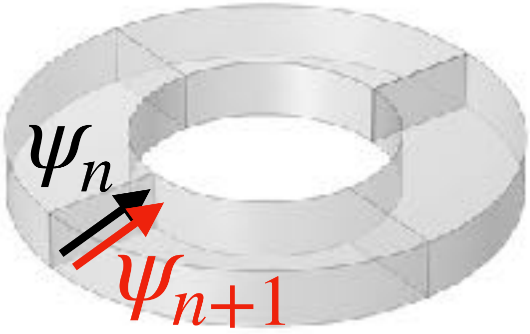

$$\psi_n = \psi_{n+1}$$
$$\psi_n = \psi_{n+N}$$
$$\theta = 0$$

Boson

Möbius

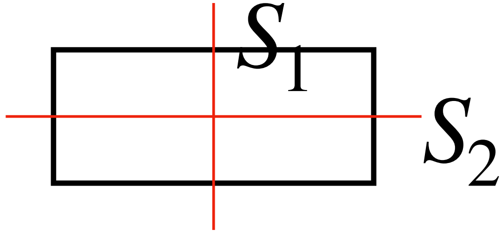

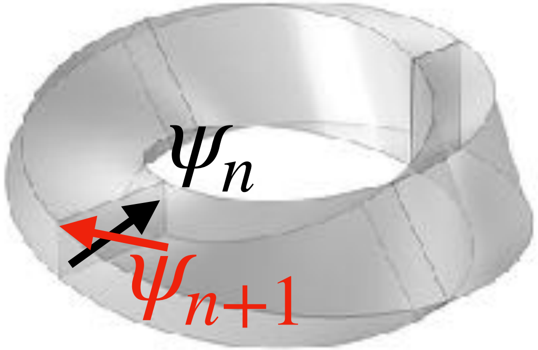

$$\psi_n = -\psi_{n+1}$$
$$\psi_n = \psi_{n+2N}$$
$$\theta = \pm\pi$$

Fermion

Anyon Cavity

Dihedral group of regular convex polygons: D_p

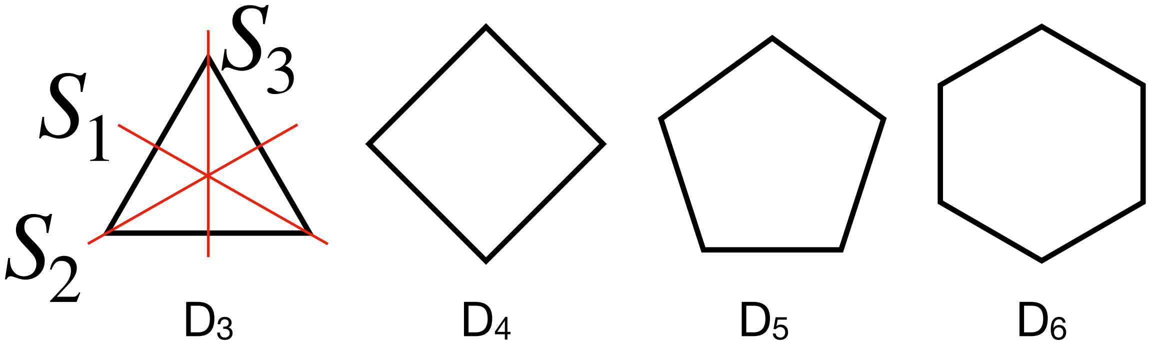

$2p$ symmetries: p rotational + p reflection
Rotation by $2\pi/p$ preserves the object

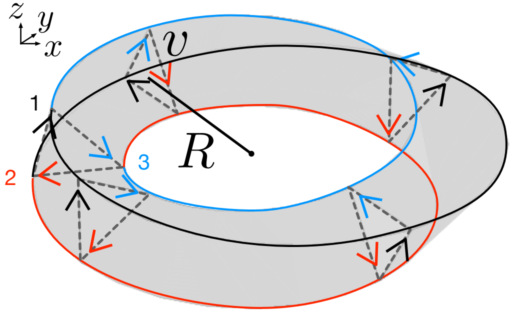

$$\psi_n = e^{i\theta}\psi_{n+1}$$
$$\theta = (2\pi/p)Z$$
$$Z \in \pm\mathbb{Z}$$

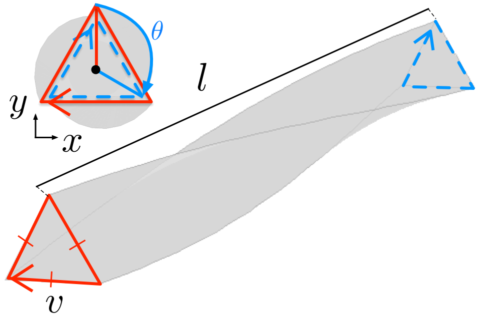

$$\psi_n = e^{i\theta}\psi_{n+1}$$
$$\theta \in \mathbb{R}$$

Anyon

3D Printed Super Conducting Aluminium Cavities

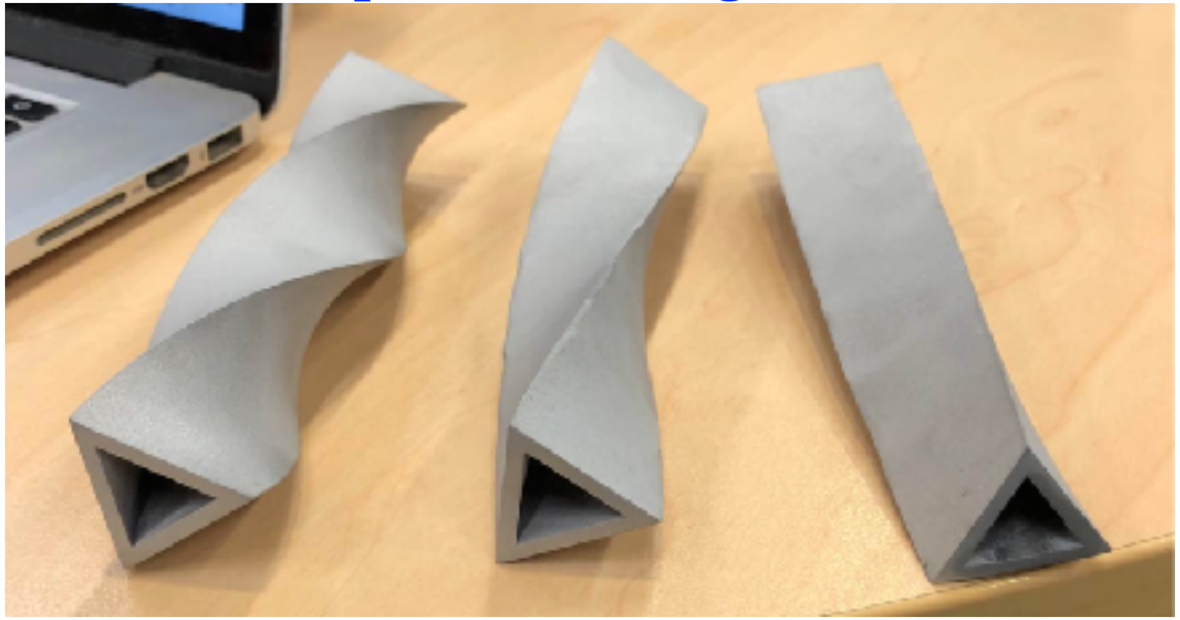

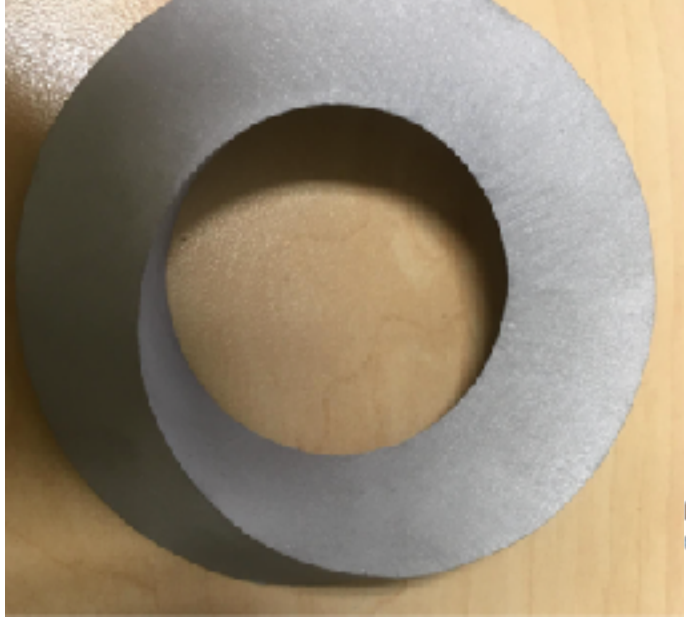

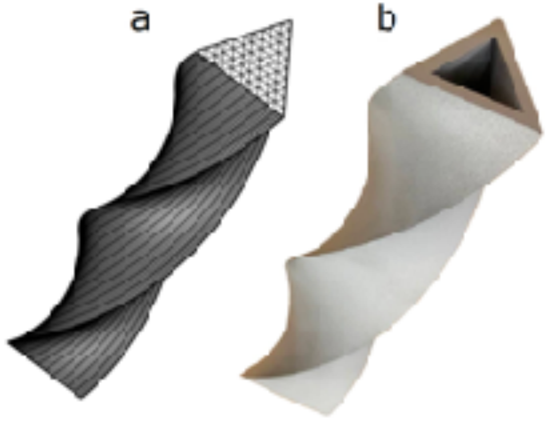

FIG. 5. a 3D mesh of waveguide resonator used for finite element simulations and b Aluminium 3D printed cavity.

$$\mathscr{H}_p = \frac{2\,\mathrm{Im}[\int \mathbf{B}_p(\vec{r})\cdot\mathbf{E}_p^*(\vec{r})\,d\tau]}{\sqrt{\int \mathbf{E}_p(\vec{r})\cdot\mathbf{E}_p^*(\vec{r})\,d\tau \int \mathbf{B}_p(\vec{r})\cdot\mathbf{B}_p^*(\vec{r})\,d\tau}},$$

Resonator	Mode	f (GHz)	G (Ω)	$\mathscr{H}$
Ring	ψ_0^-	17.221	6200	0.933
Ring	ψ_1^-	17.297	6570	0.9166
Ring	ψ_0^+	17.895	7290	-0.820
Linear	ψ_0^-	17.214	1950	0.932
Linear	ψ_1^-	17.278	2030	0.896
Linear	ψ_0^+	17.859	1920	-0.884

TABLE I. Simulated f, G and $\mathscr{H}$ values for the lowest order $\psi^{\pm}$ modes for $l = 150$ mm, $r = 20$ mm and $\theta = 120°$ ring and linear resonators.

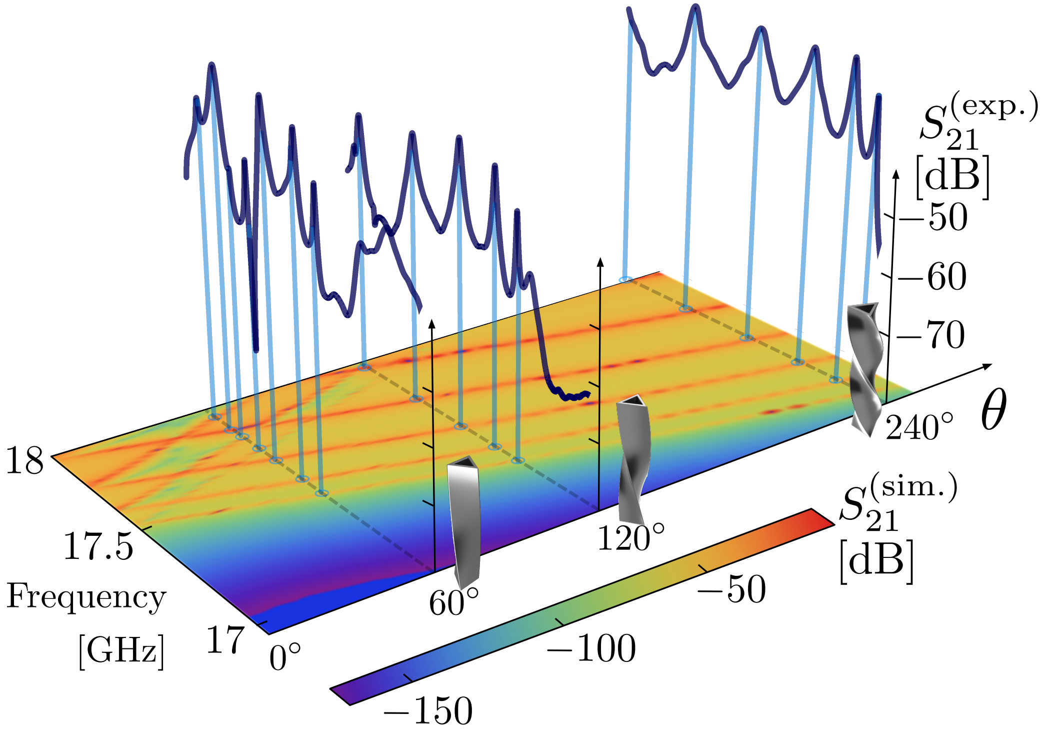

Zilch (electromagnetism)

From Wikipedia, the free encyclopedia

In physics, **zilch** is a conserved quantity of the electromagnetic field.

Daniel M. Lipkin observed that if he defined the quantities

$$Z^0 = \mathbf{E}\cdot\nabla\times\mathbf{E} + \mathbf{B}\cdot\nabla\times\mathbf{B}$$

$$\mathbf{Z} = \frac{1}{c}\left(\mathbf{E}\times\frac{d}{dt}\mathbf{E} + \mathbf{B}\times\frac{d}{dt}\mathbf{B}\right)$$

then the Maxwell equations imply that

$$\partial_0 Z^0 + \nabla\cdot\mathbf{Z} = 0$$

which implies that the total "zilch" $\int Z^0\, d^3x$ is constant ($\mathbf{Z}$ is the "zilch current").

OPEN ACCESS
IOP Publishing
Journal of Optics
J. Opt. 18 (2016) 064004 (11pp)
doi:10.1088/2040-8978/18/6/064004

On the natures of the spin and orbital parts of optical angular momentum

Stephen M Barnett[1], L Allen[2], Robert P Cameron[1], Claire R Gilson[3], Miles J Padgett[1], Fiona C Speirits[1] and Alison M Yao[2]

[1] School of Physics and Astronomy, University of Glasgow, Glasgow G12 8QQ, UK
[2] Department of Physics, University of Strathclyde, Glasgow G4 0NG, UK
[3] School of Mathematics and Statistics, University of Glasgow, Glasgow G12 8QW, UK

Optical chirality: Twisted light

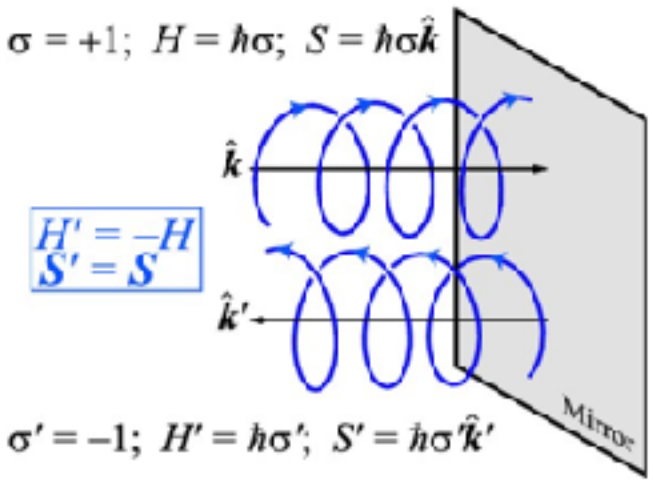

Circularly polarized light

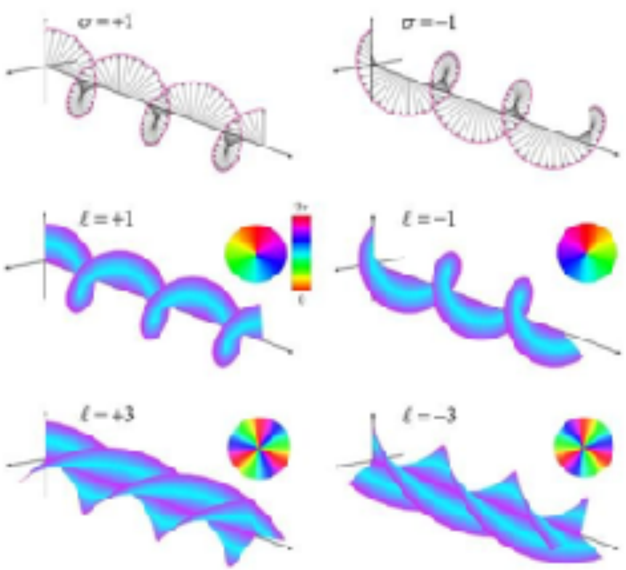

optical vortex beams

Helicity of light plays an important part in the coupling between electromagnetic fields and chiral objects

Axion is a Chiral Object

$$\mathscr{H}_p = \frac{2\,\mathrm{Im}[\int \mathbf{B}_p(\vec{r})\cdot\mathbf{E}_p^*(\vec{r})\ d\tau]}{\sqrt{\int \mathbf{E}_p(\vec{r})\cdot\mathbf{E}_p^*(\vec{r})\ d\tau \int \mathbf{B}_p(\vec{r})\cdot\mathbf{B}_p^*(\vec{r})\ d\tau}},$$

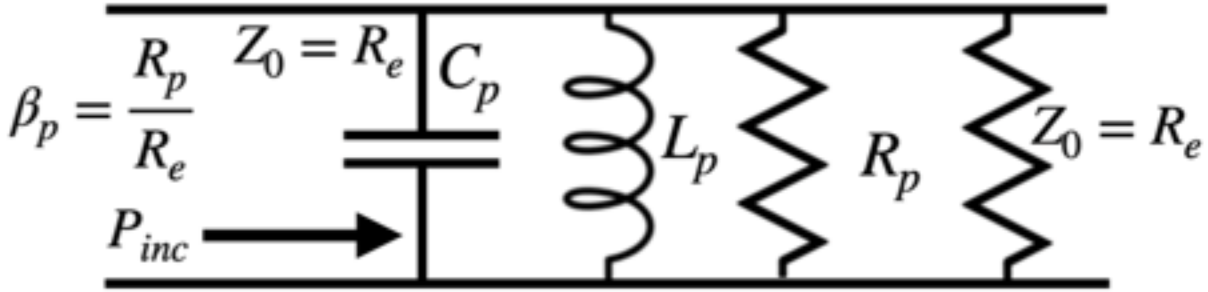

FIG. 7. Equivalent parallel LCR circuit model of a resonant mode with a coupling of β_p, when impedance matched $\beta_p = 1$.

$$P_p = \frac{\beta_p P_d}{\beta_p + 1} = \frac{4\beta_p^2}{(1+\beta_p)^2} P_{inc}.$$

$$\frac{P_{am}}{P_{inc}} = \frac{m_{am}^2 P_p}{P_{inc}} = Q_p^2 \frac{4\beta_p^2}{(1+\beta_p)^2}\left(\frac{\omega_a}{\omega_p}\right)^2 \frac{\langle\theta_0\rangle^2}{8} \mathscr{H}_p^2.$$

$$SNR = \frac{g_{a\gamma\gamma}\beta_p|\mathscr{H}_p|}{\sqrt{2}(1+\beta_p)} \frac{Q_p}{\sqrt{1+4Q_p^2(\frac{\omega_a}{\omega_p})^2}} \frac{\left(\frac{10^6 t}{\omega_a}\right)^{\frac{1}{4}}\sqrt{\rho_a c^3}}{\omega_p\sqrt{S_{am}}}$$

$$SNRp_{a\gamma\gamma} \sim g_{a\gamma\gamma}|\xi_{10}|\sqrt{\frac{2Q_{L0}Q_{L1}P_{0inc}\rho_a c^3}{\omega_1\omega_0 k_B(T_1+T_{amp})}}\left(\frac{10^6 t}{f_a}\right)^{\frac{1}{4}},$$

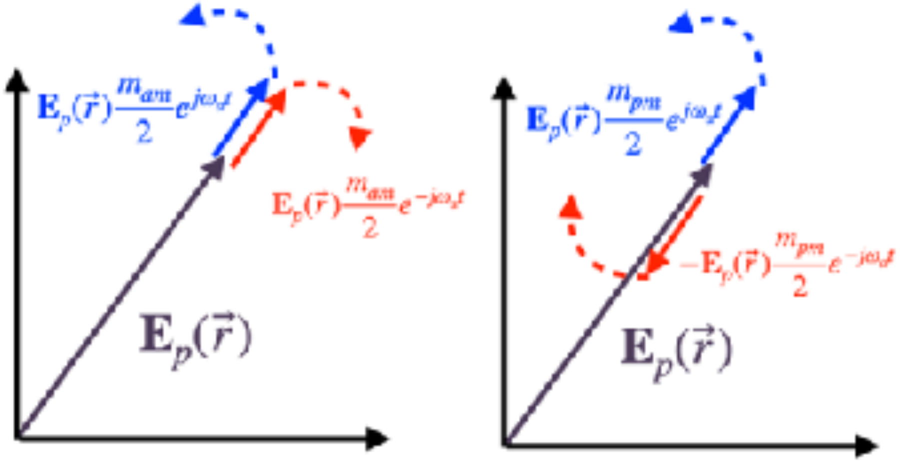

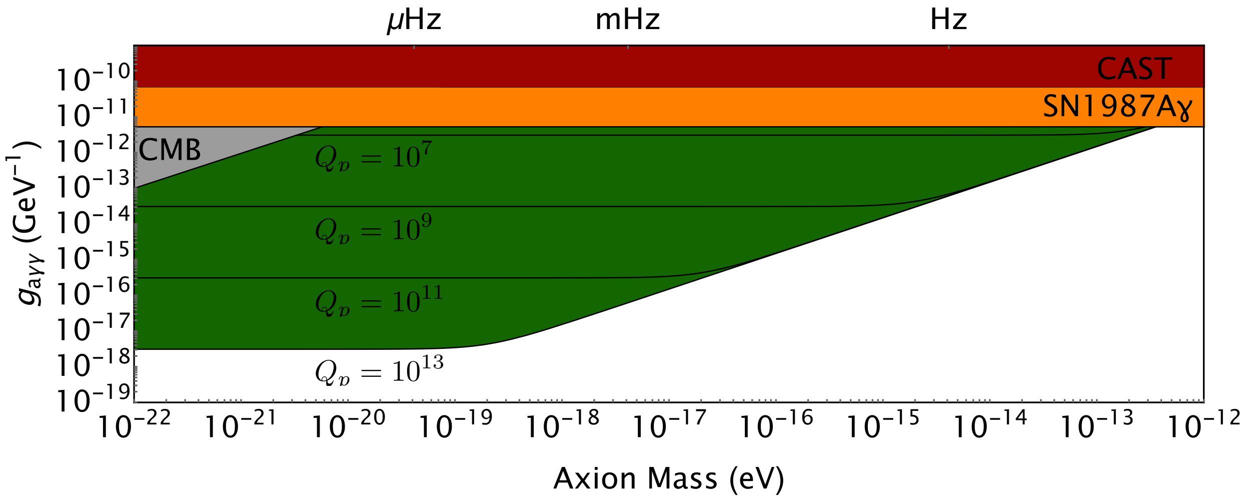

Sensitivity ~ $|\mathscr{H}|(g_{a\gamma\gamma} + g_{aBB})$

Electromagnetic Couplings of Axions

Anton V. Sokolov, Andreas Ringwald

Deutsches Elektronen-Synchrotron DESY, Notkestr. 85, 22607 Hamburg, Germany

E-mail: anton.sokolov@desy.de, andreas.ringwald@desy.de

AXION MAXWELL EQUATIONS

Classical equations of motion corresponding to this Lagrangian are the axion Maxwell equations:

$$\partial_\mu F^{\mu\nu} - g_{aAA}\,\partial_\mu a\,F^{d\,\mu\nu} + g_{aAB}\,\partial_\mu a\,F^{\mu\nu} - \frac{e^2 a}{4\pi^2 v_a} f_m^{\mu\nu} = j_e^\nu\,,$$

$$\partial_\mu F^{d\,\mu\nu} + g_{aBB}\,\partial_\mu a\,F^{\mu\nu} - g_{aAB}\,\partial_\mu a\,F^{d\,\mu\nu} = j_m^\nu\,,$$

$$(\partial^2 - m_a^2)\,a = -\frac{1}{4}(g_{aAA} + g_{aBB})\,F_{\mu\nu}F^{d\,\mu\nu} - \frac{1}{2}g_{aAB}F_{\mu\nu}F^{\mu\nu}$$

In the experimentally relevant case, in terms of electric and magnetic fields:

$$\nabla\times\mathbf{B}_a - \dot{\mathbf{E}}_a = g_{aAA}(\mathbf{E}_0\times\nabla a - \dot a\mathbf{B}_0) + g_{aAB}(\mathbf{B}_0\times\nabla a + \dot a\mathbf{E}_0)\,,$$

$$\nabla\times\mathbf{E}_a + \dot{\mathbf{B}}_a = -g_{aBB}(\mathbf{B}_0\times\nabla a + \dot a\mathbf{E}_0) - g_{aAB}(\mathbf{E}_0\times\nabla a - \dot a\mathbf{B}_0)\,,$$

$$\nabla\cdot\mathbf{B}_a = -g_{aBB}\,\mathbf{E}_0\cdot\nabla a + g_{aAB}\,\mathbf{B}_0\cdot\nabla a\,,$$

$$\nabla\cdot\mathbf{E}_a = g_{aAA}\,\mathbf{B}_0\cdot\nabla a - g_{aAB}\,\mathbf{E}_0\cdot\nabla a\,,$$

$$(\partial^2 - m_a^2)\,a = (g_{aAA} + g_{aBB})\,\mathbf{E}_0\cdot\mathbf{B}_0 + g_{aAB}(\mathbf{E}_0^2 - \mathbf{B}_0^2)\,,$$

where we separated external fields sustained in the detector and axion-induced fields.

arXiv:2207.14437 [pdf, other]

Searching for Scalar Field Dark Matter using Cavity Resonators and Capacitors

V.V. Flambaum, B.T. McAllister, I.B. Samsonov, M.E. Tobar

$$\oint \mathrm{Re}\,(\mathbf{S})\cdot\hat n\,ds = \frac{j\omega_a\epsilon_0 c g_{a\gamma\gamma}\sqrt{2}\langle a_0\rangle}{4}\int(\mathbf{E}_1\cdot\mathbf{B}_0^* - \mathbf{E}_1^*\cdot\mathbf{B}_0)\,d\tau + \frac{j\omega_a\epsilon_0 c g_{aBB}\sqrt{2}\langle a_0\rangle}{4}\int(\mathbf{B}_1^*\cdot\mathbf{E}_0 - \mathbf{B}_1\cdot\mathbf{E}_0^*)\,d\tau$$
$$+\frac{j\omega_a g_{aAB}\sqrt{2}\langle a_0\rangle}{4\mu_0}\int(\mathbf{B}_1\cdot\mathbf{B}_0^* - \mathbf{B}_1^*\cdot\mathbf{B}_0)\,d\tau + \frac{j\omega_a g_{aAB}\epsilon_0\sqrt{2}\langle a_0\rangle}{4}\int(\mathbf{E}_1^*\cdot\mathbf{E}_0 - \mathbf{E}_1\cdot\mathbf{E}_0^*)\,d\tau$$
$$-\frac{1}{4}\int(\mathbf{E}_1\cdot\mathbf{J}_{e1}^* + \mathbf{E}_1^*\cdot\mathbf{J}_{e1})\,d\tau$$

Constant DC Background Magnetic field

$$\oint \mathrm{Re}\,(\mathbf{S})\cdot\hat n\,ds = \frac{j\omega_a\epsilon_0 c g_{a\gamma\gamma}}{4}\int(\mathbf{E}_1\cdot\tilde a^*\vec B_0 - \mathbf{E}_1^*\cdot\tilde a\vec B_0)\,d\tau$$
$$\cancel{+\frac{j\omega_a g_{aAB}}{4\mu_0}\int(\mathbf{B}_1\cdot\tilde a^*\vec B_0 - \mathbf{B}_1^*\cdot\tilde a\vec B_0)\,d\tau}$$
$$-\frac{1}{4}\int(\mathbf{E}_1\cdot\mathbf{J}_{e1}^* + \mathbf{E}_1^*\cdot\mathbf{J}_{e1})\,d\tau$$

$$\int(\mathbf{B}_1\cdot\tilde a^*\vec B_0 - \mathbf{B}_1^*\cdot\tilde a\vec B_0)\,d\tau = 0$$

in constant magnetic field,

needs a gradient field to be non zero

$$g_{\alpha AB}\sim g_{\phi\gamma\gamma}$$

Professor Mike Tobar
Director

Dr Maxim Goryachev
Research Associate

Dr Ben McAllister
Research Associate

Professor Eugene Ivanov
Winthrop Research Professor—Dept of Physics

Dr Jeremy Bourhill
Postdoctoral Research Associate

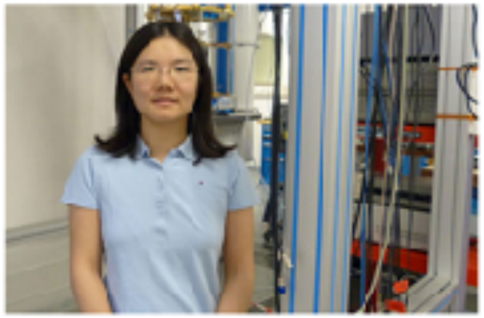

Dr Cindy Zhao
Deborah Jin Fellow—EQUS

Professor Alexey Veryaskin
Adjunct Professor

Graeme Flower
PhD

Aaron Quiskamp
PhD

Will Campbell
PhD

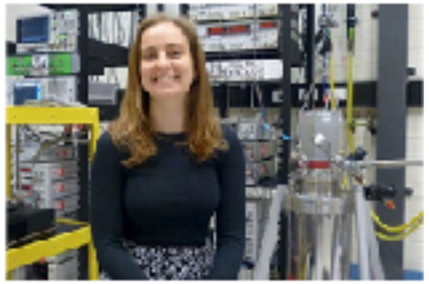

Catriona Thomson
PhD

Elrina Hartman
PhD

Jay Mummery
Masters

Robert Crew
BPhil (Hons) Placement

Daniel Tobar
BPhil (Hons) Placement

Michael Hatzon
BPhil (Hons) Placement

Steve Osborne
Technician

ARC CENTRE OF EXCELLENCE FOR DARK MATTER

EQUS
Australian Research Council
Centre of Excellence for
Engineered Quantum Systems

THE END
THE TEAM

QDM